41st ANNUAL GASEOUS ELECTRONICS CONFERENCE

October 18-21, 1988
University of Minnesota
Minneapolis, Minnesota

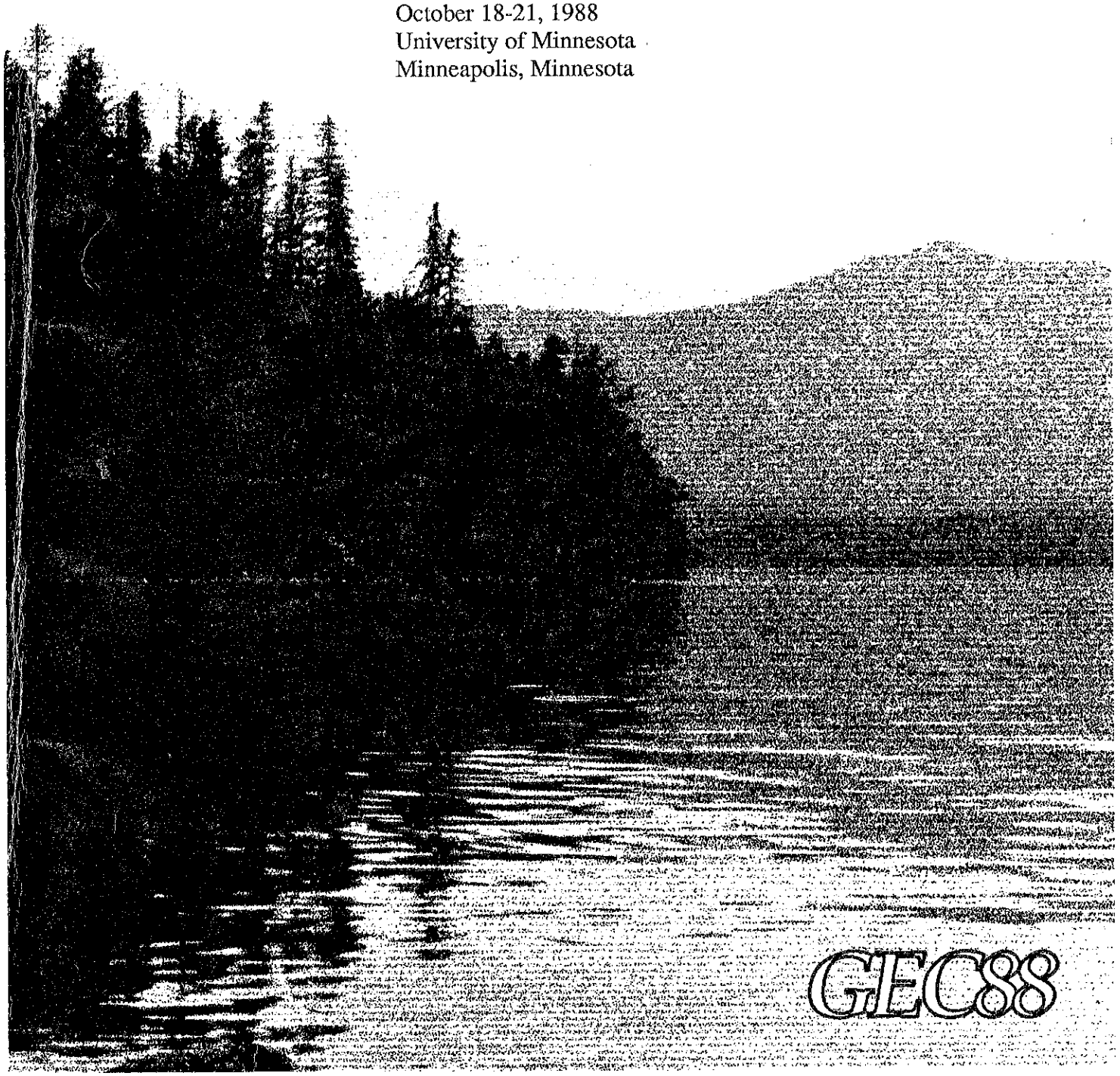

41st Annual Gaseous Electronics Conference

GEC88

18-21 October, 1988
Minneapolis, Minnesota

PROGRAM AND ABSTRACTS

A Topical Conference of the American Physical Society

Sponsored by:
The University of Minnesota
The American Physical Society: Division of Atomic, Molecular and Optical Physics

ACKNOWLEDGEMENTS

The Gaseous Electronics Conference gratefully acknowledges the support of the University of Minnesota, and in particular the staffs of the Department of Electrical Engineering and the Department of Professional Development and Conference Services, for assistance with the local arrangements. Financial support for the Gaseous Electronics Conference has been provided by:

The Air Force Office of Scientific Research

The National Science Foundation

The General Electric Company

GTE Incorporated

The Gaseous Electronics Conference is a Topical Conference of the American Physical Society with sponsorship by the Division of Atomic, Molecular and Optical Physics.

CONTENTS

TECHNICAL PROGRAM

FORTY FIRST ANNUAL GASEOUS ELECTRONICS CONFERENCE

REGISTRATION AND RECEPTION

6:30 PM - 9:30 PM
Monday, October 17, 1988
Radisson Plaza Hotel - Prefunction Area and Minnesota Room

The Stockholm Room is available most times during the Conference for use as a discussion room.

WELCOMING REMARKS. Dr. V. Rama Murthy, Vice Provost, University of Minnesota

8:00 AM - 8:10 AM, Tuesday, October 18
Radisson Plaza Hotel - Ballroom

SESSION A. ELECTRON-ATOM COLLISIONS

8:10 AM - 10:00 AM, Tuesday, October 18
Radisson Plaza Hotel - Ballroom
Chairperson: S. Trajmar, Jet Propulsion Laboratory

8:10 - 8:45	A-1.	THE STATUS OF ELECTRON ATOM AND ELECTRON MOLECULE COLLISION THEORY P. G. Burke (Invited Paper)
8:45 - 9:20	A-2.	ELECTRON SCATTERING FROM ATOMIC OXYGEN AND HYDROGEN J. F. Williams (Invited Paper)
9:20 - 9:45	A-3.	SUPERELASTIC SCATTERING OF SPIN-POLARIZED ELECTRONS FROM SODIUM ATOMS J. J. McClelland, M. H. Kelley and R. J. Celotta (Long Paper)
9:45 - 9:58	A-4.	ELECTRON EXCITATION OF THE 3^3S, 3^3P, 3^3D, 4^3S, AND 4^3D LEVELS OF He FROM THE 2^3S METASTABLE LEVEL D. L. A. Rall, F. A. Sharpton, M. B. Schulman, L. W. Anderson, J. E. Lawler and C. C. Lin

SESSION B. CHARGED PARTICLE DISTRIBUTIONS AND ELECTRIC FIELDS

10:20 AM - 12:00 Noon, Tuesday, October 18
Radisson Plaza Hotel - Ballroom
Chairperson: J. Wormhoudt, Aerodyne Research Incorporated

10:20 - 10:55	B-1.	NONINTRUSIVE MEASUREMENTS OF GLOW DISCHARGE PROPERTIES BY VELOCITY MODULATION LASER SPECTROSCOPY R. Saykally and M. B. Radunsky (Invited Paper)
10:55 - 11:20	B-2.	MICROSCOPIC ELECTRIC FIELDS IN PLASMAS FROM STARK EFFECTS IN MICROWAVE SPECTRA R. C. Woods and W. T. Conner (Long Paper)
11:20 - 11:33	B-3.	NON-GAUSSIAN VELOCITY DISTRIBUTIONS OF IONS IN A DRIFT TUBE J. P. M. Beijers, S. M. Penn, R. A. Dressler, V. M. Bierbaum and S. R. Leone
11:33 - 11:46	B-4.	DOPPLER BROADENED AND SHIFTED ABSORPTION PROFILES OF N_2^+ AS A PROBE FOR THE ELECTRIC FIELD IN N_2 DISCHARGES J. Borysow and A. V. Phelps
11:46 - 11:59	B-5.	ELECTRON TEMPERATURE AND DENSITY IN THE NEGATIVE GLOW OF A He DISCHARGE E. A. Den Hartog and J. E. Lawler

SESSION CA. THERMAL AND HIGH PRESSURE PLASMA PROCESSES

1:30 PM - 3:30 PM, Tuesday, October 18
Radisson Plaza Hotel - East Ballroom
Chairperson: S. Girshick, University of Minnesota

1:30 - 2:05	CA-1.	NONEQUILIBRIUM EFFECTS IN THERMAL PLASMA PROCESSING C. H. Kruger (Invited Paper)
2:05 - 2:40	CA-2.	RADIATIVE EFFECTS IN THERMAL PLASMAS M. Boulos (Invited Paper)
2:40 - 2:53	CA-3.	TIME RESOLVED TEMPERATURE MEASUREMENTS IN A FREE-BURNING ARGON ARC A. J. D. Farmer and G. N. Haddad

2:53 - 3:06	CA-4.	SPECTROSCOPIC INVESTIGATION OF AN ARC DISCHARGE IN PURE FLUORINE H. L. Hausmann and J. Mentel
3:06 - 3:19	CA-5.	SINTERING YTTRIA-ZIRCONIA CERAMICS IN AN RF PLASMA: EFFECTS OF PLASMA PRESSURE AND COMPOSITION M. E. Ruhland, P. C. Kong, Y. C. Lau and E. Pfender
3:19 - 3:32	CA-6.	AN RF PLASMA SYSTEM FOR THE SYNTHESIS OF CERAMIC POWDERS USING A NOVEL LIQUID INJECTION TECHNIQUE H. Zhu, Y. C. Lau and E. Pfender

SESSION CB. ELECTRON AND PHOTON INTERACTIONS

1:30 PM - 3:30 PM, Tuesday, October 18
Radisson Plaza Hotel - West Ballroom
Chairperson: M. Dillon, Argonne National Laboratory

1:30 - 1:55	CB-1.	PHOTO-REIONIZATION SPECTROSCOPY OF MOLECULAR HYDROGEN L. J. Lembo, D. L. Huestis and H. Helm (Long Paper)
1:55 - 2:08	CB-2.	MEASUREMENT OF NUMBER DENSITY OF METASTABLE NEON ATOMS IN AN ELECTRON BEAM SYSTEM M. B. Schulman, F. A. Sharpton, L. W. Anderson and C. C. Lin
2:08 - 2:21	CB-3.	TEMPORARY NEGATIVE IONS IN COMPLEX MOLECULES: ANGULAR DISTRIBUTIONS AND VIBRATIONAL EXCITATION T. M. Stephen and P. D. Burrow
2:21 - 2:34	CB-4.	ENHANCED ELECTRON ATTACHMENT TO LASER-IRRADIATED THIPHENOL AND THIOANISOLE MOLECULES L. A. Pinnaduwage, L. G. Christophorou and S. R. Hunter
2:34 - 2:47	CB-5.	ATTACHMENT AND DETACHMENT IN N_2O T. H. Teich
2:47 - 3:00	CB-6.	EXACT NON-LOCAL OPTICAL POTENTIALS FOR CLOSE-COUPLING CALCULATIONS D. H. Madison, I. Bray and I. E. McCarthy
3:00 - 3:13	CB-7.	ALIGNMENT AND ORIENTATION OF HYDROGENIC 2p STATES BY ELECTRON, POSITRON, PROTON AND ANTIPROTON IMPACT C. D. Lin, A. Jain and N. C. Deb

3:13 - 3:31 CB-8. A REVIEW OF PHOTOEMISSION CROSS SECTIONS FOR ATOMIC TRANSITIONS IN THE EXTREME ULTRAVIOLET DUE TO ELECTRON COLLISIONS WITH ATOMS AND MOLECULES
P. J. M. Van der Burgt, W. B. Westerveld and J. S. Risley
(Long Paper)

SESSION D. WORKSHOP ON THE DESIGN, CALIBRATION, AND MODELING OF RESEARCH RF PLASMA PROCESSING SYSTEMS

3:45 PM - 5:45 PM, Tuesday, October 18
Radisson Plaza Hotel - West Ballroom
Moderator: J. Gerardo, Sandia National Laboratories

The goal of this workshop is to establish some quidelines that may be used in designing, calibrating, and modeling research rf plasma systems of the type widely used to deposit, etch, or surface-treat materials. The workshop is expected to encourage the adoption of "standards", so as to foster improved communications between scientists and between scientists and technologists working in this area, thus enhancing their ability to compare data sets and to exchange insight into the underlying physics and chemistry. The workshop will consist of short presentations of several preliminary design proposals followed by a free flowing discussion based on these preliminary proposals. The final product of this workshop should be a standard "reference system" based on a consensus of both scientists and technologists working in the field.

SESSION E. POSTERS: GASEOUS ELECTRONICS I

7:30 PM - 10:00 PM, Tuesday, October 18
Radisson Plaza Hotel - East Ballroom and Minnesota Room
Chairperson: P. Moskowitz, GTE Electrical Products

All posters may be posted from 5:00 PM onwards, manned from 7:30 PM to 10:00 PM, and taken down at 10:00 PM.

E-1. ELECTRON ENERGY DISTRIBUTION FUNCTIONS AND RATE COEFFICIENTS IN O_2 DISCHARGES
M. Pinheiro, P. A. Sá, C. M. Ferreira and J. Loureiro

E-2. AN EXACT NUMERICAL SOLUTION OF THE TIME DEPENDENT BOLTZMANN EQUATION
P. J. Drallos and J. M. Wadehra

E-3. PARTICLE MODELLING OF AN RF DISCHARGE
G. J. Hofmann and W. N. G. Hitchon

E-4. LOCAL FIELD AND BALLISTIC ELECTRON MODELS FOR LOW PRESSURE GLOW DISCHARGES
R. A. Gottscho, A. Mitchell, G. R. Scheller, D. B. Graves and J. P. Boeuf

E-5. NUMERICAL SIMULATION OF 13.56 MHz SYMMETRIC PARALLEL PLATE RF GLOW DISCHARGES IN ARGON
A. P. Paranjpe, J. P. McVittie and S. A. Self

E-6. A NUMERICAL AND EXPERIMENTAL STUDY OF AN ARGON DC AND RF NEGATIVE GLOW
M. Surendra and D. B. Graves

E-7. MODELING OF VOLUME H^- ION SOURCES
M. Bacal, P. Berlemont, J. Bretagne, M. Capitelli, C. Gorse and D. A. Skinner

E-8. ANALYSIS OF THE RADIAL CHARGED PARTICLE FLUXES IN THE POSITIVE COLUMN
D. W. Ernie, H. J. Oskam and A. Metze

E-9. A FRAMEWORK FOR MODELING THE CATHODE FALL ILLUSTRATED WITH A SINGLE BEAM MODEL
T. J. Sommerer, J. E. Lawler and W. N. G. Hitchon

E-10. THEORY OF THE CATHODE SHEATH IN A VACUUM ARC
K. U. Reimann

E-11. PLASMA PARAMETERS IN LOW PRESSURE Ar-Hg DISCHARGE USED FOR A FLUORESCENT LAMP
T. Arai, T. Goto and S. Murayama

E-12. TRANSIENT ANALYSIS OF GLOW DISCHARGES IN NITROGEN
S. K. Dhali

E-13. IN SITU MONITORING OF PLASMA PROCESSES USING ADVANCED DIODE LASER DIAGNOSTICS
H. M. Anderson, A. C. Stanton and J. A. Silver

E-14. PLASMA DIAGNOSTICS USING PLIF AND WAVELENGTH MODULATION SPECTROSCOPY
D. S. Baer, A. Y. Chang, P. H. Paul and R. K. Hanson

E-15. LASER DIAGNOSTIC DENSITY MEASUREMENTS OF Hg ($6^3P_{0,1,2}$) IN A NARROW-DIAMETER Hg-Ar DISCHARGE
L. Bigio and J. T. Dakin

E-16. THE EFFECTS OF LOW LEVEL («0.1%) HYDROCARDONS ON HELIUM ATOMIC (2^3S) AND MOLECULAR ($^3\Sigma$) METASTABLES IN A LONG-PULSED ELECTRON-BEAM DISCHARGE
L. W. Downes, S. D. Marcum and W. E. Wells

E-17. ON THE IMPORTANCE OF VIBRATIONAL AND ELECTRONIC METASTABLE STATES ON THE RELAXATION OF ELECTRON ENERGY DISTRIBUTION FUNCTION OF He-N_2 AFTERGLOW
G. Dilecce, C. Gorse, S. Debenedictis and M. Capitelli

E-18. STOKES PARAMETERS AND ABSOLUTE PHASE ANGLES FOR THE 3^1D STATE OF HELIUM.
E. J. Mansky

E-19. MEASUREMENT AND MODELING OF ATOMIC CHLORINE CONCENTRATIONS IN PLASMA PROCESSES
J. P. Nicolai, H. H. Sawin and K. D. Allen

E-20. PLASMA INJECTION THROUGH RF MULTIPOLES TO A FOURIER TRANSFORM MASS SPECTROMETER
J. L. Shohet

E-21. RELATIVE ABUNDANCE OF IONS IN CH_4-H_2 DISCHARGE PLASMA
R. E. Miers, L. W. Anderson, J. E. Lawler, C. C. Lin and R. B. Lockwood

E-22. LANGMUIR PROBE MEASUREMENTS IN RF DISCHARGES
W. G. Graham, C. A. Anderson and M. B. Hopkins

E-23. LANGMUIR PROBE DIAGNOSTICS IN RF PLASMAS, CRITICAL REVIEW
V. A. Godyak

E-24. AUTOMATIC EMISSION SPECTROSCOPIC DIAGNOSTICS FOR INDUCTION PLASMA PROCESSING
J. Vattulainen and R. Hernberg

E-25. STUDY OF SOFT VACUUM ELECTRON BEAM GENERATION IN He-O_2 DISCHARGE USING LASER OPTO-GALVANIC SPECTROSCOPY
S. Moriya, P. Zeller, Z. Yu and G. J. Collins

E-26. MODELLING OF SILENT DISCHARGES WITH EXCIMER-GAS FILLING
H. Muller and M. Neiger

E-27. ANALYSIS OF THE REACTION He (2^3S)+2He$\rightarrow$$He_2(a^3\Sigma)$+He
J. Stevefelt

E-28. COLLISIONAL DETACHMENT CROSS SECTIONS FOR SF_6^-, SF_5^- AND F^- ON SF_6 AND RARE GAS TARGETS
Y. Wang, R. L. Champion, L. D. Doverspike, J. K. Olthoff and R. J. Van Brunt

E-29. DISSOCIATIVE CHARGE TRANSFER REACTIONS OF ATMOSPHERIC IONS WITH DIMETHYL-METHYLPHOSPHONATE
R. Johnsen, B. K. Chatterjee, R. Tosh

E-30. £^{2} QUANTUM MECHANICAL VARIATIONAL SOLUTION OF THE SCHROEDINGER EQUATION FOR CHEMICAL REACTIONS
M. Zhao, P. Halvick, M. Mladenovic, D. Chatfield, D. G. Truhlar, D. W. Schwenke, Y. Sun, C. H. Yu, D. J. Kouri, C. Duneczky and R. E. Wyatt

E-31. A NEW POTENTIAL ENERGY SURFACE FOR THE F + H_2 REACTION
G. Lynch, A. J. C. Varandas, D. G. Truhlar and B. C. Garrett

E-32. MEASUREMENT OF PLASMA SHEATH POTENTIAL PROFILES IN THE PRESENCE OF HIGH FREQUENCY RF
M. H. Cho, N. Hershkowitz and T. Intrator

E-33. MEASUREMENT AND ANALYSIS OF RF GLOW DISCHARGE ELECTRICAL IMPEDANCE
J. W. Butterbaugh, L. D. Baston and H. H. Sawin

E-34. TEMPORAL AND SPATIAL PLASMA POTENTIAL MEASUREMENT IN PARALLEL PLATE RF GLOW DISCHARGE
C. H. Nam, N. Hershkowitz, M. H. Cho and J. DeKock

E-35. EMISSION SPECTROSCOPY OF MICROWAVE DISCHARGES IN AIR
M. Passow and M. Brake

E-36. MEASUREMENTS AND MODELLING OF THE RADIAL CURRENT DISTRIBUTION IN A PLANAR MAGNETRON
A. E. Wendt and M. A. Lieberman

E-37. PLASMA PROPERTIES OF A MAGNETIZED, INDUCTIVELY COUPLED DISCHARGE FOR THIN FILM APPLICATIONS
K. R. Stalder, S. E. Savas and W. G. Graham

E-38. TIME DEPENDENT THEORY OF MOLECULAR PHOTODISSOCIATION OF H_3^+
K. C. Kulander and A. E. Orel

E-39. SPUTTERING APPARATUS USING MODIFIED HIGH VOLTAGE HOLLOW CATHODE DISCHARGE
T. Sumii, S. Masuda and T. Iijima

E-40. DIAMOND-LIKE CARBON (DLC) FILM DEPOSITION USING PARALLEL PLATE RF DISCHARGE
H. Mishurda, M. H. Cho, N. Hershkowitz and R. Breun

E-41. TRANSIENT RESPONSES OF THE STEADY STATE GLOW DISCHARGE TO PERTURBATIONS
Y. M. Li

E-42. SOFT X-RAY MEASUREMENT OF A PLASMA DENSITY PROFILE
B. Brill, B. Arad and M. Kishinevski

SESSION FA. MODELS AND DIAGNOSTICS OF LIGHTING DISCHARGES

8:00 AM - 9:50 AM, Wednesday, October 19
Radisson Plaza Hotel - East Ballroom
Chairperson: H. Witting, General Electric-Corporate Research Division

8:00 - 8:35 FA-1. PROGRESS AND PROSPECTS FOR LASER DIAGNOSTICS OF LIGHT SOURCES
R. Devonshire
(Invited Paper)

8:35 - 9:00 FA-2. ELECTRODELESS HIGH PRESSURE MICROWAVE DISCHARGES
S. Offermanns
(Long Paper)

9:00 - 9:25 FA-3. FLUID DYNAMICS OF ENCLOSED HIGH PRESSURE DISCHARGES
P. A. Vicharelli
(Long Paper)

9:25 - 9:50 FA-4. ANATOMY OF A 400 WATT HIGH PRESSURE MERCURY DISCHARGE WITH METAL HALIDE ADDITIVES
J. T. Dakin and T. H. Rautenberg Jr.
(Long Paper)

SESSION FB. ELECTRON COLLISIONS, INCLUDING EXCITED STATES

8:00 AM - 9:55 AM, Wednesday, October 19
Radisson Plaza Hotel - West Ballroom
Chairperson: C. C. Lin, University of Wisconsin

8:00 - 8:25 FB-1. MULTICHANNEL EIKONAL THEORY OF ELECTRON-(EXCITED) ATOM COLLISIONS
M. R. Flannery
(Long Paper)

8:25 - 8:50 FB-2. REVIEW OF TOTAL ELECTRON IMPACT CROSS SECTION MEASUREMENTS
R. A. Bonham
(Long Paper)

8:50 - 9:15 FB-3. THE IMPORTANCE OF INDIRECT PROCESSES IN ELECTRON-IMPACT IONIZATION OF IONS
D. C. Gregory
(Long Paper)

$S(2^1S - 2^3P) \sim 25.5, 57.7$

9:15 - 9:28	FB-4.	LOW ENERGY ELECTRON COLLISIONS WITH EXCITED MOLECULAR NITROGEN W. M. Huo
9:28 - 9:41	FB-5.	ABSOLUTE ANGULAR DISTRIBUTIONS OF ELASTIC SCATTERING CROSS SECTIONS OF ATOMIC HYDROGEN BY ELECTRON IMPACT T. W. Shyn and S. Y. Cho
9:41 - 9:54	FB-6.	ELECTRON-ATOM SCATTERING CROSS SECTIONS: PROGRESS ON OI AND OTHER SPECIES J. P. Doering

SESSION GA. LASERS

10:10 AM - 12:05 PM, Wednesday, October 19
Radisson Plaza Hotel - East Ballroom
Chairperson: J. G. Eden, University of Illinois

10:10 - 10:23	GA-1.	ELECTION DRIFT VELOCITY MEASUREMENT IN HYDROGEN AZIDE (NH_3) GAS MIXTURES C. A. Denmann and L. A. Schlie
10:23 - 10:36	GA-2.	MODEL CALCULATIONS OF AMPLIFICATION OF SHORT WAVELENGTH RADIATION IN CAPILLARY PLASMAS J. J. Rocca, D. Beethe and M. Marconi
10:36 - 10:49	GA-3.	TIME RESOLVED MEASUREMENT OF THE PLASMA DENSITY IN A HIGHLY IONIZED HELIUM CAPILLARY DISCHARGE M. Villagran and J. J. Rocca
10:49 - 11:02	GA-4.	A SELF-CONSISTENT MODEL OF A HOLLOW CATHODE DISCHARGE HELIUM MERCURY LASER G. J. Fetzer, N. R. Reesor and J. J. Rocca
11:02 - 11:15	GA-5.	A SELF-CONSISTENT MODEL FOR LONGITUDINAL DISCHARGE EXCITED He-Sr^+ RECOMBINATION LASERS R. J. Carman and J. A. Piper
11:15 - 11:28	GA-6.	UV-EMISSION FROM SILENT DISCHARGES IN XeCl* GAS MIXTURES V. Schorpp, K. Stockwald and M. Neiger
11:28 - 11:41	GA-7.	THE TIME RESPONSE OF ELECTRON BEAM PUMPED PLASMAS AND LASERS M. J. Kushner and H. Pak
11:41 - 11:54	GA-8.	EXCITATION KINETICS OF THE ATOMIC Xe LASER IN Ar/Xe MIXTURES T. J. Moratz and M. J. Kushner

11:54 - 12:07 GA-9. DISSOCIATION AND VIBRATIONAL RELAXATION OF XeF BY VARIOUS COLLISION PARTNERS
J. F. Bott, R. F. Heidner, J. S. Holloway, J. B. Koffend and M. A. Kwok

SESSION GB. PLASMA-SURFACE PHENOMENA

10:10 AM - 11:55 AM, Wednesday, October 19
Radisson Plaza Hotel - West Ballroom
Chairperson: D. Graves, University of California-Berkeley

10:10 - 10:23 GB-1. THEORY OF THE PLASMA-SHEATH TRANSITION AND THE BOHM CRITERION
K. U. Riemann

10:23 - 10:48 GB-2. IN SITU SURFACE DIAGNOSTICS FOR PLASMA CHEMISTRY
A. Mitchell, R. A. Gottscho, S. W. Downey and G. R. Scheller (Long Paper)

10:48 - 11:01 GB-3. ELECTRON YIELD OF GLOW DISCHARGE CATHODE MATERIALS UNDER NOBLE GAS ION BOMBARDMENT
B. Szapiro, J. J. Rocca and T. Prabhuram

11:01 - 11:14 GB-4. THE USE OF TRANSPORT COEFFICIENTS FOR ELECTRON SCATTERING ON DIELECTRIC SURFACES
T. L. Peck and M. J. Kushner

11:14 - 11:27 GB-5. SPONTANEOUS THRESHOLD BEHAVIOR FOR A DISTRIBUTED-ELEMENT MODEL OF SURFACE ARCS
A. Kadish, W. B. Maier II and R. T. Robiscoe

11:27 - 11:40 GB-6. SIMULATION OF SPUTTERING OF LIQUID AND SOLID METALS
W. L. Morgan

11:40 - 11:53 GB-7. THERMALIZATION OF ATOMS EJECTED FROM THE CATHODE OF A MAGNETRON SPUTTERING DISCHARGE
I. S. Falconer, G. M. Turner, B. W. James and D. R. McKenzie

SESSION H. POSTERS: GASEOUS ELECTRONICS II

1:30 PM - 3:45 PM, Wednesday, October 19
Radisson Plaza Hotel - Ballroom and Minnesota Room
Chairperson: J. Evans, University of Minnesota

All posters may be posted from 1:00 PM onwards, manned from 1:30 PM to 3:45 PM, and taken down at 6:00 PM.

H-1. A COMPLETE AND SELF-CONSISTENT THEORY OF SURFACE WAVE PRODUCED DISCHARGES
A. B. Sá and C. M. Ferreira

H-2. VALIDITY OF THE EFFECTIVE FIELD CONCEPT AT VERY HIGH E/N
Y. M. Li and L. C. Pitchford

H-3. SELF-CONSISTENT SOLUTION OF BOLTZMANN EQUATION IN RF PLASMAS: APPLICATION TO EXIMER Ne-Xe-HCl LASER
C. Gorse and M. Capitelli

H-4. ION DIFFUSION AND ELECTRODE BIAS VOLTAGE IN ASYMMETRIC, CAPACITIVE R.F. DISCHARGES
M. A. Lieberman and S. E. Savas

H-5. RATE EQUATION MODELING OF A LOW PRESSURE RF ARGON GLOW DISCHARGE
M. J. Colgan, D. E. Murnick and R. B. Robinson

H-6. PARTICLE SIMULATION OF A LOW PRESSURE RF DISCHARGE
I. J. Morey and R. W. Boswell

H-7. KINETIC MODELING OF RF DISCHARGES
D. J. Koch and W. N. G. Hitchon

H-8. OBSERVED AND CALCULATED CURRENT OVERSHOOT IN Ar-Hg AND Ne-Hg DISCHARGES
M. E. Duffy and J. H. Ingold

H-9. CRITERION FOR CHARACTERIZING THE SLOPE OF THE I-E RELATIONSHIP OF A POSITIVE COLUMN
G. L. Rogoff

H-10. FLUID TREATMENT OF PLASMA PRESHEATH FOR COLLISIONLESS TO COLLISIONAL PLASMAS
J. T. Scheuer and G. A. Emmert

H-11. SHEATH STRUCTURE AND CURRENT LIMITATION FOR AN ELECTRODE CONTACTING A THERMAL PLASMA
L. D. Eskin and S. A. Self

H-12. THE PULSED DISCHARGE ARC RESISTANCE AND ITS FUNCTIONAL BEHAVIOR
T. G. Engel, A. L. Donaldson and M. Kristiansen

H-13. ELECTRON DENSITY AND COLLISION FREQUENCY MEASUREMENTS IN MICROWAVE BREAKDOWN PLASMAS IN AIR
K. R. Stalder and D. J. Eckstrom

H-14. ATOMIC TRANSITION PROBABILITIES FOR Sc I AND Sc II
G. Marsden, J. E. Lawler and J. T. Dakin

H-15. LIFETIMES, BRANCHING RATIOS, AND ABSOLUTE TRANSITION PROBABILITIES IN HgI
E. C. Benck and J. E. Lawler

H-16. Zn-RARE GAS ATOM ABSORPTION SPECTRA
Y. Tamir, I. Aharon and R. Shuker

H-17. THE CALCULATION OF MOLECULAR ELECTRON AFFINITIES
T. Gorczyca and D. W. Norcross

H-18. A NUMERICAL MULTICONFIGURATION HARTREE-FOCK CALCULATION ON ^3P (nsnp) Rb and Cs ANION STATES
D. Chen and C. F. Fischer

H-19. ANISOTROPIC POTENTIALS OF RARE GAS - N_2 SYSTEMS
M. S. Bowers, K. T. Tang and J. P. Toennies

H-20. THEORETICAL TREATMENT OF SHAPE RESONANCES IN MOLECULES USING FANO'S METHOD
D. Chen and G. A. Gallup

H-21. ELECTRON IMPACT EXCITATION OF HELIUM TO TRIPLET STATES
R. E. H. Clark, D. C. Cartwright, J. Abdallah, Jr., J. B. Mann and G. Csanak

H-22. CALCULATION OF DIFFERENTIAL CROSS SECTIONS, ELECTRON IMPACT COHERENCE PARAMETERS, AND FINE-STRUCTURE EFFECT SPIN-POLARIZATION FUNCTIONS FOR THE ELECTRON IMPACT EXCITATION OF NEON
L. E. Machado, M. C. Ferraz, G. D. Meneses, G. Csanak and D. C. Cartwright

H-23. ORIENTATION AND ALIGNMENT PARAMETERS IN $e^{\pm}$ IMPACT EXCITATION OF HYDROGEN-LIKE POSITIVE IONS
A. Jain, N. C. Deb, N. C. Sil and C. D. Lin

H-24. COMPARISON OF THE DIFFERENTIAL MAGNETIC SUBLEVEL (m_l=0) CROSS SECTION FOR THE 3^1P STATE OF HELIUM FOR 60 AND 80 ev ELECTRONS
N. W. P. H. Perera and D. J. Burns

H-25. DENSITY AND ROTATIONAL TEMPERATURE OF $SiH_3(X^2A_1)$ RADICAL IN SILANE PLASMA
T. Goto, N. Itabashi, N. Nishiwaki, K. Kato, C. Yamada and E. Hirota

H-26. TIME-DEPENDENCE OF THE SCATTERING AMPLITUDES FOR THE 3^1D STATE OF HELIUM
E. J. Mansky

H-27. ELECTRON-PHOTON COINCIDENCE STUDIES OF HEAVY RARE GAS EXCITATION BY ELECTRON IMPACT
J. J. Corr, P. Plessis and J. W. McConkey

H-28. POLARIZATION OF VUV RADIATION FROM THE RARE GASES EXCITED BY ELECTRON IMPACT
W. Karras, K. Bird, P. Hammond and J. W. McConkey

H-29. MOLECULAR DISSOCIATION STUDIES USING LASER INDUCED FLUORESCENCE
M. Darrach and J. W. McConkey

H-30. FRAGMENTATION OF CF_4 FOLLOWING ELECTRON IMPACT
S. Wang and J. W. McConkey

H-31. VUV EMISSIONS PRODUCED BY ELECTRON COLLISIONS WITH HALOGEN-CONTAINING MOLECULES
F. M. Olchowski, Z. J. Jabbour and K. Becker

H-32. ELECTRON DEGRADATION SPECTRA AND YIELDS BY SUBEXCITATION ELECTRONS IN O_2 AND CO_2 GASES
M. Kimura, K. Kowari, M. A. Ishii, A. Pagnamenta and M. Inokuti

H-33. ELECTRON DISTRIBUTION IN A DENSE GAS OF REPULSIVE SCATTERERS
T. F. O'Malley

H-34. MEASUREMENT OF THE MOBILITY AND LONGITUDINAL DIFFUSION COEFFICIENTS OF SF_5^+ IN SF_6
J. De Urquijo, I. Alvarez, H. Martinez and C. Cisneros

H-35. EXCITED STATES IN PARTIALLY IONIZED HYDROGEN
S. S. Popovic

H-36. MEASUREMENTS OF ELECTRODE TEMPERATURE EVOLUTION BY LASER LIGHT REFLECTION
H. Kempkens, W. W. Byszewski and W. P. Lapatovich

H-37. EXPERIMENTAL INVESTIGATION OF ARC ROOT IGNITION ON COLD CATHODES
K. P. Nachtigall and J. Mentel

H-38. EFFECT OF UV RADIATION ON OPERATING VOLTAGE IN THE HIGH-VOLTAGE HOLLOW CATHODE DISCHARGE
T. Arai, H. Akiba, T. Iijima and T. Goto

SESSION I. POSTERS: GASEOUS ELECTRONICS III

3:45 PM - 6:00 PM, Wednesday, October 19
Radisson Plaza Hotel - Ballroom
Chairperson: L. Bigio, General Electric R&D Center

All posters may be posted from 1:00 PM onwards, manned from 3:45 PM to 6:00 PM, and taken down at 6:00 PM.

I-1. ELECTRICAL CONDUCTIVITY MEASUREMENTS OF THE NRL LASER-INITIATED-REDUCED-DENSITY CHANNELS
K. R. Stalder, M. S. Williams and D. J. Eckstrom

I-2. TEMPERATURE DEPENDENCE OF VUV FLUORESCENCE YIELD OF Xe_2
I. Messing, M. S. Williams and D. J. Eckstrom

I-3. EXCITATION TEMPERATURE DETERMINATION IN NON-EQUILIBRIUM, LOW-PRESSURE, Ar-Cs PLASMAS
M. A. Gieske, J. Myers, S. D. Marcum and B. N. Ganguly

I-4. ELECTRON TEMPERATURE RELAXATION IN Ar-Cs PLASMAS AS A FUNCTION OF CATHODE TEMPERATURE
J. L. Myers, M. A. Gieske, S. D. Marcum and B. N. Ganguly

I-5. MEASURED AND PREDICTED ETCH CHARACTERISTICS OF SULFUR HEXAFLUORIDE RF DISCHARGES
H. M. Anderson

I-6. PULSED-LASER GENERATION OF ACOUSTIC RESONANCES IN HIGH PRESSURE MERCURY AND METAL HALIDE DISCHARGES
J. Kramer and W. Lapatovich

I-7. RADIAL TEMPERATURE DISTRIBUTIONS IN HIGH PRESSURE XENON DISCHARGES
S. S. Popovic and J. Koceic

I-8. EMISSION OF RADIATION FROM A XENON DISCHARGE AT MEDIUM PRESSURES
J. K. Berkowitz and P. Moskowitz

I-9. STARK SPECTROSCOPY OF RYDBERG STATES IN PLASMAS
J. R. Shoemaker, B. N. Ganguly and A. Garscadden

I-10. ELECTRIC FIELD PROFILE MEASUREMENT IN AN OBSTRUCTED HYDROGEN DISCHARGE
B. N. Ganguly, J. R. Shoemaker and A. Garscadden

I-11. SPACE AND TIME RESOLVED ELECTRIC FIELD VECTOR MEASUREMENTS IN TWO DIMENSIONAL DC AND RF DISCHARGES USING LASER STARK SPECTROSCOPY OF NaK
H. Debontride, J. Derouard and N. Sadeghi

I-12. ELECTRIC FIELD MEASUREMENTS IN THE CATHODE FALL REGION OF DC GLOW DISCHARGES USING THE RELATIVE INTENSITY OF STARK ENHANCED FORBIDDEN TRANSITIONS
H. Shan, M. A. Cappelli and S. A. Self

I-13. ION BOMBARDMENT ANGLE AND ENERGY DISTRIBUTIONS IN ARGON AND SF_6 RF DISCHARGES
J. Liu, J. W. Butterbaugh, G. L. Huppert and H. H. Sawin

I-14. NUMERICAL CALCULATION OF BREAKDOWN CHANNELS IN A DIELECTRIC-BARRIER DISCHARGE
B. Eliasson and W. Egli

I-15. THE ROLE OF IONIZATION BY FAST ATOMS AND IONS IN THE ELECTRICAL BREAKDOWN OF Ar AT HIGH VOLTAGES AND LOW PRESSURES
A. V. Phelps and B. M. Jelenkovic

I-16. STREAMER PROPAGATION IN ATTACHING GASES
S. K. Dhali and A. Sarkar

I-17. COPPER CONTAMINATION IN AN ELECTRIC ARC
G. Y. Zhao, M. Dassanayaki and K. Etemadi

I-18. EXPERIMENTAL STUDIES OF ANODE BOUNDARY LAYERS IN HIGH-INTENSITY ARCS
E. Leveroni and E. Pfender

I-19. NUCLEATION AND GROWTH OF PLASMA-SYNTHESIZED POWDERS
C. P. Chiu, R. Muno and S. L. Girshick

I-20. TWO-DIMENSIONAL MAGNETIC FIELD EFFECTS IN INDUCTIVELY COUPLED ATMOSPHERIC-PRESSURE HYDROGEN PLASMAS
W. Yu and S. L. Girshick

I-21. PHOTODISSOCIATION OF H_3
P. C. Cosby and H. Helm

I-22. LASER-INDUCED PHOTODETACHMENT OF O^- IN AN OXYGEN DC GLOW DISCHARGE
G. Gousset, J. Jolly and M. Touzeau

I-23. RESONANT MULTIPHOTON IONIZATION SPECTROSCOPY IN A HYDROGEN FLOWING AFTERGLOW EXPERIMENT
G. Sultan, G. Baravian, G. Jolly and P. Persuy

I-24. POSITRON AND ELECTRON DIFFERENTIAL ELASTIC SCATTERING FROM INERT GASES AT INTERMEDIATE ENERGIES
S. J. Smith, G. M. A. Hyder, W. E. Kauppila, C. K. Kwan and T. S. Stein

I-25. TOTAL CROSS SECTION MEASUREMENTS FOR POSITRON AND ELECTRON-Na and Rb COLLISIONS
T. S. Stein, M. S. Dababneh, W. E. Kauppila, C. K. Kwan, R. A. Lukaszew, S. P. Parikh and Y. J. Wan

I-26. ABSOLUTE ELASTIC DIFFERENTIAL CROSS SECTIONS OF ELECTRONS SCATTERED BY $3^2P_{3/2}$ SODIUM
M. Zuo, T. Y. Jiang, L. Vuskovic and B. Bederson

I-27. ELECTRON IMPACT IONIZATION CROSS SECTION MEAUSREMENTS OF THE Cu, Fe, P AND Si ATOMS
R. S. Freund, R. C. Wetzel and R. J. Shul

I-28. ELECTRON-IMPACT EXCITATION OF ATOMIC OXYGEN
S. S. Tayal and R. J. Henry

I-29. INTEGRAL AND DIFFERENTIAL CROSS SECTIONS FOR e^-+He($2^{1,3}S$) COLLISIONS
E. J. Mansky and M. R. Flannery

I-30. ELECTRON IMPACT VIBRATIONAL EXCITATION OF SMALL MOLECULES
S. Alston, G. Snitchler and D. Norcross

I-31. STUDIES OF LOW-ENERGY ELECTRON SCATTERING BY MOLECULES
H. Pritchard, C. Winstead, K. Watari, V. McKoy, M. A. P. Lima, F. J. daPaixao and L. M. Brescansin

I-32. USE OF THE PDE METHOD IN DISSOCIATIVE RECOMBINATION
C. A. Weatherford and W. M. Huo

I-33. DISSOCIATIVE IONIZATION OF LASER EXCITED N_2^* BY ELECTRON IMPACT
D. P. Wang, L. C. Lee and S. K. Srivastava

I-34. ELECTRON IMPACT EXCITATION OF THE $a^3\Pi$, $a'^3\Sigma^+$, $d^3\Delta$ AND $A^1\Pi$ STATES OF CO AT LOW ENERGIES
P. W. Zetner, I. Kanik, J. C. Nickel and S. Trajmar

I-35. TOTAL LOW-ENERGY ELECTRON SCATTERING CROSS SECTIONS FOR SiF_4
P. B. Liescheski, Ce Ma, K. H. Chung and R. A. Bonham

I-36. A STUDY OF THE ANGULAR MOMENTUM DEPENDENCE OF PHASE SHIFT FOR FINITE RANGE AND COULOMB POTENTIALS
S. R. Valluri and W. J. Romo

I-37. LASER INDUCED FLUORESCENCE STUDIES IN Hg-Ar RF DISCHARGES
J. L. Streete, J. M. Christman and L. Maleki

I-38. NEW VARIATIONAL APPROACHES TO ELECTRON-MOLECULE SCATTERING
T. N. Rescigno and C. W. McCurdy

SESSION JA. SILANE PLASMAS

8:00 AM - 8:50 AM, Thursday, October 20
Radisson Plaza Hotel - East Ballroom
Chairperson: G. Hays, Sandia National Laboratories

8:00 - 8:13 JA-1. NEGATIVE ION KINETICS IN SILANE PLASMAS
A. Garscadden

8:13 - 8:26 JA-2. MEASUREMENTS OF ELECTRON SWARM PARAMETERS IN SILANE
D. K. Davies

8:26 - 8:39 JA-3. THE PLASMA-SURFACE INTERFACE IN PECVD OF AMORPHOUS SILICON
M. J. McCaughey and M. J. Kushner

8:39 - 8:52 JA-4. LOW TEMPERATURE, LOW PRESSURE, RF PLASMA SYNTHESIS OF ULTRAFINE, ULTRAPURE CERAMIC POWDERS
H. M. Anderson

SESSION JB. BEAM-PLASMA INTERACTIONS

8:00 AM - 9:20 AM, Thursday, October 20
Radisson Plaza Hotel - West Ballroom
Chairperson: J. L. Shohet, University of Wisconsin

8:00 - 8:13 JB-1. A HOLLOW CATHODE ARC SOURCE FOR BEAM-PLASMA EXPERIMENTS
J. B. Rosenzweig

8:13 - 8:26 JB-2. MONTE CARLO SIMULATION OF ION COOLING IN EBIT
B. M. Penetrante and J. N. Bardsley

8:26 - 8:39 JB-3. ELECTRON ENERGY DEPOSITION IN PARTIALLY IONIZED ATOMIC NITROGEN PLASMAS
B. M. Penetrante and J. N. Bardsley

8:39 - 8:52 JB-4. MODEL OF MULTIPHOTON IONIZATION RESONANT UV LASER-ATMOSPHERE INTERACTIONS
J. E. Stockley, G. J. Fetzer, L. D. Nelson and L. J. Radziemski

8:52 - 9:05 JB-5. HIGH ENERGY HEAVY ION BEAM PUMPED PLASMAS
D. E. Murnick, A. Ulrich, B. Busch, W. Krotz and G. Ribitzki

9:05 - 9:18 JB-6. ELECTRON BEAM INITIATED DISCHARGE STUDIES IN HYDROGEN AZIDE (HN_3) GAS MIXTURES
M. W. Wright and L. A. Schlie

SESSION KA. NON-EQUILIBRIUM ELECTRON TRANSPORT

8:50 AM - 9:45 AM, Thursday, October 20
Radisson Plaza Hotel - East Ballroom
Chairperson: Y. Li, GTE Laboratories

8:52 - 9:05 KA-1. LOCAL MOMENT THEORY OF ELECTRON TRANSPORT IN GASES
E. E. Kunhardt and I. T. Lu

9:05 - 9:18 KA-2. THE INFLUENCE OF ELECTRON GENERATION AND DEPLETION ON THE ELECTRON KINETICS IN GASES
G. Schaefer and P. Hui

9:18 - 9:31 KA-3. CONVECTIVE SCHEME MODELING OF SWARM EXPERIMENTS AND THE CATHODE FALL
T. J. Sommerer, W. N. G. Hitchon and J. E. Lawler

9:31 - 9:44 KA-4. FLUX-CORRECTED TRANSPORT FOR SOLUTION OF THE SPATIALLY DEPENDENT BOLTZMANN'S EQUATION
J. V. Dicarlo and M. J. Kushner

SESSION LA. NEUTRAL PARTICLE DISTRIBUTIONS

10:00 AM - 11:30 AM, Thursday, October 20
Radisson Plaza Hotel - East Ballroom
Chairperson: M. Cappelli, Stanford University

10:00 - 10:25 LA-1. MEASUREMENT OF THE DENSITY AND TEMPERATURE OF GROUND-STATE HYDROGEN ATOMS AND OF VIBRATIONALLY EXCITED HYDROGEN MOLECULES IN A PLASMA.
A. S. Schlachter, G. C. Stutzin, A. T. Young, J. W. Stearns, K. N. Leung, W. B. Kunkel, G. T. Worth, R. R. Stevens, H. V. Smith and E. Pitcher
(Long Paper)

10:25 - 10:38	LA-2.	SPATIALLY RESOLVED TEMPERATURE MEASUREMENTS IN AN ABNORMAL GLOW N_2-Ar DISCHARGE USING COHERENT ANTI-STOKES RAMAN SPECTROSCOPY (CARS) P. P. Yaney, J. E. Oleksy, W. A. Fowler and S. W. Kizirnis
10:38 - 10:51	LA-3.	PLASMA ETCHING DIAGNOSTICS USING GATED-RF DISCHARGES P. J. Hargis, Jr. and K. E. Greenberg
10:51 - 11:04	LA-4.	CHARACTERIZATION OF CF_4 PLASMA KINETICS BY MODULATED POWER RELAXATION L. D. Baston and H. H. Sawin
11:04 - 11:17	LA-5.	INFARED ABSORPSION LASER DIAGNOSTICS OF DEPOSITION PLASMAS J. Wormhoudt
11:17 - 11:30	LA-6.	DETECTION OF SULFUR DIMERS IN SULFUR HEXAFLUORIDE ETCHING DISCHARGES K. E. Greenberg and P. J. Hargis, Jr.

SESSION LB. HEAVY PARTICLE INTERACTIONS

10:00 AM - 11:30 AM, Thursday, October 20
Radisson Plaza Hotel - West Ballroom
Chairperson: B. Bederson, New York University

10:00 - 10:25	LB-1.	INTERACTION OF LOW-ENERGY $O^-(^2P)$ AND $O(^3P)$ BEAMS WITH A MgF_2 SURFACE A. Chutjian, O. J. Orient and E. Murad (Long Paper)
10:25 - 10:38	LB-2.	RATE CONSTANTS FOR THE REACTION $^{22}Ne^+ + {}^{20}Ne$ AS A FUNCTION OF COLLISION ENERGY AT SEVERAL TEMPERATURES R. A. Morris, A. A. Viggiano, T. Su and J. F. Paulson
10:38 - 10:51	LB-3.	MUTUAL NEUTRALIZATION STUDIES USING CHEMICAL RELEASES IN SPACE PLASMAS P. A. Bernhardt and P. Rodriguez
10:51 - 11:04	LB-4.	PREDISSOCIATION PRODUCT DISTRIBUTIONS FROM H_3 P. Devynck, W. G. Graham and J. R. Peterson
11:04 - 11:17	LB-5.	DISSOCIATIVE CHARGE TRANSFER IN $H^+(H_3^+) + SiH_4$ REACTIONS H. H. Michels and R. H. Hobbs

11:17 - 11:30 LB-6. CENTER OF MASS DISTRIBUTION OF H^- PRODUCED BY THE DISSOCIATION OF H_3^+
O. Yenen, L. Wiese and D. H. Jaecks

BUSINESS MEETING

11:30 AM - 12:00 Noon, Thursday, October 20
Radisson Plaza Hotel - East Ballroom
Chairman: J. Proud, GTE Laboratories

SESSION M. RF GLOW DISCHARGE MODELING

1:30 PM - 3:20 PM, Thursday, October 20
Radisson Plaza Hotel - Ballroom
Chairperson: A. Mitchell, AT&T Bell Laboratories

1:30 - 2:05 M-1. MODELING OF RF GLOW DISCHARGES
J. P. Boeuf
(Invited Paper)

2:05 - 2:18 M-2. CONTINUUM MODELING OF SF_6 AND Ar RF DISCHARGES, AND COMPARISON WITH EXPERIMENTAL MEASUREMENTS
E. Gogolides, J. P. Nicolai and H. H. Sawin

2:18 - 2:31 M-3. MODELING OF MOLECULAR RF GLOW DISCHARGES FOR SEMICONDUCTOR PROCESSING
T. J. Grimard, M. S. Barnes and M. E. Elta

2:31 - 2:44 M-4. COMPUTATIONAL LIMITATIONS IN RF GLOW DISCHARGE MODELING
M. S. Barnes, T. J. Grimard and M. E. Elta

2:44 - 3:19 M-5. MODELING OF RF GLOW DISCHAGE PLASMAS
T. Makabe
(Invited Paper)

SESSION N. BREAKDOWN AND SWITCHING

3:40 PM - 5:35 PM, Thursday, October 20
Radisson Plaza Hotel - Ballroom
Chairperson: M. Gundersen, University of Southern California

3:40 - 4:05 N-1. STOCHASTIC PROPERTIES OF NEGATIVE CORONA (TRICHEL) PULSE DISCHARGES IN ELECTRONEGATIVE GASES
R. J. Van Brunt and S. V. KulKarni
(Long Paper)

11:17 - 11:30 LB-6. CENTER OF MASS DISTRIBUTION OF H^- PRODUCED BY THE DISSOCIATION OF H_3^+
O. Yenen, L. Wiese and D. H. Jaecks

BUSINESS MEETING

11:30 AM - 12:00 Noon, Thursday, October 20
Radisson Plaza Hotel - East Ballroom
Chairman: J. Proud, GTE Laboratories

SESSION M. RF GLOW DISCHARGE MODELING

1:30 PM - 3:20 PM, Thursday, October 20
Radisson Plaza Hotel - Ballroom
Chairperson: A. Mitchell, AT&T Bell Laboratories

1:30 - 2:05 M-1. MODELING OF RF GLOW DISCHARGES
J. P. Boeuf
(Invited Paper)

2:05 - 2:18 M-2. CONTINUUM MODELING OF SF_6 AND Ar RF DISCHARGES, AND COMPARISON WITH EXPERIMENTAL MEASUREMENTS
E. Gogolides, J. P. Nicolai and H. H. Sawin

2:18 - 2:31 M-3. MODELING OF MOLECULAR RF GLOW DISCHARGES FOR SEMICONDUCTOR PROCESSING
T. J. Grimard, M. S. Barnes and M. E. Elta

2:31 - 2:44 M-4. COMPUTATIONAL LIMITATIONS IN RF GLOW DISCHARGE MODELING
M. S. Barnes, T. J. Grimard and M. E. Elta

2:44 - 3:19 M-5. MODELING OF RF GLOW DISCHAGE PLASMAS
T. Makabe
(Invited Paper)

SESSION N. BREAKDOWN AND SWITCHING

3:40 PM - 5:35 PM, Thursday, October 20
Radisson Plaza Hotel - Ballroom
Chairperson: M. Gundersen, University of Southern California

3:40 - 4:05 N-1. STOCHASTIC PROPERTIES OF NEGATIVE CORONA (TRICHEL) PULSE DISCHARGES IN ELECTRONEGATIVE GASES
R. J. Van Brunt and S. V. KulKarni
(Long Paper)

4:05 - 4:18	N-2.	IONIZATION AND CURRENT GROWTH IN N_2 AT VERY HIGH E/N V. T. Gylys, B. M. Jelenkovic and A. V. Phelps
4:18 - 4:31	N-3.	OVERSHOOT IN IONIZATION RATES AT HIGH E/N J. T. Verdeyen, L. C. Pitchford, Y. M. Li, J. B. Gerardo and G. N. Hays
4:31 - 4:44	N-4.	AN INVESTIGATION OF STREAMER PROPERTIES AND MULTI-STREAMER INTERACTIONS M. C. Wang and E. E. Kunhardt
4:44 - 4:57	N-5.	DISTRIBUTED ELEMENT MODEL GIVING SPONTANEOUS THRESHOLDS FOR ELECTRIC DISCHARGES W. B. Maier II, A. Kadish and R. T. Robiscoe
4:57 - 5:10	N-6.	EFFECTS OF UNSTEADY FLOW AND RADIATION ON RECOVERY OF A SPARK GAP SWITCH A. K. Cousins, V. C. H. Lo and W. J. Thayer
5:10 - 5:23	N-7.	SIMULATION OF AN OPTICALLY TRIGGERED PSEUDO SPARK THYRATRON H. Pak and M. J. Kushner
5:23 - 5:36	N-8.	EXCITATION OF MERCURY IN A DIELECTRIC-BARRIER DISCHARGE B. Eliasson, B. Gellert and U. Kogelschatz

SOCIAL HOUR AND BANQUET

6:30 PM - , Thursday, October 20
Radisson Plaza Hotel - Ballroom
After Dinner Speaker: Dr. G. Edward Schuh, Dean, Hubert H. Humphrey Institute, University of Minnesota

SESSION O. PHYSICS IN A POSITRON TRAP

8:30 AM - 9:05 AM, Friday, October 21
Radisson Plaza Hotel - Ballroom
Chairperson: R. Gottscho, AT&T Bell Laboratories

8:30 - 9:05	O-1.	PHYSICS IN A POSITRON TRAP C. M. Surko (Invited Paper)

SESSION PA. LOW-PRESSURE DISCHARGES: EXPERIMENTAL

9:20 AM - 11:15 AM, Friday, October 21
Radisson Plaza Hotel - East Ballroom
Chairperson: R. Gerber, Sandia National Laboratories

9:20 - 9:33	PA-1.	NEGATIVE ION FLUX ENHANCEMENT FROM RF PROCESSING DISCHARGES L. J. Overzet and J. T. Verdeyen
9:33 - 9:46	PA-2.	ELECTRICAL CHARACTERISTICS OF RF PARALLEL PLATE DISCHARGES WITH ADDED ATTACHERS AND THEIR INTERPRETATION P. Bletzinger
9:46 - 9:59	PA-3.	SPATIAL DISTRIBUTIONS OF a-Si:H FILM PRODUCING SPECIES IN SILANE GLOW DISCHARGES D. A. Doughty and A. Gallagher
9:59 - 10:12	PA-4.	RF POTENTIAL MEASUREMENTS IN THE MODEL 5000 MAGNETRON ETCHER S. E. Savas and K. G. Donohoe
10:12 - 10:25	PA-5.	ELECTRICAL CHARACTERISTICS OF CYLINDRICAL MAGNETRON RF DISCHARGES FOR ETCHING AND DEPOSITION G. Y. Yoem and M. J. Kushner
10:25 - 10:38	PA-6.	A MICROWAVE DISCHARGE FOR PLASMA PROCESSING USING A SLOTTED METAL COUPLER S. Kuo, E. E. Kunhardt and G. Schaefer
10:38 - 10:51	PA-7.	ELECTRODE DESIGN FOR DIFFUSE GAS DISCHARGES A. E. Rodriguez and W. M. Moeny
10:51 - 11:04	PA-8.	A REFLEX ELECTRON BEAM DISCHARGE AS A PLASMA SOURCE FOR ELECTRON BEAM GENERATION C. Murray, J. J. Rocca and B. Szapiro
11:04 - 11:17	PA-9.	DESIGN CRITERIA FOR AN OPTICAL IONIZING RADIATION PARTICLE TRACK DETECTOR S. R. Hunter, W. A. Gibson and G. S. Hurst

SESSION PB. ELECTRON-MOLECULE COLLISIONS

9:20 AM - 11:15 AM, Friday, October 21
Radisson Plaza Hotel - West Ballroom
Chairperson: R. Bonham, University of Indiana

9:20 - 9:45	PB-1.	MULTICHANNEL STUDIES OF LOW - ENERGY ELECTRON IMPACT EXCITATION OF MOLECULES C. Winstead, H. Pritchard, K. Watari, V. McKoy, M. A. P. Lima, F. J. daPaixao and L. M. Brescansin (Long Paper)
9:45 - 10:10	PB-2.	ELECTRON-IMPACT DISSOCIATION OF SIMPLE MOLECULES P. C. Cosby and H. Helm (Long Paper)
10:10 - 10:35	PB-3.	NEW DEVELOPMENTS IN DISSOCIATIVE RECOMBINATION J. B. A. Mitchell and F. B. Yousif (Long Paper)
10:35 - 10:48	PB-4.	ATTACHMENT AND IONIZATION CROSS SECTIONS IN CF_4 P. J. Chantry and C. B. Freidhoff
10:48 - 11:01	PB-5.	MONTE CARLO CALCULATIONS OF ELECTRON TRANSPORT IN CF_4 WITH ANISOTROPIC SCATTERING L. E. Kline and T. V. Congedo
11:01 - 11:14	PB-6.	LOW ENERGY STRUCTURES IN EMISSION CROSS SECTIONS FROM CCl_2F_2 and BCl_3 Z. J. Jabbour and K. Becker

SESSION Q. FOLLOW-UP TO THE WORKSHOP ON THE DESIGN, CALIBRATION, AND MODELING OF RESEARCH RF PLASMA PROCESSING SYSTEMS

11:15 AM - 12:00 Noon, Friday, October 21
Radisson Plaza Hotel - East Ballroom
Chairperson: J. Gerardo, Sandia National Laboratories

SESSION A

8:10 AM - 10:00 AM, Tuesday, October 18

Radisson Plaza Hotel - Ballroom

ELECTRON-ATOM COLLISIONS

Chairperson: S. Trajmar, Jet Propulsion Laboratory

A-1 The Status of Electron Atom and Electron Molecule Collision Theory. P. G. BURKE, The Queen's University of Belfast, Belfast, Northern Ireland. - Over the last few years, developments in collision theory together with the increasing availability of supercomputers and the ever increasing sophistication of experiments have enabled substantial progress to be made in the theoretical understanding of electron atom and electron molecule collisions. At low energies, accurate scattering amplitudes can now be determined for light atoms and molecules using configuration interaction expansion approaches while at high energies perturbative approaches give reliable results. For example, recent work has yielded accurate low energy cross sections for highly excited states of H and He and for the electronic excitation of simple diatomic molecules such as O_2. However, for heavy atoms, where relativistic effects are important, and for polyatomic molecules much work still remains to be done to obtain reliable theoretical results. In addition, there are still fundamental theoretical difficulties in obtaining excitation and ionization cross sections at intermediate energies where an infinite number of strongly coupled channels are open. This review will survey recent progress in electron atom and electron molecule collision theory comparing wherever possible with experiment and will describe attempts to develop new approaches for areas where major theoretical uncertainties exist. It will conclude with a brief survey of possible future directions of research.

A-2 Electron Scattering from Atomic Oxygen and Hydrogen. J. F. WILLIAMS, Physics Department, The University of Western Australia, Nedlands, Perth 6009 Australia - - In atomic oxygen, the angular distribution of electrons elastically scattered through angles from 10 to 150 degrees at energies of 0.54, 4.990 and 8.71 eV have been analyzed by a phase shift analysis technique. Absolute differential cross sections are in good agreement with polarized-orbital pseudostate values. In atomic hydrogen, observations of Lyman-alpha radiation have revealed nine resonances converging to the n=3 threshold. Their positions and widths agree with the pseudostate close-coupling values and fit the supermultiplet structure using K, T and A quantum numbers. Electron-photon angular correlations near the n=2 threshold indicate large perturbations from the ^1P resonance. Similar angular correlations but from the Stark-perturbed 2S and 2P states for an incident energy of 350 eV and a scattering angle of 10^o show quantum beats in the circular polarization and permit the complete state multipoles of the n=2 excited state to be deduced.

A-3 Superelastic Scattering of Spin-polarized Electrons from Sodium Atoms,* J.J. McCLELLAND, M.H. KELLEY and R.J. CELOTTA, National Bureau of Standards, Gaithersburg, MD — Orientation parameters have been measured for superelastic scattering of spin-polarized electrons from laser-excited Na(3P) using circularly polarized excitation. Data at 2, 17.9 and 52.3 eV over the angular range 10-120 degrees will be presented. Polarized electrons are obtained from a GaAs source. The use of spin-polarized electrons allows $L_\perp$, the angular momentum transferred perpendicular to the scattering plane, to be separated into singlet and triplet contributions, and also allows the ratio of singlet to triplet cross sections to be measured. Comparison of these three parameters with close-coupling calculations reveals interesting agreements and discrepancies.

*Work supported in part by U.S. Dept. of Energy, Office of Basic Energy Sciences, Division of Chemical Sciences.

A-4 Electron Excitation of the 3^3S, 3^3P, 3^3D, 4^3S, and 4^3D Levels of He from the 2^3S Metastable Level, D. L. A. RALL, F. A. SHARPTON, M. B. SCHULMAN, L. W. ANDERSON, J. E. LAWLER, and CHUN C. LIN, Univ. of Wisconsin, Madison--Electron excitation cross sections from the 2^3S metastable level of He to the 3^3S, 3^3P, 3^3D, 4^3S, and 4^3D levels have been measured by means of the optical method. A beam of He(2^3S) metastable atoms produced from a hollow cathode discharge is crossed by a low-energy electron beam, and the emission from the various excited states is detected. Absolute calibration is made by comparing the electron excitation cross section with the known optical absorption cross section. At 10 eV the cross section for 3^3D is larger than that for 3^3P in contrast to excitation from the ground level to 3^1P and 3^1D.

SESSION B

10:20 AM - 12:00 Noon, Tuesday, October 18

Radisson Plaza Hotel - Ballroom

CHARGED PARTICLE DISTRIBUTIONS AND ELECTRIC FIELDS

Chairperson: J. Wormhoudt, Aerodyne Research Incorporated

B-1 Nonintrusive Measurements of Glow Discharge Properties by Velocity Modulation Laser Spectroscopy. M.B. RADUNSKY AND R.J. SAYKALLY, University of California, Berkeley -- We have used the method of velocity modulation to study the positive column of a glow discharge in a nonintrusive manner. We have measured the axial electric field in the positive column by observing the field induced drift velocity of the ions. By half wave rectification of a sine wave driven discharge, the absolute Doppler shift in frequency of an ionic transition can be observed, thus allowing calculation of the drift velocity of the ion in the direction of the laser beam propagation. In this experimental configuration a non-derivative absorption signal is obtained and therefore the ionic translational temperature can also be measured. A He/N_2 discharge was studied using this method and axial electric fields of about 13 V/cm were observed. Translational temperatures for the N_2^+ ion were also measured and found to be slightly above the neutral gas temperature. In addition estimates of the vibrational temperature were obtained.

B-2 Microscopic Electric Fields in Plasmas from Stark Effects in Microwave Spectra, R. CLAUDE WOODS and WILLIAM T. CONNER, Department of Chemistry, U. of Wisconsin-Madison --Observation of Stark broadening in the microwave rotational spectra of HCN and HCO^+ in degenerate excited states of their bending vibrations have been used to infer values for microscopic electric fields in DC glow discharge plasmas. A computer model based on the simple Holtsmark theory of the microscopic field is used to simulate the observed spectra and estimate the ion density. The latter agrees with electron densities deduced from microwave interferometry to within 20-50%, but the Stark broadening predicted from the interferometric plasma density is systematically less than that observed. Possible explanations for the discrepancy will be discussed. Probe measurements of the plasma floating potential have been used to show that the macroscopic electric fields are too small (~0.5 V/cm) to account for the observed Stark perturbation. In a magnetically enhanced negative glow discharge a reversed direction for the axial macroscopic field has been inferred from the probe measurements.

B-3 Non-Gaussian Velocity Distributions of Ions in a Drift Tube* J. P. M. BEIJERS, S. M. PENN, R. A. DRESSLER, V. M. BIERBAUM, and S. R. LEONE, JILA, Univ. of Colo. and NBS -- Experimental evidence is presented for skewed velocity distributions of atomic ions drifted in a buffer gas under the influence of an electric field. We have probed the velocity distribution of Ba^+ drifted in He and Ar by tuning a single-mode dye laser over the $6^2S_{1/2}$ - $6^2P_{3/2}$ transition and observing the fluorescence radiation. With He as the buffer gas the observed spectra are Gaussian and their widths are in excellent agreement with the three-temperature theory of Lin et al.,[1] both when the laser propagates parallel and prependicular to the electric field. In Ar the observed temperatures are much higher and there is a significant skewing of the ion velocity distribution in the forward scattering direction. Additional results will be presented and compared with theoretical predictions.[2]

*Supported by Air Force Office of Scientific Research.

[1]S. L. Line, L. A. Viehland, and E. A. Mason, Chem. Phys. 37, 411 (1979).

[2]J. H. Whealton and S. B. Woo, Phys. Rev. A 6, 2319 (1971).

B-4 Doppler broadened and shifted absorption profiles of N_2^+ as a probe for the electric field in N_2 discharges,* JACEK BORYSOW and A.V. PHELPS,† JILA, University of Colorado and NBS. --- Doppler broadened and shifted absorption line profiles of the $A^2\Pi_u \leftarrow X^2\Sigma_g^+$ (3 - 0) Meinel band of N_2^+ near 689 nm have been used to determine time-dependent N_2 drift velocities and longitudinal electric fields in the positive column of a 10 μs discharge in N_2 (1.5 A/cm^2 and 1 torr). The absorption of the single-mode CW laser is $\leq$ 0.05% for a 1.8 m folded, axial path. The ion velocity distribution is assumed to be the convolution of the high field distribution for charge transfer collisions with a thermal distribution. The derived E/n decrease with time from 120 to 90 Td and the average agrees with positive column theory to within the measurement uncertainty of $\approx$ 15%. The N_2^+ velocities redistribute rapidly upon collapse of the discharge field.

† Quantum Physics Division, NBS and Physics Dept., CU.

* Supported in part by Air Force Wright Aeronautical Laboratories and National Science Foundation.

B-5 Electron Temperature and Density in the Negative Glow of a He Discharge. *E. A. DEN HARTOG and J. E. LAWLER, U. of Wisconsin-Madison--The negative glow of a dc He discharge contains a high density of low energy electrons. These electrons cause a severe suppression of the 2^1S metastable density via the reaction:

$$He(2^1S) + e^- \rightarrow He(2^3S) + e^- + 0.79 \text{ eV}.$$

The 2^1S and 2^3S metastable densities are mapped using laser-induced fluorescence and absorption. These maps are analyzed to yield an effective rate for the above reaction from which a relation between n_e and T_e is determined. An independent relation between n_e and T_e is derived by balancing ion production and loss in the negative glow. Ion production is determined from Monte Carlo simulations of electron avalanches from the cathode fall region. We use a model of ion loss in the negative glow in which ions drift toward the anode by ambipolar diffusion.

*Work supported by the Air Force Office of Scientific Research under grant AFOSR 84-0328.

SESSION CA

1:30 PM - 3:30 PM, Tuesday, October 18

Radisson Plaza Hotel - East Ballroom

THERMAL AND HIGH PRESSURE PLASMA PROCESSES

Chairperson: S. Girshick, University of Minnesota

CA-1 Nonequilibrium Effects in Thermal Plasma Processing,* C.H. KRUGER, Stanford Univ. --Calculations are described which investigate conditions such that electron-temperature nonequilibrium in thermal plasmas and charged-particle reaction channels might influence chemical reactivity in plasma synthesis and plasma processing applications. Results for dissociation rates in the presence of elevated electron temperatures show that nonequilibrium in a plasma torch itself or in an auxiliary discharge can have significant effects on the state of the plasma and its reactivity. To address such effects, experiments are under way in a plasma facility incorporating a 50kW RF induction torch. Spectroscopic measurements show differences between Boltzmann excitation temperatures and those inferred assuming local thermodynamic equilibrium. Measurements of the radiation source strength in argon indicate an order-of-magnitude difference from values reported earlier at temperatures of interest in plasma processing. This difference is discussed in terms of nonequilibrium effects and an upper-bound argument with respect to the decay of radiation source strength with decreasing temperature.

*Work supported by Basic Energy Sciences, DOE.

CA-2 Radiative Effects in Thermal Plasma, MAHER I. BOULOS, University of Sherbrooke, Sherbrooke, Quebec, Canada, J1K 2R1 - An analysis will be presented of radiative energy transfer mechanism under plasma conditions. Results obtained for different thermal plasma generating devices show that more than 50% of the plasma energy can be transferred to its surroundings as radiation. The effect is particularly important in transferred arc furnaces. The presence of particles, in-flight, and of metal vapours in the plasma can also be responsible for the substantial increase of the overall radiative energy loss from the plasma. The efficient use of the plasma as a material processing device depends in such cases on the ability to recapture the radiative energy in the material being processed.

CA-3 Time-resolved Temperature Measurements in a Free-burning Argon Arc, A.J.D. FARMER and G.N. HADDAD, CSIRO, Division of Applied Physics - Time-resolved excitation temperatures derived from spectroscopic emission measurements have been obtained for a free-burning argon arc when the arc current has a significant a.c. component. A rotating mirror system is used to sweep an image of the arc across the detection optics in a time short compared to the period of the a.c. waveform and relative intensity measurements are recorded for the 696.5 nm line of neutral argon. Multiple sweeps are averaged to obtain a suitable signal-to-noise ratio and the data is analysed as described in Haddad and Farmer[1]. Arc temperatures obtained at the maximum and minimum of the a.c. cycle are found to differ markedly from each other and also from those obtained for corresponding d.c. arcs. Explanations of the results will be given in terms of the thermal time constants of the arc column and the electrodes.

[1]G.N. Haddad and A.J.D. Farmer, J. Phys. D: Appl. Phys. 17, 1189 (1984).

CA-4 Spectroscopic Investigation of an Arc Discharge in Pure Fluorine,* H.L. HAUSMANN and J. MENTEL, Allgemeine Elektrotechnik und Elektrooptik, Ruhr-Universität Bochum, FRG - Radially resolved spectroscopic measurements are performed at a low current arc in pure fluorine. A radial distribution of an excitation temperature is determined from the intensity ratio of two fluorine lines and the distribution of the electron temperature from a Boltzmann-plot of the F^--affinity continuum. Two groups of electrons are found. At the axis the temperature of one group corresponds to the gas temperature of 4000 K that of the other group to the excitation temperature of 7800 K. Electron densities are determined from the absolute intensity of the F^--continuum and ion densities from the half width of the contamination line H_β. At the arc axis an electron density of $1.3\ 10^{20}\ m^{-3}$, a density of the F^+-ions of $9\ 10^{20}\ m^{-3}$ and of the F^--ions of $7.7\ 10^{20}\ m^{-3}$ are found.

*Research supported by DFG.

CA-5 **Sintering Yttria-Zirconia Ceramics in an RF Plasma: Effects of Plasma Pressure and Composition.*** M.E. RUHLAND, PETER C. KONG, Y.C. LAU AND E. PFENDER, Mechanical Engineering, U. of Minnesota -- Yttria-Stabilized Zirconia powder compacts have been rapidly sintered (< 5 mins.) to high densities in RF plasmas. Final sintered densities varied with plasma composition (Ar, Ar/O_2, Ar/He, and Ar/N_2) and pressure (5 Torr to 1 atm). Mixed-gas plasmas generally gave higher sintered densities This effect is due to the increased enthalpy of the mixed-gas plasmas. Greater than 95% of the theoretical density was achieved using atmospheric Ar/O_2 plasmas. The sintered densities decreased with plasma pressure until the degree of ionization in the plasma greatly increased at low pressures. At these pressures (< 15 Torr), the sample densities increased to higher values. This effect is due to increased release of the recombination energies of atomic and ionic species on the sample surface. SEM micrographs of the sintered samples show uniformly fine-grained microstructures. X-ray diffraction was used for phase identification.

*This work is supported by grant #NSF/DMR8511748.

CA-6 **An RF Plasma System for the Synthesis of Ceramic Powders Using a Novel Liquid Injection Technique.*** H. Zhu, Y.C. Lau and E. Pfender, Mechanical Engineering, University of Minnesota -- A complete (15 kW) rf plasma processing system has been constructed for the synthesis of ultrafine ceramic powders by injection of liquid precursors into the plasma. A water-cooled gas-blast atomizer is used to spray fine droplets of the liquid reactants inside the fire ball of the argon rf plasma at a typical feed rate of 300 ml/hr. The product powders are collected on the surface of a downstream collection chamber (by thermal precipitation), by an in-line cyclone and by a porous metal filter. Fine powders of MgO, pure and Y_2O_3 stabilized zirconia (YSZ) have been synthesized by this method using nitrate solution precursors. The success in synthesizing YSZ powders suggests that other solid solutions of oxide powders (e.g. superconducting oxides) can be produced in a similar fashion. The reactant concentration and feed rate are the control parameters to produce powders of desirable size and morphology. The product powders are characterized by X-ray diffraction and scanning electron microscopy.

*This work is supported by grant #NSF/CBT-8514180.

SESSION CB

1:30 PM - 3:30 PM, Tuesday, October 18

Radisson Plaza Hotel - West Ballroom

ELECTRON AND PHOTON INTERACTIONS

Chairperson: M. Dillon, Argonne National Laboratory

CB-1 Photo-Reionization Spectroscopy of Molecular Hydrogen.* L. J. LEMBO, D. L. HUESTIS, and H. HELM, SRI International -- The metastable states of diatomic and triatomic hydrogen, 2p $c^3\Pi_u^-$ and 2p $\bar{B}^2A_2''$, are produced by charge transfer in Cs vapor of keV H_2^+ or H_3^+ ion beams, respectively. Photoabsorption is observed by detecting H_2^+ or H_3^+ ions produced from metastable neutrals by photoionization, field ionization, or vibrational and rotational autoionization. The absorption spectrum of H_3 is simple, consisting of atomic-like transitions (e.g. nd ← 2p). It provides detailed information about the relatively weak coupling between the Rydberg electron and the rotational and vibrational modes of the H_3^+ core. On the other hand, the absorption spectrum of metastable H_2 is very rich and difficult to assign, due to vibrational and rotational excitation of the H_2^+ parent and the large rotational constant. Using an ionization-dissociation double-resonance technique we have investigated the rapidly-predissociated high vibrational levels of the $j^3\Delta_g$ state.

*This work was supported by NSF and AFOSR

CB-2 Measurement of Number Density of Metastable Neon Atoms in an Electron Beam System, M. BRUCE SCHULMAN, FRANCIS A. SHARPTON, L. W. ANDERSON, and CHUN C. LIN, Univ. of Wisconsin, Madison--The number density of metastable Ne atoms produced by an electron beam through Ne gas has been measured. The $1s_5(2p^5 3s\ ^3P_2)$ metastable atoms are pumped to the $2p_7$ level $(2p^5 3p\ J=1)$ by a pulsed laser and the resulting $2p_7 \rightarrow 1s_4(2p^5 3s, J=1)$ laser-induced fluorescence is used to determine the $1s_5$ metastable number density. The electron beam is turned on and off periodically. The laser is fired with an adjustable time delay after the electron beam is turned off. By repeating the experiment for a series of time delay, we determine the temporal decay of the metastable number density. The decay curve is close to a single exponential form with a time constant 19 μsec.

CB-3 Temporary Negative Ions in Complex Molecules: Angular Distributions and Vibrational Excitation,* T.M. STEPHEN and P.D. BURROW, Behlen Lab. U. of NE, Lincoln--Angular scattering distributions and vibrational excitation functions are widely used to study temporary negative ion formation in small molecules. We examine the extent to which such methods work in a more complex molecule, 1,4-cyclohexadiene. This planar compound has two low-lying unfilled pi* orbitals and considerable symmetry. A well-isolated totally symmetric vibrational mode of the neutral, associated with C=C motion, is found to be excited by the resonances. The angular scattering dependence of electrons exciting this mode reflects the orbital symmetries of the resonances and permits an unambiguous ordering of the two anion states. The ^2A_u state is observed to lie below the $^2B_{3g}$ state.[1,2]

*Supported by NSF.

[1]R. McDiarmid and J.P. Doering, JCP 75, 2687 (1981).
[2]A. Modelli, D. Jones, S. Rossini and G. Distefano, Chem. Phys. Letters 123, 375 (1986).

CB-4 Enhanced Electron Attachment to Laser-Irradiated Thiophenol and Thioanisole Molecules, L. A. PINNADUWAGE, L. G. CHRISTOPHOROU, and S. R. HUNTER, Oak Ridge National Laboratory and The University of Tennessee, Knoxville - Following our initial report,[1] we have conducted a series of experiments to identify the specific electron attachment mechanisms involved in the enhanced electron attachment to excimer-laser-irradiated thiophenol (C_6H_5SH) and thioanisole ($C_6H_5SCH_3$) molecules. Experimental results to date indicate that the photoenhanced electron attachment which occurs within a few μs following laser irradiation is due to dissociative electron attachment to molecules in their first excited triplet state. At longer times (μs to ~ 10 ms) following laser irradiation photoenhanced attachment increases further. This latter is attributed to electron capture by diphenyl disulfide ($C_6H_5SSC_6H_5$) formed by the interaction of first excited triplet state parent molecule(s) and/or thiophenoxy radical(s) ($C_6H_5S\cdot$) produced by laser irradiation.

*Research sponsored by OHER, USDOE under contract DE-AC05-840R21400 with Martin Marietta Energy Systems, and The University of Tennessee, Knoxville.
[1]L.G.Christophorou,et al.,Phys.Rev.Lett. 58,1316 (1987)

CB-5 Attachment and Detachment in N_2O. T. H. TEICH, ETH, Zurich - Conventional measurement of steady state current vs. gap spacing in N_2O at constant E/N with Townsend, Gosseries, Nikamura plots or curve fitting has been applied to determine ionization (α) and attachment (η) coefficients. The measured η values are at least one order of magnitude lower than those determined by solving the Boltzmann equation.[1] Current transients originating from large electron swarms generated at the cathode of a homogeneous field discharge gap show a peculiar discharge development: The attachment rate is very high, and at gas densities, n, above $n_{crit}=8x10^{17}$ cm^{-3} no electrons are observed. Reducing net attachment by increasing E/N leads to immediate breakdown in spite of $\eta>\alpha$, and "critical" field strength with $\alpha=\eta$ can only be attained for $n<n_{crit}$. On the other hand, $\alpha=\eta$ is then clearly observed for $(E/N) \cong 200$ Td. This $(E/N)_{crit}$ remains constant for densities from 0.6 to $7.5.x10^{17}$ cm^{-3}. The observed high $(E/N)_{crit}$ suggests N_2O as a candidate for gas insulation. However, because of very high rates of detachment, the high currents due to detached electrons reach their maximum several hundred ns after injection of the primary swarm. For E/N fixed the detached electron current increases as n increases. Even for $n= 0.6x10^{17}$ cm^{-3}, detachment is still obvious and conventional discharge current analysis should not be uncritically applied. However, determination of electron drift velocity etc. is straight-forward over a wide range of E/N at low n.

1) M. Hayashi, et al. Proc. ICPIG XVIII, Swansea 1987, 13-15.

CB-6 Exact Non-Local Optical Potentials for Close-Coupling Calculations. D. H. MADISON*, University of Missouri-Rolla, and I. BRAY and I. E. MCCARTHY, Flinders University of South Australia. - In a close-coupling calculation, the total wave function is expanded in terms of a complete set which includes a sum over all discrete states and an intergal over all possible continuum states. For practical calculations, this sum must be limited to a finite number of states of the discrete type. It is well known, however, that the neglected continuum states make a significant contribution. The effects of the continuum can be incorporated into a close-coupling calculation through the use of optical potentials. However, optical potentials are non-local and are very difficult to calculate and as a result many simplyfing approximations of often questionable validity are made. Since it is necessary to include the effects of the neglected states properly, we have developed the techniques to calculate optical potentials exactly for any hamiltonian of the distorted wave type. These non-local optical potentials are numerically summed over all neglected discrete states and intergated over all contributing continuum states. In this paper, we will describe our calculation and present some results for the electron-hydrogen problem.

*Work supported by the NSF

CB-7 **Alignment and Orientation of hydrogenic 2p states by electron, positron,proton and antiproton impact***. C. D. Lin, A. Jain, N. C. Deb, Kansas State University — The alignment and orientation of 2p states of hydrogenlike ions excited by electron and positron impact are calculated in the Coulomb-Born approximation. It is found that the results are similar to those seen in helium target. Simple scaling with respect to the incident energy and the target nuclear charge have been observed. Comparisons are made with respect to the impact parameter dependence of the alignment and orientation of H(2p) by proton and antiproton impact. Analysis of the 2s and 2p coherence will also be discussed.

* Supported in part by the US Department of Energy, Office of Energy Sciences, Division of Chemical Sciences.

CB-8 A Review of Photoemission Cross Sections for Atomic Transitions in the Extreme Ultraviolet due to Electron Collisions with Atoms and Molecules.* PETER J. M. VAN DER BURGT, W. B. WESTERVELD and J. S. RISLEY, N. C. State University, Raleigh. -- Over 500 photoemission cross sections in the extreme ultraviolet have been measured for a variety of atomic and molecular targets during the last 25 years. On reviewing the literature severe inconsistencies are found between cross sections reported by different laboratories, sometimes extending far outside the quoted accuracies. Almost all reported cross sections are based on relative measurements, and are either directly or via earlier reported cross sections normalized to the Bethe or Born approximations. An important element in this normalization is the molecular branching-ratio technique, used to determine the relative spectral response of the spectrometer-detector system. There is clearly a need for: (1) more careful attention for the difficulties associated with accurate measurement of the essential parameters, and (2) accurate measurements, independent of the molecular branching-ratio technique, that are either relative to transitions in the visible, or absolute by using absolute calibration of the spectrometer-detector system with synchrotron radiation.

*Work supported in part by the Experimental Plasma Research of the DOE, Grant No. DE-FG05-87-ER53259.

SESSION D

3:45 PM - 5:45 PM, Tuesday, October 18

Radisson Plaza Hotel - West Ballroom

WORKSHOP ON THE DESIGN, CALIBRATION, AND MODELING OF RESEARCH RF PLASMA PROCESSING SYSTEMS

Moderator: J. Gerardo, Sandia National Laboratories

D-1 Workshop on the Design, Calibration, and Modeling of Research RF Plasma Processing Systems -- The goal of this workshop is to establish some quidelines that may be used in designing, calibrating, and modeling research rf plasma systems of the type widely used to deposit, etch, or surface-treat materials. The workshop is expected to encourage the adoption of "standards", so as to foster improved communications between scientists and between scientists and technologists working in this area, thus enhancing their ability to compare data sets and to exchange insight into the underlying physics and chemistry. The workshop will consist of short presentations of several preliminary design proposals followed by a free flowing discussion based on these preliminary proposals. The final product of this workshop should be a standard "reference system" based on a consensus of both scientists and technologists working in the field.

SESSION E

7:30 PM - 10:00 PM, Tuesday, October 18

Radisson Plaza Hotel - East Ballroom and Minnesota Room

POSTERS: GASEOUS ELECTRONICS I

Chairperson: P. Moskowitz, GTE Electrical Products

(All posters may be posted from 5:00 PM onwards, manned from 7:30 PM to 10:00 PM, and taken down at 10:00 PM.)

E-1 **Electron Energy Distribution Functions and Rate Coefficients in O_2 Discharges**, M. PINHEIRO, P. A. SÁ, C. M. FERREIRA, and J. LOUREIRO, Centro de Electrodinâmica, Lisbon Tech. U. - We have solved the steady-state, homogeneous electron Boltzmann equation as derived from the usual two-term expansion approximation for the conditions of a low pressure positive column in $O_2(p \sim 0.1 - 5Torr$, $E/N \sim 30 - 100$Td). The calculation includes the effects of superelastic collisions of the electrons with vibrationally excited molecules $O_2(X\ ^3\Sigma_g^-)$ and with metastable molecules $O_2(a\ ^1\Delta_g)$, and of the presence of dissociated oxygen atoms in large amounts ($O_2 + O$ mixture). Typical experimental values[1] of the relative concentrations $\delta_m = [O_2(a)]/[O_2] \sim 15 - 20\%$ and $\delta_a = [O]/[O_2] \sim 10\%$ have been used. The characteristic vibrational temperature of $O_2(X)$ molecules, T_V, is taken as a parameter. The basic set of electron cross sections for O_2 is the same as proposed by Phelps[2] from his analysis of swarm experiments. The calculated data, i.e., the electron transport parameters, the ionization and the excitation rate coefficients, and the percentage energy losses vs. E/N as a function of δ_m, δ_a, and T_V, are compared to those obtained for the conditions of a swarm (S), i.e., for $T_V = 300K$ and $\delta_m = \delta_a = 0$. At the lower E/N values the effect of superelastic collisions can increase the total ionization rate, C_i, by a factor of about 4 with respect to case S, but at the higher E/N the increase only is $\sim 50\%$. It appears that this increase in C_i is not sufficient to explain the discrepancy between the theoretical and experimental values of E/N vs. NR previously reported[1].

[1] C. M. Ferreira, G. Gousset, M. Touzeau, and M. Vialle, Bull. Am. Phys. Soc. 33, 154(1988); J. Phys. D (to appear)
[2] A. V. Phelps, JILA Report No. 28(1985)

E-2 An Exact Numerical Solution of the Time Dependent Boltzmann Equation,* P.J. DRALLOS and J.M. WADEHRA, Dept. of Physics, Wayne State Univ.-- An exact, time dependent numerical solution of the Boltzmann equation for charged particle swarms in a dilute gas and uniform electric field is presented in detail. The method incorporates the full anisotropy of both the velocity distribution function and the collision cross sections as it does not involve any term expansions. An exact analysis of the collision terms is described and conditions for numerical stability of the solution are discussed. Results are presented for electron and positron swarms in gaseous Neon and Argon and in some model gases at various values of E/N.

*This work was supported by the Air Force Office of Scientific Research through Grant No. AFOSR-87-0342.

E-3 Particle Modelling of an RF Discharge. G.J. Hofmann and W.N.G. Hitchon, Electrical and Computer Engineering, University of Wisconsin-Madison. -- A 1D Particle model of a 13.56 MHz RF O_2 plasma etching discharge will be presented. The electron and ion trajectories are integrated self-consistently, with respect to the electric fields due to the charged species. The model thus determines the electron and ion distributions as functions of energy and position. It also determines the potential distribution in the etching reactor and the production rate of oxygen ions as a function of position. Electron collisions (elastic and inelastic) are allowed with O_2 only. The inelastic collisions result in either metastable formation, ionization, dissociation or excitation. Ions are allowed elastic and charge exchange collisions with O_2. The effect of secondary electron emission on the energy distributions, ionization rate and potential distribution in a low density case (10 mTorr), and a high density case (300 mTorr), has been investigated. Results for the electron and ion energy distributions, ionization rate and potential distribution will be presented. The role of negative ions will be discussed.

E-4 Local Field and Ballistic Electron Models for Low Pressure Glow Discharges, R.A. GOTTSCHO, A. MITCHELL, and G.R. SCHELLER, AT&T Bell Laboratories, D.B. GRAVES, University of California, Berkeley, and J.-P. BOEUF, Université Paul Sabatier - Local field and ballistic electron models for dc and rf glow discharges are tested by comparing calculated current-voltage characteristics, ion densities, emission intensities, electric fields, and electric field reversals with experiment. In general, the local field model, that assumes transport and rate coefficients are completely specified by the electric field to gas density ratio, is in poor agreement with results obtained from low-frequency and dc glows. This is because of large field and density gradients in the sheath. A single-beam electron model that treats electrons created by secondary emission processes at the cathode as a separate group is in better agreement with experiment. But discrepancies remain because momentum randomization and energy spreading of the beam has been neglected. The beam model appears to offer a useful compromise between complexity and accuracy in modeling glow discharge processes.

E-5 Numerical Simulation of 13.56 MHz Symmetric Parallel Plate RF Glow Discharges in Argon, A.P. PARANJPE, J.P. McVITTIE and S.A. SELF, Stanford University - A fast and numerically stable technique based on the systematic decoupling of the equations has been developed. First the time-averaged equations of continuity (i.e. particle and momentum conservation) for charged particles together with Poisson's equation are solved for an assumed ionization rate profile across the discharge. This is followed by a time-dependent solution of the continuity and Poisson's equations for a specified RF discharge current. Finally an electron energy balance equation is solved for the calculated power deposition density to compute the electron energy and hence the ionization rate. Rate coefficients (for electron-impact processes) used in the electron energy balance are obtained by solving the Boltzmann equation in conjunction with a four level collisional-radiative model for argon. The calculated ionization rate is used to revise the previous estimate, and the whole procedure is repeated until satisfactory convergence is achieved. Calculated spatial emission profiles agree qualitatively with experiment.

A typical case executes in 6 minutes on a Micro Vax II, and in a minute for a simplified formulation which predicts the charged particle concentrations and total generation rates to within 10% of the exact solution.

E-6 A Numerical and Experimental Study of an Argon DC and RF Negative Glow,* M. SURENDRA and D. B. GRAVES, University of California, Berkeley - The numerical model combines a multibeam approach for fast electrons together with a continuum description for ions and slow electrons. The multibeam method, which allows for a fairly detailed description of the nonequilibrium cathode fall region, is used to obtain the inelastic rates. The generation rates are used in the continuum model (species conservation for slow electrons and ions, Poisson's equation for a self-consistent electric field). The model predictions show qualitative agreement with experimental measurements over a range of conditions. A comparison between the multibeam method and a computationally simpler single-beam approach is also presented.

*Work supported in part by San Diego Supercomputer Center.

E-7 Modeling of Volume H^- Ion Sources, M. BACAL, P. BERLEMONT, J. BRETAGNE, M. CAPITELLI, C. GORSE and D. A. SKINNER, Ecole Polytechnique, Universite de Paris Sud (France) and Universita di Bari (Italy).-- We applied a recently developed code[1] for modeling the driver section of a tandem volume H- ion source, with the purpose of identifying the reason for the observed saturation at high discharge current. It is currently assumed that dissociative electron attachment to highly vibrationally excited molecules is the main formation mechanism for hydrogen negative ions. We found that the reason for saturation was the reduction of the density of hydrogen molecules as a result of dissociation. It was also found that ionization in electron collisions was the principal destruction process of the vibrationally excited molecules.

[1]C. Gorse et al, Chem. Phys., 117, 177 (1987)

E-8 Analysis of the Radial Charged Particle Fluxes in the Positive Column, D. W. ERNIE and H. J. OSKAM, Univ. of Minnesota and A. METZE, Honeywell Systems and Research Center, Minneapolis, MN -- The model previously developed for the positive column of a direct current gaseous discharge produced in a monatomic electropositive gas has been used for a detailed analysis of the radial charged particle fluxes. The purpose of the study was to obtain more information about the relative contributions to the radial charged particle flow by the density gradient (diffusion), the radial electric field and the charged particle inertia. The results show that the relative importance of the three components of the radial charged particle flux depends on the type of charged particle, the gas pressure and the discharge tube radius. The data relate to a discharge produced in helium with a positive ion density at the axis equal to 10^{10} cm^{-3} and for products of the gas pressure and the tube radius of 5 Torr cm and 0.5 Torr cm.

E-9 A Framework for Modeling the Cathode Fall Illustrated with a Single Beam Model.* T.J.SOMMERER, J.E.LAWLER, and W.N.G. HITCHON. U. of Wisconsin.—A framework for a model of the cathode fall region of a DC glow discharge is presented, and a simple model is solved as an illustration. An extremum condition independent of the model is placed on the electric field behavior to produce a unique solution that agrees with experiment. The zeroth and second moments of the Boltzmann equation are solved for the electrons with a self-consistent electric field. A single beam model with only two parameters (number density and beam velocity) is assumed for the electron distribution function. Ion motion is modeled with a parametric fit to experimentally known ion mobilities. The model is solved for conditions corresponding to the experimental results and Monte Carlo simulations of Doughty, *et al.*[1] and Den Hartog, *et al.*[2] The results are in good qualitative and "factor-of-two" quantitative agreement with the published results.

* Supported by the AFOSR.

[1] D. A. Doughty, E. A. Den Hartog, and J. E. Lawler, Phys. Rev. Lett. **58**, 2668 (1987); D. A. Doughty, Ph.D. thesis, University of Wisconsin.

[2] E. A. Den Hartog, D. A. Doughty, and J. E. Lawler, to be published in Phys. Rev. A.

E-10 Theory of the Cathode Sheath in a Vacuum Arc, K.-U. RIEMANN, Ruhr-Universität Bochum, FRG. — We consider the plasma-sheath-transition of a partially ionized plasma in front of a negative wall. A previous theory of the boundary layer of a collision dominated plasma [1] is extended to account for ionization and recombination and applied to the plasma ball in front of an arc cathode spot. We find an essential potential and density drop from the plasma ball to the sheath edge. This potential drop is accounted for in a unified theory of the arc cathode which starts from Ecker's existence diagram method [2] and indicates possible areas of arc spot operation in the T_c-j-plane (T_c = spot temperature, j = spot current density). We evaluate the theory for the case of a Cu-metal vapor arc and discuss the difference to Ecker's results.

[1] K.-U. Riemann, Phys. Fluids 24, 2163 (1981).
[2] G. Ecker in: J.M. Lafferty (Ed.) Vacuum Arcs - Theory and Application, Wiley, New York 1980.

E-11 Plasma Parameters in Low Pressure Ar-Hg Discharge Used for a Fluorescent Lamp, T.ARAI, Kanagawa Inst. of Tech., T. GOTO, Nagoya U., and S. MURAYAMA, Cen. Res. Lab., Hitachi Ltd., --The purpose of this work is the detamination of plasma parameters in the Ar-Hg discharge used for the efficient fluorescent lamp of the small diameter. The fluorescent lamp of a smaller diameter below 15mm has recently been developed as a more efficient and compact light source for illumination and its importance is increasing. In order to clarify the excitation mechanism in the smaller bore lamp, quantitatively, various parameters must be measured directly. The tube used is 12mm in bore diameter and the Ar filling pressure is 3Torr. The electron temperature and electron density were measured with the single probe methode in discharge current 100-400mA and wall temperature region 0-80°C. Also the electron density was measured with the modified double probe method used the continuity relation of the discharge current. The result was similar to that by the single probe method.

E-12 Transient Analysis of Glow Discharges in Nitrogen,* S. K. DHALI, Southern Illinois University -- The growth of the discharge current, reduced field (E/N), vibrational population (VP), excited-state population, nitrogen atom population, i-v characteristics and energy partitioning in a pulsed nitrogen discharge is simulated using a self-consistent calculation of the electron distribution function (EDF) and the vibrational population (VP). The model developed includes diffusion losses to the wall and the external circuit parameters. The results discussed are for pressures of 1 - 100 Torr, discharge currents in the range of 10^{-3} - 5.0 A, and reduced field (E/N) in the range of 150 - 250 Td. For a typical discharge in a tube of 2 cm diameter and a current of few amperes, the energy stored in the vibrational manifold saturates after few milliseconds from the initiation of the discharge.

*Research supported by AFOSS, Bolling AFB, DC.

E-13 *In Situ* Monitoring of Plasma Processes Using Advanced Diode Laser Diagnostics,* H.M. ANDERSON, University of New Mexico, and A.C. STANTON and J.A. SILVER, Southwest Sciences, Inc.--Tunable diode laser absorption spectroscopy has broad capability for detection of most gas phase species, and thus has potential applications in monitoring of low pressure plasma processes used in microelectronics fabrication. The major impediment to using this method as a process diagnostic has been that the sensitivity of usual low frequency detection methods is inadequate for measurement of important reactive plasma species. This limitation could only be overcome by resorting to multiple pass optics internal to the plasma reactor. We have obtained significant improvements in detection sensitivity using high frequency FM spectroscopy with new single-mode double heterostructure diode lasers. This technique is capable of measuring optical absorbance of 10^{-6} or lower, corresponding to species concentrations in the range of 10^{9} to 10^{11} cm^{-3} for a 10 cm absorption path length. We describe the results of preliminary experiments to measure CF_4 dissociation and reactive intermediates in a dc discharge and discuss the application of this method to *in situ* measurements in boron halide rf discharges used in etching of aluminum.

*Supported by the National Science Foundation under Grant No. ISI-8661031.

E-14 Plasma Diagnostics Using PLIF and Wavelength Modulation Spectroscopy* D.S. BAER, A.Y. CHANG, P.H. PAUL and R.K. HANSON, Mechanical Engineering Department, Stanford University -- Planar laser-induced fluorescence and wavelength modulation spectroscopy diagnostics are being developed for measurements in thermal plasmas. 2-dimensional imaging of NO in an air plasma is accomplished using a Raman-shifted tunable KrF laser to excite A-X (0,0) transitions at λ=225.2 nm. Broadband fluorescence is collected and imaged onto an intensified 2D CCD array. The experiments are performed in 50 kW (4 MHz) and 3 kW (27 MHz) atmospheric pressure inductively coupled plasma torches. Laser wavelength modulation spectroscopy is being used to monitor the fluorescence of Na and H in the 3 kW torch. An Ar^{+}-pumped cw ring dye laser is rapidly tuned across selected transitions of Na (λ=588.9 nm, 568.2 nm) and H (λ=656.3 nm). The technique discriminates against broadband interferences such as elastic scattering and plasma emission. Analysis of the spatially resolved profiles can yield Doppler temperatures and electron densities.

*Research supported by the Air Force Office of Scientific Research.

E-15 Laser Diagnostic Density Measurements of $Hg(6^3P_{0,1,2})$ in a Narrow-diameter Hg-Ar Discharge, L. BIGIO and J.T. DAKIN General Electric R&D Center - Two laser techniques are used to measure absolute and radial density distributions of mercury atoms in the three (6^3P_J) states populated in the positive column of a narrow (13.7 mm diameter) low-pressure Hg-Ar dc discharge. Relative densities are obtained as a function of radial position using a saturated laser absorption technique,[1] while on-axis absolute densities are measured uing the hook method (an interferometric technique).[2] Results are shown for two mercury vapor pressures (6.4 and 13.3 mTorr) at a discharge current of 270 mA and argon pressure of 3.0 Torr. These results are compared with recent computer model predictions and show good agreement.

[1] L. Bigio, J. Appl. Phys. 63, 5259 (1988).
[2] W.C. Marlow, Appl. Opt. 6, 1715 (1967).

E-16 The Effects of Low Level (≪0.1%) Hydrocarbons on Helium Atomic (2^3S) and Molecular ($^3\Sigma$) Metastables in a Long-Pulsed Electron-Beam Discharge, by L. W. Downes, S. D. Marcum and W. E. Wells -- Miami University, Oxford, Ohio. -- We are investigating the effects of low concentrations of CH on helium atomic and molecular metastable densities in high-pressure, electron-beam-generated plasmas. These studies are derived from earlier research that showed the CH(A→X) at 431.2 nm to be a major emission in the afterglow, despite having a concentration less than 1 part in 10^8. We find that the CH(B→X) at 388.9 nm is also a major source of afterglow emission. The electron temperatures and densities for a long-pulsed, electron-beam-generated helium plasmas will also be reported for a range of pressures (25-2500 Torr).

E-17 On the Importance of Vibrational and Electronic Metastable States on the Relaxation of Electron Energy Distribution Function of He-N_2 Afterglow, G. DILECCE, C. GORSE, S. DEBENEDICTIS and M. CAPITELLI, Centro Studio Chimica Plasmi (CNR), University of Bari - Italy -- The importance of excited states in affecting the electron energy distribution function (EDF) of He-N_2 (99.5:0.5) mixture in afterglow plasmas has been studied from both theoretical and experimental points of view. Theoretically we have solved selfconsistently the Boltzmann equation for EDF coupled to plasmachemistry and to the kinetics of excited states, while experimentally we have measured EDF through the second derivative of Langmuir I/V characteristics. A satis_ factory agreement has been found between experimental and theoretical values, both of them emphasizing the importance of excited states in increasing the lifetime of EDF in the post discharge conditions. In particular He(^3S) and $N_2(A\,^3\Sigma_u^+)$ excited states take an important role in affecting EDF relaxation.

E-18 Stokes Parameters and Absolute Phase Angles for the $3\,^1D$ State of Helium,* E. J. MANSKY, Georgia Institute of Technology - The multichannel eikonal theory results for the Stokes parameters for the $3\,^1D$ state of helium are examined. A detailed examination of the Stokes parameters P_1, P_2, P_3 and P_4 in both the collision-frame and natural-frame provides a clear picture of the effect couplings between the n=2 and n=3 states of helium have on the final state probabilities and the polarization properties of the emitted radiation. Comparing the systematic trends in the Stokes parameters with the behavior of the absolute phase angles of the scattering amplitudes for the $3\,^1D_m$ magnetic substates of helium then yields information about the dynamics of the charge cloud of the $3\,^1D$ state of helium during the scattering event.

*Research supported by U. S. Air Force Office of Scientific Research under Grant No1 AFOSR-84-0233.

E-19 Measurement and Modeling of Atomic Chlorine Concentrations in Plasma Processes, J.P. NICOLAI, and H.H. SAWIN, Massachusetts Institute of Technology, and K.D. ALLEN, Honeywell SSED -- We have used the two-photon laser induced fluorescence technique to detect ground-state chlorine atoms and obtain spatially resolved concentration profiles of ground state chlorine atoms in CF_3Cl/Ar and Cl_2/Ar RF plasmas. A significant Cl gradient was found between the two electrodes under conditions typical for polysilicon etching. This experimental observation compares favorably with previous model predictions[1] which assumed the primary loss of Cl in polysilicon etching was a second-order surface recombination on the opposing stainless steel electrode which was partially limited by gaseous diffusion. The observation of significant Cl gradients is dependent upon process conditions and electrode material, e.g. electrodes of stainless steel were found to be good catalysts for recombination and induced Cl gradients, but Si and SiO_2 are poor recombination surfaces.

[1]K.D. Allen, H.H. Sawin, M.T. Mocella, M.W. Jenkins, J. Electrochem. Soc. 133, 2315 (1986).

E-20 Plasma Injection Through RF Multipoles to a Fourier Transform Mass Spectrometer, J.L. Shohet, Center for Plasma Processing and Technology, University of Wisconsin-Madison* -- Fourier Transform Mass Spectrometry[1] (FTMS) is a mass analysis technique capable of ultrahigh resolution and operates in a dc magnetic field which makes it particularly well suited for processing plasmas. For analysis, it is required that ions must be injected in the analysis cell so that they are not reflected in the fringe solenoid fields. Ion injection methods are direct coupling, acceleration and deceleration, and rf multipoles. Plasma injection has been done via direct coupling. In this work we inject plasma into an FTMS cell via rf multipole guides. The multipole fields dominate the magnetic field in the fringing field regions, while in the central field region, the magnetic field dominates the particle motions. As a result, injection without acceleration is feasible.

1 M.B. Comisarow, Adv. Mass. Spec., 7, 1042(1978).

* Work supported in part by the Wisconsin Plasma Processing and Technology Research Consortium.

E-21 Relative Abundance of Ions in CH_4-H_2 Discharge Plasma. R. E. MIERS, L. W. ANDERSON, J. E. LAWLER, CHUN C. LIN, and R. B. LOCKWOOD, U. of Wisconsin-Madison.— There are many potential applications of the diamond or diamondlike carbon films produced using CH_4-H_2 discharge plasmas. It is therefore timely to study the quantitative properties of these discharge plasmas. We report mass spectrometry of both the positive and negative ions formed in a duoplasmatron ion source using CH_4-H_2 input gas. The identification of positive and negative ions is important for the identification of the various molecular and ionic species present in the plasma. Negative ions are also important because negative ion formation can change the electron concentration in the plasma dramatically. We have studied discharges run at a total pressure of 200 - 300 mTorr containing 2% and 100% CH_4. We observe H^+, H_2^+, H_3^+, and positive ions of the form $C_nH_m^+$ where n = 1 - 9, and we observe H^- and negative ions of the form $C_nH_m^-$ where n = 1 - 6. The ions $C_nH_m^+$ decrease in abundance as n increases. The most abundant negative ions are $C_2H_m^-$ with the second most abundant ions being CH_m^-.

E-22 Langmuir Probe Measurements in RF Discharges. W. G. GRAHAM, C. A. ANDERSON, Physics Department, University of Ulster, Coleraine, N. Ireland, and M. B. HOPKINS, Physics Department, N.I.H.E., Dublin 9, Ireland. - The use of Langmuir probes to obtain reliable plasma parameter measurements in rf driven discharges is difficult due to the effects of rf fluctuations on the local plasma-probe potential. The time-resolved techniques used at the University of Ulster allows the effect of rf fluctuations on the plasma-probe potential to be eliminated.

Time resolved plasma parameters, including the electron energy distribution function, measured in low frequency, less than 500 kHz, rf driven discharges will be presented. The electron distribution function can be highly non-Maxwellian and can be strongly influenced by atomic collision processes. The measured thermal electron temperatures are found to be lower than those previously reported in similar discharges.

E-23 Langmuir Probe Diagnostics in RF Plasmas, Critical Review, V. A. GODYAK, GTE Products Corporation, Danvers, MA -- Properly used, the Langmuir probe is a powerful tool for diagnostics of low temperature plasmas at low pressures. A specific problem arising from its application in rf discharges is the distortion of probe characteristics which can yield improper conclusions concerning plasma parameters. A comparative analysis of several well known approaches to probe measurements in capacitive rf discharges is presented. It is shown that the majority of these approaches either ignore the effects of the nonlinear interaction of the rf field with the probe and/or with the rf electrode sheaths, or are based on a model which is too simplistic. Typical rf distortions found in probe characteristics are considered for single probes and double probes, as well as for electron energy distribution measurements. It is shown that the shape of the second derivative of the probe characteristics can be an indicator of rf distortion on the probe measurement and thus can itself be used in adjusting the probe circuit as to minimize the rf distortion.

E-24 Automatic Emission Spectroscopic Diagnostics for Induction Plasma Processing,* J. Vattulainen and R. Hernberg, Tampere U. of Technology, Finland --A fully automated diagnostic system has been designed and tested at a 60 kW, 1.76 MHz induction plasma unit. The system is used for measuring the intensities and widths of emission lines and continuum intensities. Light is collected by means of a specially designed collimator, and transferred by fiber optics. The collimator is mounted on a stepper-motor driven 2-dimensional translation stage allowing for rapid scanning of the plasma with a lateral accuracy of 0.01 mm. Single or array detectors can be used. Wavelength selection and collimator movement are controlled by a PC/AT through a multiple-processor arrangement. Data processing and printout is also done by the same PC. The software includes an Abel inversion routine. The measurement of the temperature distribution in one plane for a 70 mm diameter plasma with 0.5 mm step length takes about 1 minute.

E-25 Study of Soft Vacuum Electron BEam Generation in a He-O2 Discharge Using Laser Opto-Galvanic Spectroscopy. S. MORIYA*, P. Zeller*, Z. Yu, G. J. Collins, Colorado State University - Electron Beam generation in soft vacuum using an abnormal glow discharge has been well documented. [1] The oxide layer in-situ on the aluminum cathode plays an important role in emitting secondary electrons and is also highly resistant to sputtering. The cathode electron field and its spatial variation has been explored in the He-O2 discharge using the LOGS method. [2,3] Varying optogalvanic signals show that the oxide layer contributes strongly to the secondary electron emission from the cathode surface.

[1] R.A. Dugdale, J. Materials Science, 10, 896, (1974).
[2] D.K. Doughty and J.E. Lawler, Appl. Phys. Lett. 45, 611 (1984).
[3] S. Moriya, P. Zeller, G.J. Collins, 40th GEC, Atlanta, GA (1987).
*Present address: Kawasaki Steel Corp. JAPAN
*Present address: University Paris-sud, FRANCE

E-26 Modelling of Silent Discharges with Excimer–Gas Filling** H.MÜLLER, M.NEIGER, LTI University of Karlsruhe FRG —The plasma of high pressure glow discharges and silent discharges is an excellent source for incoherent, spectral selectiv excimer radiation. In addition to experiments, we examine silent discharges theoretically, using a reaction kinetic model, to get a better understanding of the microscopic production mechanisms of the radiation in order to optimize operation conditions. So far we examined Ar,Ne,-Xe,HCl mixtures for building the excimer XeCl*. In these plasmas the heavy particles are not in thermal equilibrium with electrons, but because of the short duration of each pulse, they stay near a temperature of 300 K. To model the plasma, we made an approximation of the electron distribution function and solved energy, momentum and particle balance equations using different measured or theoretically determined cross section data sets. The equations for the driving electric circuit were solved simultaneously with the plasma equations. By numerical integration we solved for particle densities, average electron energy as well as for observable macroscopic quantities as voltages and currents in the external circuit and the radiation as a function of time.
** Supported by the German Ministry of R&D (BMFT)

E-27 Analysis of the reaction $He(2^3S)+2He \rightarrow He_2(a^3\Sigma)+He$
J.STEVEFELT, GREMI, U. of Orléans, France. Recent experimental work[1] has suggested that highly vibrationally excited molecules play an important role in the high pressure kinetics of metastables. In the formation of $He_2(a^3\Sigma)$ molecules, the initial capture involves tunneling through a barrier of the order of 500 cm^{-1}, and subsequent vibrational relaxation may control the overall rate at which the product $He_2(v=0)$ appears. A classical trajectory method is employed to calculate the rate of vibrational and rotational transfer, and a phenomenology is predicted that largely agrees with measured three-body rates, [2,3] choosing reasonable values for the parameters describing collisions with the background gas.

1. J.M. Pouvesle, A. Khacef, J. Stevefelt, H. Jahani, V.T. Gylys, and C.B. Collins, J. Chem. Phys., 88, 3061 (1988).
2. K.H. Ludlum, L.P. Larson and J.M. Coffrey, Jr., J. Chem. Phys., 46, 127 (1967).
3. C.B. Collins and F.W. Lee, J. Chem. Phys., 70, 1275 (1979).

E-28 Collisional Detachment Cross Sections for SF_6^-, SF_5^-, and F^- on SF_6 and Rare Gas Targets,*
YICHENG WANG, R.L. CHAMPION, L.D. DOVERSPIKE, College of William and Mary, J.K. OLTHOFF, R.J. VAN BRUNT, National Bureau of Standards--Absolute collisional electron-detachment cross sections for SF_6^-, SF_5^-, and F^- on SF_6 and rare gas targets have been measured for relative (center-of-mass) energies in the range of 3 to 250 eV. Apparent onsets for direct detachment are observed at 90 eV, 90 eV, and 8 eV, respectively for SF_6^-, SF_5^-, and F^- on SF_6. Lower detachment thresholds are observed for rare gas targets. Cross sections for ion conversion and charge transfer reactions are also reported. The experimental results are compared with the predictions of a collisional model where the unimolecular decomposition of excited SF_6^- ions is described in a statistical framework.

*Research supported, in part, by the U.S. Department of Energy.

E-29 Dissociative Charge Transfer Reactions of Atmospheric Ions with Dimethyl-methylphosphonate.*, R. Johnsen, B.K. Chatterjee, and R. Tosh., University of Pittsburgh--
We have measured rate coefficients and production branching ratios for the dissociative charge-transfer reactions of atomic and molecular oxygen and nitrogen ions with Dimethyl-methylphosphonate (DMMP), i.e. the reactions

$$A^+ + (CH_3O)_2CH_3PO \longrightarrow PO_2(CH_3)_3^+ + (CH_3)_n$$

where n=0,1,2,3; $A^+ = O^+, O_2^+, N^+, N_2^+$,
in the ion energy (CM) range from 0.04 to 1 eV using a selected ion drift tube. We find that these reactions are fast (total rate coefficients $\approx$ 1(-9) cm^3/sec, independent of ion energy). Product ion distributions, however, were found to vary strongly with energy.
*Work supported in part by Air Force Wright Aeronautical Laboratories.

E-30 $\mathscr{L}^2$ Quantum Mechanical Variational Solution of the Schroedinger Equation for Chemical Reactions* M. ZHAO, P. HALVICK, M. MLADENOVIC, D. CHATFIELD, and D. G. TRUHLAR, Minnesota Supercomputer Institute, University of Minnesota, D. W. SCHWENKE, Eloret Institute, Y. SUN, C.–H. YU, and D. J. KOURI, University of Houston, and C. DUNECZKY and R. E. WYATT, University of Texas — The Schrödinger equation describing a chemical reaction is converted to coupled integral equations for reactive amplitude density components and is solved by expanding the solutions in a square–integrable ($\mathscr{L}^2$) basis set. The coefficients are found by a variational prescription, and the resulting linear equations are solved variationally by direct or iterative (minimal residual, Lanczos) methods. The method has been applied successfully to $H + H_2$, $D + H_2$, $O + H_2$, $H + HBr$, $Cl + H_2$, and $F + H_2$, and we will present some results for the branching ratio $O + HD \rightarrow OH + D$ or $OD + H$.

*Work supported by the Minnesota Supercomputer Institute, University of Minnesota Graduate School, National Science Foundation, the Petroleum Research Fund of the American Chemical Society, Cray Research, Inc., and the Robert A. Welch Foundation.

E-31 A New Potential Energy Surface for the F + H_2 Reaction.* G. LYNCH, A. J. C. VARANDAS, and D. G. TRUHLAR, Minnesota Supercomputer Institute, University of Minnesota and B. C. GARRETT, Chemical Dynamics Corporation — We will present a new potential energy surface for the reaction F + H_2 → HF + H based on *ab initio* calculations employing the method of scaled external correlation and a double many–body expansion to include the long–range forces. The calibration of the surface is based on variational transition state theory with bend–rotation coupling.

*Work supported by the Minnesota Supercomputer Institute, the Chemical Sciences and Engineering Fund of the Council for Chemical Research, and the U.S. Department of Energy, Office of Basic Energy Sciences.

E-32 Measurement of Plasma Sheath Potential Profiles in the Presence of High Frequency RF , M.H. CHO, N. HERSHKOWITZ, and T. INTRATOR:University of Wisconsin -Madison--Characteristics of plasma sheaths in the presence of high frequency rf have been measured using a parallel plate plasma capacitor placed in a multi-dipole plasma device. Argon plasma is produced by a hot-filament discharge, and the typical plasma parameters are $P \sim 1 \times 10^{-4}$ torr, $n_e \sim 1 \times 10^{9} cm^{-3}$, and $T_e \sim 3eV$. The plasma potentials in sheaths and bulk plasmas are measured using emissive probes. It is observed that a potential dip occurs in the sheath of an electrode to which an rf is applied, and the overall structure of potential profiles show close resemblance for the rf frequencies below or above the ion plasma frequency. It is also observed from the 2-d potential measurement that rf sheaths have 2-dimensional characteristics. The experimental results and the detailed potential diagnostic techniques are presented.

*Work supported in part by NASA Grant No. NAGW-905 and NSF Grant No. ECS-8704529

E-33 Measurement and Analysis of RF Glow Discharge Electrical Impedance, J.W. BUTTERBAUGH, L.D. BASTON, and H.H. SAWIN, Massachusetts Institute of Technology - Impedance measurement of RF glow discharges is a convenient diagnostic tool and can be used to estimate specific discharge properties based on a simple electrical analog model. Accurate measurements require minimization and characterization of stray impedances. Minimization of stray impedances is accomplished by using a triaxial power feed and electrode shield configuration. Characterization is accomplished by "unterminating" the reactor system network[1] which involves measuring the impedance of the reactor system with at least three known impedances inserted between the electrodes. The discharge impedance can then be determined from the reactor system impedance measured during discharge operation. This method of stray impedance correction can be easily applied to commercial reactors and avoids the inaccuracies inherent in estimating the stray impedance of a distributed network.

[1]R.F. Bauer and P. Penfield, IEEE Trans. MTT-22(3), 282(1974).

E-34 Temporal and Spatial Plasma Potential Measurement in Parallel Plate RF Glow Discharge*, CHEOL-HEE NAM**, N. HERSHKOWITZ, M.H. CHO, and J. DeKOCK: University of Wisconsin-Madison--Space and time resolved plasma potential profiles are measured in a parallel plate (10cm dia. SS-discs) rf glow discharge system using Langmuir probes and high impedance capacitive probes.[1] The system is equipped with the active control devices capable of maintaining constant flow of gases and constant neutral pressure. The system is normally operated with conditions of $\leq$50 W rf load power, ~100 kHz rf frequency, and ~100 mTorr neutral gas pressure with a choice of working gases (Ar, O_2, and C_3H_6), and it produces typical plasma parameters of $n_e \sim 1 \times 10^9 cm^{-3}$ and $T_e \sim$ 5eV for argon gas. The detailed diagnostic techniques and the experimental results are presented.

*Work supported in part by NSF Grant No. ECS-8704529

**In memory of his untimely death by tragic a accident

[1]N. Hershkowitz, M.H. Cho, C.H. Nam, and T. Intrator, Plasma Chem. & Plasma Process. 8, 35 (1988)

E-35 Emission Spectroscopy of Microwave Discharges in Air*, M. PASSOW AND M. BRAKE, University of Michigan -- The interaction of microwave radiation and the atmosphere has been studied spectroscopically (180 - 800 nm) using a cw microwave discharge in air at 2.45 GHz. We have investigated the radiation signatures from microwave discharges in low pressure air (0.1 - 100 Torr) with input power levels ranging from 30 to 300 W. The discharges are produced in one of two quartz tubes (23 mm and 4 mm ID) placed along the axis of an Asmussen resonant cavity excited in the TM_{012} mode. The majority of the intense emission is due to N_2 (Second Positive system) and NO (γ system) as well as lines due to atomic hydrogen. Weak lines due to O_2^+ and N_2^+ also are observed. A broadband continuum peaking at 600 nm is observed and is believed to be due to the recombination of NO + O. This continuum is observed outside the microwave cavity as well and is quite long-lived. The effects of pressure and absorbed power on the emission will be discussed.

*Supported by SDIO-IST

E-36 Measurements and Modelling of the Radial Current Distribution in a Planar Magnetron, A. E. WENDT AND M. A. LIEBERMAN, U. C. Berkeley— We will present results from our investigation of a DC planar magnetron sputtering system. The discharge is operated in argon between parallel 9" D copper electrodes, and a variable magnetic field is provided by an iron core electromagnet. Our studies have focused on the spatial structure of the plasma discharge and the dependence of the structure on external parameters. The radial distribution of current at the cathode has been measured with a radially separated array of 1 mm current probes imbedded in the cathode plate. We have made measurements of the radial distribution for magnetic fields ranging from 171 to 855 G, discharge currents from less than 100 mA to greater than 1.5 A, and pressures from 5 to 50 mtorr. We have developed a model of the distribution of current at the cathode based on the Hamiltonian dynamics of energetic electrons which are released from the cathode through secondary electron emission and are responsible for the ionization which maintains the discharge. In this model the sheath is assumed to be thin compared to the axial extent of the electron motion, so that the electrons acquire an initial energy from the sheath but spend most of their time outside of the electric field. The data are consistent with this model for higher current cases, where the thin sheath assumption is expected to hold. For lower current cases, a modified theory which employs electron motion entirely within the sheath fits the data more accurately.

E-37 Plasma Properties of a Magnetized, Inductively Coupled Discharge for Thin Film Applications, K. R. STALDER, S. E. SAVAS and W. G. GRAHAM, SRI International--Increased use of plasmas for materials processing has prompted a need for a better understanding and control of plasma parameters. We have constructed an inductively coupled rf plasma with Helmholtz coils providing an axial magnetic field. The discharge is confined in a 5 cm diam. by 20 cm long quartz vessel and is excited by up to 500 watts of 13.56 MHz rf power coupled by an external multiturn coil. Electrical properties (from Langmuir probes and capacitive probes), optical properties (from time averaged and time resolved emission spectra) and external discharge parameters (rf voltage and current) are measured as a function of magnetic field strength, gas pressure and gas composition. For nitrogen plasmas there is a decrease in the on-axis electron density, a decrease in the N_2^+ (1st Neg.) and N_2 (2nd Pos.) emission strengths and an increase in the on-axis electron temperature with increasing magnetic field. Time dependent optical measurements shows a modulation in H_α emission in hydrogen plasmas.
*Work supported by IR&D funds from SRI International.

E-38 Time Dependent Theory of Molecular Photodissociation of H_3^+ KENNETH C. KULANDER and ANN E. OREL Lawrence Livermore National Laboratory,* --The photodissociation process, $H_3^+ + h\nu \rightarrow [(H_3^+)^*] \rightarrow 2H + H^+$, or $H_2 + H^+$ has been studied for a final state which includes two Born-Oppenheimer surfaces which intersect in the Franck-Condon region. A wave packet was propagated by numerical integration of the Schrödinger equation,[1] including the full coupling between the surfaces, into the asympotic region. The effects of variations of the coupling strength on the absorption profile and final state distributions were investigated.
[1]K. C. Kulander, J. Chem. Phys. 69 5064 (1978).
*Work performed under the auspices of the U. S. Department of Energy by the Lawrence Livermore National Laboratory under contract number W-7405-ENG-48.

E-39 Sputtering Apparatus using Modified High Voltage Hollow Cathode Discharge, T. SUMII, S. MASUDA and T. IIJIMA, Tokyo Voca. Train. College --The so-called high voltage hollow cathode discharge(HV-HCD)[1-2] having special anode system placed inside the cathode is available for ion production. The HV-HCD is considerably increased the ion concentration and resulted cathode sputtering. Further advantage is the high stability against arcing. This HV-HCD device was applied to the sputtering apparatus utilizing the deposition of solid thin film. The length of the cylindrical hollow cathode was 120mm and inner diameter(ID) 56.5mm. The anode pipe(ID 52.5mm) with eight openings 60mm long and 10mm wide was placed inside the cathode pipe. The distance between the anode and cathode walls was 1mm.

[1]K. Rózsa, Rep. Hungarian Academy of Sciences, Central Research Institute for Physics,No.63, (1975)

[2]K. Rózsa, Z. Naturforsch., 35a, 649 (1980)

E-40 Diamond-like Carbon (DLC) Film Deposition Using Parallel Plate RF Discharge, H. MISHURDA, M. H. CHO, N. HERSHKOWITZ, R. BREUN: U. of Wisconsin-Madison--The deposition of hard carbon (DLC) films on single crystal silicon substrates is studied using a parallel plate rf discharge. Typical deposition parameters are: 100 kHz, 100 W rf load power, and 100 mTorr neutral gas pressure of a mixture of methane and hydrogen. The resultant films are analyzed using X-ray diffraction, Auger electron spectroscopy, and microhardness tests. The characteristics of the films, especially the dependence on substrate temperature, are presented together with the detailed rf glow discharge conditions and the plasma parameters.

*Work supported by NSF Grant No. ECS-8704529

E-41 Transient responses of the steady state glow discharge to perturbations, Y.M. Li, GTE Laboratories Inc., Waltham, MA -- The transient and steady states of the glow discharge are simulated using one dimensional charged particle continuity equations, Poisson equation and circuit equations. The model equations are discretised spatially by exponentially weighted finite-differencing [1,2] and the resulting equations are integrated implicitly in time until steady state is reached. Two different perturbations are considered. A small sinusoidal voltage is added and the perturbed discharge currents, voltages, charged particle distributions and electric fields are studied as functions of the applied frequency. The glow discharge is resistive and inductive at lower frequencies and becomes capacitve at high frequencies. For the second type of perturbation, equal numbers of electrons and ions are introduced into the steady state discharge simulating the additional ionization produced by laser irradiation. The time-dependent perturbed currents and voltages (simulated optogalvanic signals) are examined and the relation between the two types of perturbations will be discussed.

[1]D.L. Scharfetter and H.K. Gummel, IEEE Trans. Electron. Devices, ED-16, 64 (1969).

[2]J.-P. Boeuf, Phys. Rev. A, 36, 2782 (1987).

E-42 **Soft X-ray Measurement of a Plasma Density Profile** , **B. BRILL, B. ARAD and M. KISHINEVSKI, Soreq NRC, ISRAEL** -- **The density profile of a dense plasma, emerging from a capillary discharge, was measured using the soft X-ray backlighting technique. Two dimensional time-resolved imaging of the plasma was achieved with a spatial resolution of 0.1 mm. A laser-produced plasma served as X-ray source. A maximum ion density of $2.5*10^{19}$ cm^{-3} was measured. A minimum in the radial density profile close to the capillary axis is observed. This minimum has been predicted by a theoretical model suggested by A. Loeb.**

SESSION FA

8:00 AM - 9:50 AM, Wednesday, October 19

Radisson Plaza Hotel - East Ballroom

MODELS AND DIAGNOSTICS OF LIGHTING DISCHARGES

Chairperson: H. Witting, General Electric-Corporate Research Division

FA-1 Progress and Prospects for Laser Diagnostics of Light Sources, R. DEVONSHIRE, Chemistry Department Sheffield University, Sheffield S3 7HF, UK - The paper will attempt to systematize past and present activity in the laser diagnostics of low and high pressure light sources and related systems. Laser techniques based on a wide range of linear and non-linear spectroscopies, and on simple refractive/diffractive effects, are being exploited to recover spatially and temporally resolved information on temperature, pressure, number density, electric field, fluid dynamics, transport properties, and surface effects. Improvements in the performance of laser systems themselves as well as developments in the techniques continue to create new opportunities. Amongst these are experiments of interest to the author in which short pulses are used to achieve spatial resolution.

FA-2 Electrodeless High Pressure Microwave Discharges*, S. OFFERMANNS, Philips Research Laboratories, Aachen, F.R.G. - A one-dimensional numerical model has been developed to solve Maxwell's equations together with the energy balance equation for a cylindrical high pressure Hg-plasma within a microwave cavity. In addition to the model of Parosa[1] for H_2 and N_2 a full description of Hg-radiation following Stormberg et al.[2] was taken into account. An experimental microwave circuit has been designed to observe the resonance behaviour of cavity plus discharge. A coupling efficiency >99% can always be achieved with proper adjustments. Variation of discharge parameters leads to different types of temperature distributions ranging from conventional arc profiles to strongly skin-broadened distributions with a local minimum in the axis. The temperature distributions predicted by the model are in good agreement with results from spectroscopic experiments.

* Research supported by BMFT

1 R. Parosa, Material Science Vol. VI, 4, pp. 161 (1980)

2 H.P. Stormberg and R. Schäfer, J. Appl. Phys. 54, 8 pp. 4338 (1983)

FA-3 *Fluid Dynamics of Enclosed High Pressure Discharges*, P.A. VICHARELLI *GTE Laboratories Incorporated, Waltham, MA* -- Results of computational experiments on the fluid dynamics of high pressure discharges enclosed in vessels of various axisymmetric shapes are presented. The discharge plasma is viewed as a viscous, compressible, laminar fluid in local thermodynamic equilibrium. The calculations are based on the numerical solution of the energy, momentum, and mass conservation equations for this fluid, coupled with the radiation transport and current continuity equations. In addition, heat transfer from the plasma to the enclosure has been included in the model by means of a fluid-solid energy balance. A finite element formulation of these equations allows the treatment of arbitrary discharge tube geometries. Through these calculations we can predict the behavior of convective circulation patterns and their effect on the plasma and discharge-tube temperature distributions. Results for vertically oriented Hg arcs simulated at several pressures, power loadings, and arc tube shapes will be presented.

FA-4 Anatomy of a 400 Watt High Pressure Mercury Discharge with Metal Halide Additives, J.T. Dakin and T.H. Rautenberg Jr., GE Corporate R&D -- Experimental diagnostics and computer model calculations are used to develop a self consistent picture of the complex physics and chemistry occurring in a vertical high pressure Hg discharge with NaI and ScI_3 additives. The 400 W arc tube with 43 mm arc gap, 20 mm^3 bore and 5 atm pressure is used since its large size and commercial availability make it a convenient benchmark for scientific investigation. Experimental diagnostics emphasize Abel inversion of emission data from optically thin spectral lines. The model assumes local thermodynamic equilibrium, and includes convection. Results emphasize temperatures, pressures, chemical compositions, convective velocities and radiative spectra, all as a function of location in both the condensed and gaseous phases. These results are linked to key results of previous investigators as appropriate.

SESSION FB

8:00 AM - 9:55 AM, Wednesday, October 19

Radisson Plaza Hotel - West Ballroom

ELECTRON COLLISIONS, INCLUDING EXCITED STATES

Chairperson: C. C. Lin, University of Wisconsin

FB-1 Multichannel Eikonal Theory of Electron-(Excited) Atom Collisions,* M. R. FLANNERY, Georgia Tech - The Multichannel Eikonal Treatment (MET) is successful not only for the calculation of integral and differential cross sections for e-H(1s) and e-He(1^1S) inelastic collisions to the n=2 and n=3 levels at intermediate and higher impact energies $E \geq 25$ eV but also for various orientation and alignment parameters. It is particularly suited to e-excited atom collisions where the scattering is mainly about the forward direction $\theta \lesssim 40^o$ and where long range interactions are extremely important. MET provides an efficient method of including many internal quantum levels of the target atom within an eikonal treatment for the relative motion which is rapidly convergent in impact-parameter space. Integral and differential cross sections for e-H(2s) and e-He($2^{1,3}S$) collisions are presented and difficulties with implementation of the standard quantal close-coupling method are discussed.

*Research supported by AFOSR grant No. AFOSR-84-0233.

FB-2 Review of Total Electron Impact Cross Section Measurements.* R. A. BONHAM, Department of Chemistry, Indiana University, Bloomington, IN 47405 - Existing experimental data sets for absolute total electron impact cross sections will be reviewed and standard cross sections will be suggested for gases where three or more laboratories have presented results which are in agreement. Such reliable cross section data sets should prove valuable for both plasma modelers and experimentalists interested in checking the reliability of complete cross section data sets of the type needed to model low temperature plasmas. Reliable absolute total electron impact cross section data sets are proposed for the species He, H_2, CH_4, SF_6 and Ne. In addition absolute cross section data exist for many other species and a number of these sets may also be reliable although corroboration by a sufficient number of other laboratories is not yet available.

* Work supported by the National Science Foundation through grant number CHE-8600746.

FB-3 The Importance of Indirect Processes in Electron-Impact Ionization of Ions, D. C. GREGORY, ORNL* -- A number of processes may contribute to the total cross section for ionization of ions by electron impact. In addition to direct electron removal, excitation or ionization of inner-subshell target electrons can contribute to or even dominate the total ionization cross section. Measurements and accurate calculations of ionization cross sections are now available over a wide range of charge states for a number of isoelectronic and isonuclear sequences. Examples will be presented to illustrate a number of indirect ionization processes and the systematics of their importance to single and multiple ionization.

*Operated by Martin Marietta Energy Systems, Inc., under contract DE-AC05-84OR21400 with the U.S. Department of Energy.

FB-4 Low-Energy Electron Collisions with Excited Molecular Nitrogen W. M. HUO, NASA Ames Research Center, – The collision of low-energy electrons with valence excited states of N_2, the $B^3\Pi_g$, $A^3\Sigma_u^+$, $W^3\Delta_u$, $C^3\Pi_u$, $a^1\Pi_g$, $a'^3\Sigma_u^-$, and $w^1\Delta_u$ states, has been studied using the Schwinger multichannel method. The AMES SMC code has been extended to treat the collision of unpolarized electrons with target states of high spin multiplicity. Resonances are found in both the elastic and inelastic channels. Also, the excitation cross sections from one electronic excited state to another can be as much as a factor of 50 larger than the ground to excited state cross sections. The size of these cross sections makes stepwise excitations probable in low-energy plasmas.

FB-5 Absolute Angular Distributions of Elastic Scattering Cross Sections of Atomic Hydrogen by Electron Impact*- T. W. SHYN and S. Y. CHO, Space Physics Research Laboratory, University of Michigan, Ann Arbor, MI 48109.- We have measured absolute differential elastic cross sections of atomic hydrogen by electron impact. A modulated crossed-beam method was used. The energy and angular range covered were from 5.0 to 40 eV and from 12 to 156°, respectively. The present results agree with those of J. F. Williams (J. Phys. B8, 1683,1975) below 7 eV within the experimental uncertainty, however, our results show stronger backward scatterings than those of J. F. Williams (J. Phys. B8, 2191, 1975) by more than a factor of 2 above 10 eV. The integrated and momentum cross sections will also be presented.

* Supported by National Science Foundation
Phy-8700430

FB-6 Electron-Atom Scattering Cross Sections: Progress on OI and Other Species,* J.P. DOERING, Dept. of Chemistry, Johns Hopkins U. --Work on atomic oxygen electron scattering cross sections has been completed for all the major transitions. The results will be reviewed with particular emphasis on recent results down to 4 eV impact energy for the ^1D and ^1S state excitations as well as work on the ^5S state. Preliminary work on NI and prospects for measurements on CI and SI as well as other species of interest to aeronomy and astrophysics will be discussed.

*Work supported by Grant ATM-8605992 from the National Science Foundation.

SESSION GA

10:10 AM - 12:05 PM, Wednesday, October 19

Radisson Plaza Hotel - East Ballroom

LASERS

Chairperson: J. G. Eden, University of Illinois

GA-1 Election Drift Velocity Measurement in Hydrogen Azide (HN_3) Gas Mixtures, C. A. DENMANN and L. A. SCHLIE, Advanced Laser Techology Division (AFWL/ARBI), Air Force Weapons Laboratory, Kirtland AFB, N. M. 87117-6008. - For the first time, time of flight (TOF) drift velocity (V_d) measurements have been obtained in hydrogen azide (HN_3) gas mixtures. This highly energetic azide gas is of interest because its molecular kinetics indicates it has much potential for future visible/ultraviolet laser systems. Equally important are the electron kinetics for any potential type of electrically "driven" laser system. From the V_d data, initial estimates of the elastic scattering cross sections of HN_3 are inferred. Drift velocity information plus longitudinal diffusion coefficient data were acquired using a conventional TOF drift velocity apparatus having a back illuminated photocathode, guard rings, and a very sensitive, fast current amplifier to resolve the electron current pulse. Such high current sensitivity and temporal response showed asymmetric current pulses, a phenomena not normally observed in most drift velocity apparatus. Data of this asymmetric current pulseshape for the inert gases and hydrogen azide are presented. The analysis method of such TOF current pulses is discussed.

GA-2 Model calculations of amplification of short-wavelength radiation in capillary plasmas*. J.J. ROCCA [a], D. BEETHE and M. MARCONI. Electrical Engineering Dept. Colorado State University.--We discuss the possibility of creating extreme ultraviolet lasers in recombining plasmas with large length to diameter ratio ($l/d > 100$) generated by fast capillary discharges. A time dependent collision-radiative model is used to calculate the temporal evolution of the plasma density, electron and ion temperature and the time history of all ionic ground states and relevant excited states following the excitation by the discharge pulse. In hot plasmas of such a geometry conduction cooling can be greater than radiation cooling resulting in rapid cooling of the plasma at the termination of the discharge pulse. Gain-length products > 10 are predicted to occur at XUV wavelengths.

*Work supported by the National Science Foundation.
a- N.S.F. Presidential Young Investigator

GA-3 Time resolved measurement of the plasma density in a highly ionized helium capillary discharge

*. M. VILLAGRAN and J.J.ROCCA[a] . Electrical Engineering Dept. Colorado State University.--We have used short current pulses to create dense (Ne=1 10^{16}-1 10^{17}cm $^{-3}$) highly ionized plasmas in a helium capillary discharge. Rapid cooling of these plasmas result in a large three body electron-ion recombination rate and might allow the amplification of radiation in the vacuum ultraviolet. The temporal evolution of the plasma density in a helium capillary discharge was measured from the Stark broadened profile of the 4-3 HeII transition. The plasma density at the time of maximum recombination,(occurring 150 to 200ns after peak of the discharge current pulse),was determined as a function of the discharge parameters.

*Work supported by the National Science Foundation
a- N.S.F. Presidential Young Investigator

GA-4 A Self-Consistent Model of a Hollow Cathode Discharge Helium Mercury Laser, G. J. FETZER,* N. R. REESOR, and J. J. ROCCA,** Department of Electrical Engineering, Colorado State University --A self-consistent model of a DC hollow cathode discharge has been developed. The simulation closely resembles the actual situation of operating a hollow cathode discharge in which the experimentalist determines the characteristics of the discharge by selecting the voltage between cathode and anode, the gas pressures, and the cathode material. These are the input parameters for the model. For a specific set of operating conditions the electron and ion densities in the negative glow region of the discharge are calculated self-consistently with the particle fluxes and electric field distribution in the cathode sheath. The model has been used to simulate laser oscillation on the 6149 Å transition in singly ionized mercury in a helium-mercury hollow cathode discharge. We have included the calculation of laser gain, output power, and efficiency for this transition. A comparison between experimental results and those predicted by the model is included.

Work supported in part by AFOSR Grant No. 87-0290
* OPHIR Corp., 7333 W. Jefferson Ave, Ste 210, Lakewood CO. 80235
** National Science Foundation Presidential Young Investigators Award

GA-5 A Self-Consistent Model for Longitudinal Discharge Excited He-Sr^+ Recombination Lasers, R.J. CARMAN and J.A. PIPER, Macquarie University, Sydney. There is continued interest in the He-Sr^+ recombination laser as an efficient source of high-power (>1W) laser radiation in the blue (430.5nm). A detailed rate equation analysis of the discharge kinetics for a self-heated He-Sr^+ recombination laser has been developed to evaluate the temporal and spatial (radial) behaviour of the discharge parameters (n_e, T_e, T_o, He^+, Sr^+, etc.) throughout the current pulse, recombination phase, and afterglow period. The set of coupled differential rate equations used to describe the plasma and external electrical circuit are integrated over several discharge cycles to yield fully self-consistent results. Preliminary results show that the discharge parameters exhibit strong radial dependencies (notably the gas temperature T_o and ground-state densities of He and Sr) in agreement with recent experimental results[1,2]. Such effects are important in scaling these lasers to wide-bore/high-repetition-rate operation.

[1]R. Kunnemeyer *et al.*, IEEE J.Q.E. QE-23 2028 (1987)
[2]C.E. Little and J.A. Piper, SPIE Proc. 894 (1988).

GA-6 UV–Emission from Silent Discharges in XeCl* Gas Mixtures V. SCHORPP, K. STOCKWALD and M.NEIGER, LTI University of Karlsruhe FRG —The plasma of dielectric barrier discharges (silent discharges) at high pressures is a transient glow discharge (τ = 10 – 100 ns) and well suited for the excitation of excimer radiation. We report on the experimental investigation of such discharges in Ar/Xe/HCl–mixtures in the pressure range of 0.1 to 1.5 bar with sinussoidial excitation voltages (1 – 10 kV) from 50 Hz to 50 kHz. The 308 nm UV–excimer band of XeCl* can be excited with 10% efficiency. Average output power scales linearly with both amplitude and frequency at the sinussoidial operating voltage. At f ≈ 50 kHz saturation is observed possibly due to the heating of the background gas.
Supported by the German Ministry of R&D (BMFT)

GA-7 The Time Response of Electron Beam Pumped Plasmas and Lasers,* MARK J. KUSHNER and HOSOUNG PAK, University of Illinois, Urbana, IL--Excimer lasers are commonly excited by electron beams with injection energies of 100 keV - 2 MeV. The slowing of beam electrons and generation of secondary electrons are usually assumed to be instantaneous. There is, in fact, a finite slowing down time and a disparity in the time between high threshold (ionization) and low threshold (attachment) events which may be problematic at the lower pressures (≈1 atm) being considered for large volume e-beam pumped excimer lasers. In this paper, the time response of electron beam pumped plasmas of interest to excimer lasers is discussed as a function of gas mixtures, pressure, and beam voltage using results from a Monte Carlo particle simulation. With a $Ar/Kr/F_2$ = 90/10/0.25 mixture for a KrF laser, the time response is ≈75 ns-atm/MeV based on beam voltage. Response time decreases with increasing Z of the target, ranging from 120 ns-atm/MeV for He to 15 ns-atm/MeV for Xe.

* Work supported by Los Alamos National Laboratory.

GA-8 Excitation Kinetics of the Atomic Xe Laser in Ar/Xe Mixtures,* THOMAS J. MORATZ and MARK J. KUSHNER, University of Illinois, Urbana, IL--The atomic xenon laser has demonstrated >5% intrinsic efficiency using discharge, e-beam and heavy ion excitation. We present a model for the excitation kinetics of the atomic xenon laser (1.73 μm - 2.6 μm) in Ar/Xe mixtures and compare results of the model to experiment. We find the dominant pumping to be by dissociative recombination of $ArXe^+$ and Xe^+_2 followed by a collisional cascade that selectively populates the upper laser level ($Xe(5d[3/2]_1)$). At xenon concentrations above a few percent, the laser performance deteriorates due to cascade collisions with xenon atoms that do not populate the $5d[3/2]_1$ level, by electron impact excitation of the lower laser levels from the Xe metastables and by xenon dimer formation. The unique dominance of the 1.73 μm line results from argon collisions quenching the lower level of this transition [$Xe(6p[5/2]_2$] faster than adjacent Xe(6p) levels.

* Work supported by Sandia National Laboratory.

GA-9 Dissociation and Vibrational Relaxation of XeF by Various Collision Partners,* J. F. BOTT, R. F. HEIDNER, J. S. HOLLOWAY, J. B. KOFFEND, and M. A. KWOK, The Aerospace Corporation -- The removal rates of the lower levels of the XeF(B->X) excimer laser transitions strongly affect the overall efficiency of the E-beam-pumped devices. Fast vibrational relaxation is required to empty these lower levels so that vibrational "bottlenecking" does not terminate the laser prematurely. We have measured the removal rates of XeF(X,v=3) in the rare gases, N_2, and CO_2 and the removal rates of XeF(X,v=0) in SF_6 by monitoring the vibrational levels formed by the photolysis of XeF_2. Their populations are monitored with a cw tunable dye laser tuned to absorption features of selected vibrational/rotational levels. The studies show a rapid vibrational relaxation followed by a common decay rate of the coupled vibrational levels. The rare gases remove XeF(X) with rate coefficients that differ by less than a factor of 1.6. Their rate dependence on temperature was measured between 293 and 285 K. Larger removal rate coefficients were measured for the molecular collision partners with XeF_2 having the largest rate coefficient. Rate coefficients were also determined for the concerted vibrational relaxation of v = 3 although the values do not represent state-to-state rate coefficients.

*This work reflects research supported by the Air Force Weapons Laboratory of the Department of Defense under U.S. Air Force Space Division Contract F04701-85-C-0086.

SESSION GB

10:10 AM - 11:55 AM, Wednesday, October 19

Radisson Plaza Hotel - West Ballroom

PLASMA-SURFACE PHENOMENA

Chairperson: D. Graves, University of California-Berkeley

GB-1 Theory of the Plasma-Sheath Transition and the Bohm Criterion, K.-U. RIEMANN, Ruhr-Universität Bochum, FRG. – The build-up of a stationary collision free space charge sheath in front of negative absorbing walls requires that the ion flow to the wall is accelerated in a quasineutral "presheath" at least to ion sound velocity ($v \geq v_s$, Bohm criterion). This simple "sheath condition" was generalized by Harrison and Thompson [1] for arbitrary distribution functions of the ions entering the sheath. For the Tonks-Langmuir model of the collision free and for the charge-exchange model of the collision dominated plasma the exact analytic solutions for the plasma-sheath transition are known [1-3]. The solutions (and other numerical results) fulfill the Harrison-Thompson sheath condition marginally (i.e. with the equality sign). Usually the sheath transition is indicated by a formal field singularity at the sheath edge on the presheath scale . This, however, is not true for Emmert's solution [2]. We reinvestigate and generalize (boundary conditions etc.) the sheath condition kinetically and show that - except from special singular cases - it is always fulfilled marginally and connected with the usual sheath edge field singularity. The physical background and possible exceptions (e.g. [2]) are discussed in detail.

[1] E.R. Harrison, W.B. Thompson, Proc. Phys. Soc. London) 74, 145 (1959.
[2] G.A. Emmert et al., Phys. Fluids 23, 803 (1980).
[3] K.-U. Riemann, Phys. Fluids 24, 2163 (1981).

GB-2 *In Situ* Surface Diagnostics for Plasma Chemistry, A. MITCHELL, R.A. GOTTSCHO, S.W. DOWNEY, G.R. SCHELLER, AT&T Bell Laboratories - To both monitor device processing and understand basic plasma chemistry, it is important to follow surface chemical changes during plasma treatment. We have developed two *in situ* surface diagnostics, photoemission optogalvanic spectroscopy (POGS) and second harmonic generation (SHG), to monitor real-time changes on surfaces in contact with plasmas. The effects of reactive and unreactive plasmas on SHG and POGS signals for Al and Si were studied as a function of time, wavelength, and plasma conditions. These results will be discussed in relation to changes in oxide coverage, surface states, and electronic properties.

GB-3 Electron Yield of Glow Discharge Cathode Materials under Noble Gas Ion Bombardment*, B. SZAPIRO**, J. J. ROCCA*** and PRABHURAM T., Electrical Engineering Department, Colorado State University -- The secondary electron emission coefficient of materials for helium, neon, and argon ion bombardment in the energy range 0.5-20 keV was measured for the surface conditions of cathodes in high voltage glow discharges. The materials studied, listed in order of decreasing electron yield, are: oxidized aluminum, oxidized magnesium, a molybdenum aluminum oxide sintered composite, molybdenum, stainless steel, gold, copper, and graphite. Each sample was surface conditioned by operating it as cathode of a glow discharge shortly before the electron yield measurement. The measured electron yields are in good correlation with their corresponding discharge currents. The results are relevant to the modeling of glow discharges and to cold cathode electron gun design.

* Work supported by Wright Patterson A.F.B.

** Post-Doctoral Fellow, University of Buenos Aires.

*** N.S.F. Presidential Young Investigator

GB-4 The Use of Transport Coefficients for Electron Scattering on Dielectric Surfaces,* TIMOTHY L. PECK and MARK J. KUSHNER, University of Illinois, Urbana, IL-- Surface flashover discharges (SFD's) across dielectric surfaces in gas or vacuum requires the generation of seed electrons and the net multiplication of those electrons as they scatter across the dielectric surface. The source of seed electrons is commonly by electron field emission at the triple junction between the cathode, dielectric surface, and vacuum/gas. If, however, the surface is illuminated by ultra-violet light or there is an external source of electrons, there is a tradeoff between field emission and the electrode-dielectric geometry which minmizes electron multiplication. To examine the precursor conditions for a SFD resulting from surface charging, a 3-D Monte Carlo particle simulation has been developed to model electron scattering from dielectrics. We derive transport coefficients analogous to those used for gas discharges to assist in assigning a probability for occurrence of a SFD which takes into account the geometry and past history of the surface.

* Work supported by NASA Lewis Research Center.

GB-5 Spontaneous Threshold Behavior for a Distributed-Element Model of Surface Arcs, A. KADISH and W. B. MAIER II, Los Alamos National Laboratory, and R. T. ROBISCOE, Montana State University—We model a surface arc as the discharge of an electric current I along a finite length of transmission line. The line is driven by an initially charged capacitor, is terminated by a short, and has distributed resistance $\overline{R}$, inductance $\overline{L}$, and shunt capacitance $\overline{C}$ per unit length. We write the usual transmission line equations, but with a new condition, namely: $\overline{R}|I| = E^*$, where E^* is constant. We find that the arc strikes only where the local electric field $|E| > E^*$. If at any point and time, $I = 0$ when $|E| < E^*$, then $I = 0$ for later times, unless $|E|$ again exceeds E^*. The arc current oscillates a finite number of times before stopping abruptly. These features are analogous to those found in a previous lumped circuit model of transient electric discharges.[1] Both analytic and computer solutions will be discussed.

* Work supported under the auspices of the U.S. DOE.

[1] R. T. Robiscoe, A. Kadish, and W. B. Maier II, J. Appl. Phys. (accepted July 1988).

GB-6 Simulation of Sputtering of Liquid and Solid Metals. W.L. MORGAN, JILA, Univ. of Colorado and NBS--Recent research into the distribution of atoms near a liquid metal surface[1,2] has shown that the liquid/vapor interface is stratified for several atomic diameters into the bulk liquid. This will have consequences for collisions of ions and atoms with liquid metal surfaces in a sputtering discharge environment. I have performed molecular dynamics calculations of low energy atoms colliding with an model stratified liquid, uniform density liquid, and crystalline solid surfaces. Compared to scattering from a solid surface, atomic scattering from the stratified liquid metal surface is characterized by enhanced energy loss and increased low energy sputter yield. I compare the sputter yields for these three model surfaces and a TRIM[3] Monte Carlo sputter calculation and discuss these results with reference to the scanty experimental data thac have been published.

[1]S.W. Barton, et al., Nature 321, 685 (1986).
[2]M.P. D'Evelyn and S.A. Rice, J. Chem. Phys. 78, 5081 (1983).
[3]J.P. Biersack and W. Eckstein, Appl. Phys. A 34, 73 (1984).

GB-7 Thermalization of atoms ejected from the cathode of a magnetron sputtering discharge. I.S. FALCONER, G.M. TURNER, B.W. JAMES and D.R. McKENZIE, University of Sydney, Australia -- Monte Carlo calculations of the thermalization of Cu atoms by the Ar sputtering gas in a magnetron sputtering discharge are summarized. This code gives the velocity distribution as a function of distance from the cathode for a realistic energy spectrum of the sputtered atoms and atom-atom interaction potential. The velocity distribution of the sputtered atoms has been determined from an interferometric measurement of the spectral lineshape of the Cu atoms: hyperfine structure and instrumental function were deconvolved using Fourier transfer techniques to give a Doppler broadened lineshape in good agreement with that given by the Monte Carlo code.

SESSION H

1:30 PM - 3:45 PM, Wednesday, October 19

Radisson Plaza Hotel - Ballroom and Minnesota Room

POSTERS: GASEOUS ELECTRONICS II

Chairperson: J. Evans, University of Minnesota

(All posters may be posted from 1:00 PM onwards, manned from 1:30 PM to 3:45 PM, and taken down at 6:00 PM.)

H-1 **A Complete and Self-Consistent Theory of Surface Wave Produced Discharges**, A. B. SÁ and C. M. FERREIRA, Centro de Electrodinâmica, Lisbon Tech. U. - A fully self-consistent theory of discharges produced and sustained by surface waves (SW) is presented which constitutes a complete, radial and axial description of the plasma column and the SW - field. The theory is an extension of previously reported analyses[1] and is based on a complete set of equations including Maxwell's eqs. and the boundary conditions for the SW-field, the electron Boltzmann eq.that provides local collisional and transport data vs. the electric field E, and the continuity and momentum transfer eqs. for the electrons and the ions. For given operating conditions, i.e., circular frequency ω, gas pressure p, discharge tube o. d., 2b, and i. d., 2a, and total incident power $P_i(O)$, the theory enables one to determine: i) the SW dispersion and attenuation characteristics; ii) $n_e(r,z)$ and $E(r,z)$; iii) $P_i(z)$; and iv) $\bar{\Theta}(z)$, the radially averaged, mean absorded power per electron. Though $P_i(z)$ decreases along z, both $\bar{E}(z)$, the radially averaged field in the plasma, and $\bar{\Theta}(z)$ remain practically constant. A numerical application to argon for p = 0.5 Torr, $\omega/2\pi$ = 2.45 GHz, 2a = 3 mm, and 2b = 8 mm yields results in good agreement with experiment.

[1] C. M. Ferreira, J. Phys. D 14, 1811(1981); ibid 16, 1673(1983).

H-2 Validity of the effective field concept at very high E/n, Y.M. Li and L.C. Pitchford, GTE Laboratories Inc., Waltham, MA -- Transport properties of electron swarms driven by spatially-uniform, high-frequency and high-power electric fields, are calculated by Monte Carlo simulations in the presence or absence of a uniform magnetic field. The applicability of the concept of effective field[1] to high E/n is then examined. For right-hand polarized fields at electron cyclotron resonance, the effective field formula is strictly valid for all field strengths. However, swarms driven by pure high frequency fields at high E/n, have higher average energies and ionization rate coefficients than those driven by the corresponding effective fields. Similarly, the effective field formula is also shown to be invalid at high E/n for the combination of left-hand polarized fields and a uniform magnetic field. Based on the multibeam model,[2,3] a simple analytic model is given to aid the understanding of these numerical results.

[1]W.P. Allis, in Handbuch der Physik, ed. by S. Flugge (Springer, Berlin, 1956),vol. 21, p383

[2]L.C. Pitchford, Y.M. Li, G.N. Hays, J.B. Gerardo and J.T. Verdeyen, Bull. Am. Phys. Soc., 32, 1144 (1987).

[3]Y.M. Li and L.C. Pitchford, Bull. Am. Phys. Soc., 33, 136 (1988).

H-3 Self-Consistent Solution of Boltzmann Equation in RF Plasmas: Application to Excimer Ne-Xe-HCl Laser, C. GORSE and M. CAPITELLI, University of Bari, Centro Studio Chimica Plasmi (CNR), Italy -- A self-consistent solution of Boltzmann equation in a RF field ($E=E_o \cos\omega t$) coupled to plasmachemistry and to the kinetics of excited states has been obtained by extending to RF discharges our approach discussed in ref. /1/. The present results for the uncoupled problem agree with the corresponding ones discussed in previous works/2/ and obtained by using a different numerical algorithm. The results for the mixture Ne-Xe-HCl show the importance of superelastic collisions, electron-electron collisions, dissociative attachment from vibrationally excited molecules in affecting the behaviour of the laser output in RF discharges.

/1/ C. Gorse and M. Capitelli, J. Appl. Phys. 62, 4072 (1987); /2/ M. Capitelli, R. Celiberto, C. Gorse, R. Winkler, J. Wilhelm, J. Appl. Phys. 62, 4398 (1987) and references quoted herein.

H-4 Ion Diffusion and Electrode Bias Voltage in Asymmetric, Capacitive R.F. Discharges. M.A. LIEBERMAN AND S.E. SAVAS, University of California, Berkeley — Asymmetric, capacitive discharges, which have unequal areas for the powered and grounded electrodes, are widely used for materials etching and deposition in the semiconductor industry. A spherical shell model has been developed to study such discharges, allowing the asymmetry to be modeled while preserving the simplicity of a one dimensional (along r) treatment. In the model, ions are generated by electron-neutral ionization and are lost by ambipolar diffusion. Resonant charge transfer with a constant cross section is assumed to dominate the ion transport. The ion transport velocity $u = -D_a \nabla n/n$ is assumed to be much greater than the ion thermal velocity. For this system, the ambipolar diffusion coefficient D_a is itself a function of u, and the resulting particle conservation equation reduces to a nonlinear, first order, ordinary differential equation. This equation has been solved to determine the unbalanced ion currents and the bias voltages at the powered and grounded electrodes. The results are compared to those of Godyak[1] for symmetric discharges and to a numerical model that includes ion inertial and ionization drag effects.

[1]V.A. Godyak, *Soviet Radio Frequency Discharge Research*, Technical Report (Delphic Associates, Falls Church, VA) p 86, 1986.

H-5 **Rate Equation Modeling of a Low Pressure rf Argon Glow Discharge.** *M. J. Colgan,* Physics Department, Rutgers University, Piscataway, NJ 08854, *D. E. Murnick* and *R. B. Robinson,* AT&T Bell Laboratories, Murray Hill, NJ 07974. A Laser Optogalvanic (LOG) study of the lowest metastable and resonance levels ($1s_5$ and $1s_4$) in a low power inductively coupled argon rf glow discharge showed anomalous signs and time dependences.[1] Laser absorption measurements yielding absolute densities of all 4 states in the 1s manifold have now been carried out at pressures from 0.1 to 1 torr. A collisional-radiative model describes the levels assuming a Maxwellian electron energy distribution. Iterative solution of a system of coupled rate equations determines the electron density and temperature subject to the constraints of agreement between the measured and calculated $1s_5$ densities and ionization balance. Agreement for the $1s_4$, $1s_3$ and $1s_2$ level densities is excellent below about 0.5 torr, but the resonance level densities are underestimated by factors of 2 to 3 above 0.5 torr.

1. D. E. Murnick, R. B. Robinson, D. Stoneback, M. J. Colgan and F. A. Moscatelli, to be published.

H-6 Particle Simulation of a Low Pressure RF Discharge, I.J. MOREY* and R.W. BOSWELL, ANU – RF discharges have been simulated with a bounded, one-dimensional particle-in-cell model which includes both ionization and secondary electron emission. One electrode is grounded and the other is made to oscillate between ±200V with a frequency of 20MHz. The simulations are started with a small number of cold ion and electron pairs and run until equilibrium is reached. At equilibrium the ions and electrons react to the average and instantaneous potentials respectively[1] since $\omega_{pi} < \omega_{rf} < \omega_{pe}$. A greater proportion of the ionization occurs within the sheaths at higher pressure, but there is an optimum pressure at which the highest densities are achieved. It was also found that the discharge could be sustained without any secondary electron emission, and that the effects of secondary electron emission due to the ions decreased with pressure.

* Now at UC Berkeley.

1. R.W. Boswell and I.J. Morey, Appl. Phys. Lett. **52**, 21 (1988).

H-7 Kinetic Modeling of RF Discharges. D.J. Koch and W.N.G. Hitchon, ECE Department, University of Wisconsin-Madison. -- We present a self-consistent calculation of the distribution functions of electrons and ions and the electrostatic potential in DC and RF discharges. The time evolution is calculated using a numerical scheme which is very efficient for transport with a significant flow velocity.[1] For each mesh point, at a time t_0, we have a corresponding density $d(x,v_x,t_0)$. We use 'propagators' to advance the density to new positions on the mesh after a timestep τ. The total solution, $d(x,v_x,t_0+\tau)$, is the summation over all the contributions from each mesh cell at t_0. This technique is used for ions and electrons simultaneously while the potential is updated by solving Poisson's equation. For the DC case, this is run until a steady state solution is found. For RF, the calculation is run until the solution is stationary when corresponding points in a RF cycle are compared.

[1] W.N.G. Hitchon, D.J. Koch and J.B. Adams, Sandia Report SAND88-8652 (1988).

H-8 Observed and Calculated Current Overshoot in Ar-Hg and Ne-Hg Discharges, M. E. DUFFY and J. H. INGOLD, GE Lighting, Cleveland, OH 44112. --When a square voltage pulse is applied to a long, cylindrical, low pressure discharge, then current wave-shape depends on momentum transfer cross-section, and on temporal behavior of electron density and temperature. When the pulse period is short compared with ambipolar diffusion time and long compared with energy relaxation time, then density is constant and temperature is modulated. The Ar-Hg discharge has a large current overshoot, because electrons are not in equilibrium with the electric field as the pulse begins. Later in the pulse, when electrons are in equilibrium with the electric field, current is lower because mobility is lower. The Ne-Hg discharge has less current overshoot, because mobility is a weaker function of electron energy. Calculations of current overshoot in these gases, based on moment theory, are shown to agree qualitatively with observation.

H-9 Criterion for Characterizing the Slope of the I-E Relationship of a Positive Column. G.L. ROGOFF, GTE Laboratories Incorporated--A general criterion has been derived to determine the sign of the slope of a positive column I-E characteristic. The derivation utilizes a generalized electron balance equation to allow for various electron production and loss processes. The resulting I-E slope has the same sign as the dimensionless quantity (the logarithmic derivative of I with respect to E)

$$\phi \equiv \left(\frac{E}{v_d}\frac{\partial R}{\partial n_e}\frac{dv_d}{dE} - \frac{E}{n_e}\frac{\partial R}{\partial E} - \frac{E}{n_e}\frac{\partial R}{\partial n}\frac{dn}{dE}\right)\Big/\frac{\partial R}{\partial n_e} ,$$

where R represents the expression[1] for dn_e/dt at steady state and n can represent a particle density or any other independent variable. For example, in many self-sustained discharges $\partial R/\partial E$ is positive and large, making the numerator negative, while the production rate increases with n_e more strongly than the loss rate, making $\partial R/\partial n_e > 0$. Thus $\phi < 0$, and the I-E slope is negative. The general criterion reduces to more specific criteria for combinations of particular production processes and volume- or wall-controlled loss processes. Various cases for both self-sustained and externally-sustained plasmas are considered.

[1]P.J. Chantry, in Applied Atomic Collision Physics, ed. by E.W. McDaniel & W.L. Nighan (Academic, 1982), v. 3, p. 41.

H-10 Fluid Treatment of Plasma Presheath for Collisionless to Collisional Plasmas,* J.T. SCHEUER and G.A. EMMERT, University of Wisconsin-Madison - The presheath region of a plasma is treated using ion fluid equations which are valid from collisional to collisionless regimes. The plasma is assumed to be magnetic field free with Boltzmann electrons. Effects of neutral gas-plasma interactions are included through source terms in the fluid equations. Collisions are included through the closure conditions of the fluid equations. In the collisionless regime, the ion temperature in the direction perpendicular to the flow is assumed constant and independent of the parallel ion temperature. As collisionality is increased the perpendicular temperature is allowed to relax toward the parallel temperature until, in the fully collisional regime, the temperatures are equal throughout the presheath. The resulting fluid equations are integrated until a singularity is reached, which is interpreted as the sheath edge. Profiles of ion density, velocity, and temperature will be given, and compared with previously published kinetic results.

*Work supported by National Science Foundation.

H-11 Sheath Structure and Current Limitation for an Electrode Contacting a Thermal Plasma*, L. D. ESKIN AND S. A. SELF, Mech. Engr. Dept., Stanford University - 1-D solutions of the continuity and momentum equations for electrons and ions plus Poisson's equation, in the isothermal approximation, show current limitations for non-emitting cathodes and anodes set by the net generation of electron-ion pairs in the ionization non-equilibrium layer. Inclusion of the electron energy equation, allowing for Joule heating and increased net generation, removes the current saturation, leading to a decreasing potential drop versus current characteristic which is interpreted as a transition from diffuse to constricted current transfer modes.

* Work supported by the Air Force Office of Scientific Research, Grant No. 83-0108.

H-12 The Pulsed Discharge Arc Resistance and Its Functional Behavior.* T.G. ENGEL, A.L. DONALDSON, and M. KRISTIANSEN, Texas Tech U.** -- The primary objective of this work is to determine how accurately one can predict the resistance of a high current, pulsed arc discharge. To this end, eight published theoretical and empirical arc resistance equations were compared to experimentally measured arc resistance valves for unipolar arc discharges in atmospheric air (P_o = 0.86x10^5 Pa) using approximately 20 kA peak currents of 3.5 μs pulse lengths with an arc length of 0.01 m. Each arc resistance equation was numerically evaluated and matched to the experimental results at t=0.5 μs (approximate time of maximum arc current). Additionally, the examination of a special case (i.e., two degrees of freedom) of energy balance in the arc channel resulted in a new expression for the arc channel radius. It is shown to have good agreement with experiment.

*Submitted by M. KRISTIANSEN.
**Supported by SDIO/T/IS through DNA/RAEV.

H-13 Electron Density and Collision Frequency Measurements in Microwave Breakdown Plasmas in Air,* K. R. STALDER and D. J. ECKSTROM, SRI International--We have used a 10-GHz interferometer to measure breakdown plasma parameters in low pressure air pumped by high power 2.86-GHz microwaves. The interferometer probed normal to discharge layers formed in the constructive interference regions of 2.86-GHz microwaves reflected from an inclined plate. The pressure ranged from 0.01 to 3 Torr; microwave power and pulse duration were adjusted to achieve single layer breakdowns. Electron densities, primarily measured by interferometer phase shifts, typically rose to 2-4 x 10^{11} cm^{-3} (overdense for the 2.86-GHz microwaves); electron collision frequencies, primarily measured by attenuation of the 10-GHz microwaves, was anomalously high (2 x 10^{10} sec^{-1} at 0.03 Torr). The electron density decay rate scaled linearly with the pressure and was 2.7 x 10^{-7} $cm^3 s^{-1}$ at 0.1 Torr. These results suggest the dominant decay mechanism is by two-body dissociative recombination of electrons with N_2^+, with the electron temperature rising with decreasing pressure. Upcoming experiments designed to study discharge sustainment also will be discussed.
*Work supported by AFGL through LANL.

H-14 Atomic Transition Probabilities for Sc I and Sc II.* G. MARSDEN and J. E. LAWLER, U. of Wisconsin-Madison, J. T. DAKIN, General Electric Company.--An accurate and comprehensive set of transition probabilities for Sc I and Sc II is measured using a combination of spectroscopic techniques. The results are needed for reliable radiation transport calculations in metal-halide discharge lamps. Radiative lifetimes were measured using time-resolved laser-induced fluorescence on a slow atomic beam.[1] Branching ratios are measured using the McMath 1.0 meter Fourier transform spectrometer at the National Solar Observatory on Kitt Peak. A comparison of results to previous measurements and calculations will be presented.

[1]G. C. Marsden, E. A. Den Hartog, J. E. Lawler, J. T. Dakin, and V. D. Roberts, J. Opt. Soc. Am. B5, 606 (1988).

*Supported by NSF Grant AST85-20413 and the General Electric Company.

H-15 Lifetimes, Branching Ratios, and Absolute Transition Probabilities in HgI.* E. C. BENCK and J. E. LAWLER, U. of Wisconsin.--Accurate measurements of the radiative lifetimes, branching ratios, and absolute transition probabilities of HgI are reported. The radiative lifetimes are measured using time-resolved laser-induced fluorescence on an atomic beam. Branching ratios of the UV, visible, and strong IR lines are measured from the emission spectra of a Hg lamp. The branching ratios of some additional weaker IR lines are determined by measuring the relative strength of cascade and direct fluorescence in the lifetime experiment. The lifetimes and branching ratios are compared to single configuration calculations and to other published theoretical and experimental results. Our experimental lifetimes and branching ratios are combined to derive accurate absolute transition probabilities for the UV and visible lines from the 7^3S_1, 7^1S_0, 6^3D_2, 6^3D_3, 8^3S_1, 8^1S_0, 7^1D_2, 7^3D_2, 7^3D_3, and 6^3P_1 levels.

*Supported by the General Electric Company and by NSF Grant AST85-20413.

H-16 Zn-Rare Gas Atom Absorption spectra, Y. TAMIR I. AHARON and R. SHUKER, Ben-Gurion U. ISRAEL --Absorption spectra of Zn-R mixtures (R: rare gas atom, He, Ne, Ar or Kr) are studied. The red and blue absorption wings of the 213.9 nm band are attributed to the transitions from the ground-state $X^1 0^+$ (Zn (4^1S_0) - R ($^1S_0$)) to the excited states $^1 0^+$ or $^1 1$ (Zn (4^1P_1) - R ($^1S_0$)). The R-density and temperature dependence of the absorption structure are compared with the Zn-Ar 213.9 nm emission band[1], and with the absorption structure of Hg-R 185 nm and the Cd-Kr 228.8 nm bands[2]. The possibility of a rule of thumb for the M-R pairs (M: metal atom whose electronic configuration ends with $nd^{10}s^2$) is discussed, and well depth values for the potential energy curves are deduced.

[1] Y. Tamir and R. Shuker, APS bulletin, 32, 1154 (1987).
[2] C. Bousquet and N. Bras, J. Phys. B: At. Mol. Phys., 19, 3859, (1986) and references therein.

H-17 The Calculation of Molecular Electron Affinities*
T. GORCZYCA and D. W. NORCROSS,+ JILA, Univ. of Colo. and NBS -- A new method will be presented for determining the binding energy of an electron to a molecular ion or to a neutral molecule. The technique consists of solving the close-coupled scattering equations using a non-iterative integral equation method for the exchange region and standard asymptotic solutions methods for the outer region. A smooth match of the solutions in these two regions at the correct energies yields the electron affinity and outer-electron wave function. Results for H_2^- and HF^- potential curves will be shown and compared to MC-SCF negative ion calculations.

*Research supported by National Science Foundation grant PHY86-04504 to the University of Colorado.
+Quantum Physics Division, National Bureau of Standards.

H-18 A Numerical Multiconfiguration Hartree-Fock Calculation on ^3P (nsnp) Rb and Cs Anion States,* D. Chen† and C.F. Fischer, Vanderbilt University-- The MCHF[1] method including outer- and inter-shell correlation, was used to study the 5s5p ^3P and 6s6P ^3P negative ion states of Rb and Cs, respectively. In Rb, this calculation shows a shape resonance between 0.039 and 0.052 eV. In Cs, a bound ^3P anion state is tentatively predicted with an electron affinity between 0.0012 and 0.011 eV. These calculations included the relativistic shift correction and seem to be in agreement with experimental evidence.[2,3]

* Work supported by the U.S. Department of Energy, Office of Basic Energy Sciences.
1. C.F. Fischer, Comp. Phys. Rep. V3 273 (1986)
2. A.R. Johnston and P.D. Burrow, J. Phys. B At. Mol. Phys. 15 L745 (1982)
3. I.I. Fabriakant, Opt. Secpt. (USSR) 53 223 (1982)

† Present address: University of Pittsburgh

H-19 Anisotropic Potentials of Rare Gas - N_2 Systems, M.S. BOWERS, Spectra Technology Inc., K.T. TANG, Pacific Lutheran University, AND J.P. TOENNIES, Max-Planck-Institut für Strömungsforschung, FRG - The anisotropic potentials of He-N_2, Ne-N_2, and Ar-N_2 are predicted using the Tang-Toennies potential model. This model damps the long-range ab initio dispersion terms individually using a universal damping function and adds to this a simple Born-Mayer repulsive term. The Born-Mayer parameters for the three systems were derived from SCF calculations. The dispersion coefficients were estimated from established combining rules using an effective multipole spectrum for the N_2 molecule computed by Visser and Wormer from the time-dependent coupled Hartree-Fock approximation. The resulting potentials were used to predict the second interaction virial coefficients for each system, and they are found to be in excellent agreement with experiment. It is found that the law of corresponding states for anisotropic systems, which predicts that the reduced shapes of the potentials for a given geometrical configuration are identical, holds for the highly anisotropic rare gas-N_2 systems.

H-20 Theoretical Treatment of Shape Resonances in Molecules Using Fano's Method, D. CHEN and G. A. GALLUP, Dept. of Chem., U. of Nebraska --The method, due to Fano[1], of configuration interaction between a quasi-bound state and the continuum (QBSC-CI) has been used to calculate positions and widths of shape resonances in low energy electron scattering from several hydrocarbons. This method allows treatments that range from quite approximate to those containing electron correlation. In their most complete form the calculations require the determination of the off-the-energy-shell K-matrix[2] in the subspace orthogonal to the quasi-bound state, followed by the QBSC-CI. Results for hydrogen, ethylene, cyclopropene, and cyclobutene have been obtained. The method shows the connection between resonances and the virtual orbitals from basis set SCF calculations of atoms or molecules.

1.U. Fano, Phys. Rev. 124, 1866 (1961)

2.U. Fano and F. Prats, Proc. Nat. Acad. Sci. (India) A33, 553 (1963); A. F. Starace, in Encyclopedia of Physics, Vol. XXXI, ed. W. Mehlhorn (Springer-Verlag, Berlin, 1982)

H-21

Electron Impact Excitation of Helium to Triplet States, R.E. H. Clark, D. C. Cartwright, J. Abdallah, Jr., J. B. Mann, and G. Csanak Los Alamos National Laboratory, Los Alamos, NM, USA.--Distorted wave approximation (DWA) and first order many body theory (FOMBT) calculations were performed for the electron impact excitation of helium to n^3D,n^3F,n^3G (n=3,..8) states and to the 3^1P and 3^1D states. The summed differential cross section for the 3^1P and 3^1D states shows good agreement with recent experimental data[1]. The calculated integrated cross sections for the $1^1S \rightarrow n^3D,n^3F,n^3G$ transitions are substantially lower than experimentally obtained values reported recently[2]. The theoretical studies show that configuration interaction (CI) in the ground state of helium gives substantial enhancement of the cross sections. Integrated cross sections will be presented with varying amounts of CI for comparison.

[1]D.C. Cartwright, G. Csanak,D.I. Register, and S. Trajmar, to be published (1989)

[2]R.B. Kay and C. G. Simpson, J. Phy. B. 21, 625 (1988)

H-22

Calculation of Differential Cross Sections, Electron Impact Coherence Parameters, and Fine-structure Effect Spin-Polarization Functions for the Electron Impact Excitation of Neon,* L.E. Machado, Depto. de Fisica, Univ. Federal de San Carlos, San Carlos, S. P. Brazil, M. C. Ferraz, Inst. de Fisica e Quimica, Univ. de San Paulo, San Carlos, Brazil, G. D. Meneses, Instituto de Fisica, Univ. Est. de Campinas, Campinas, S.P. Brazil, G. Csanak and D. C. Cartwright, Los Alamos National Laboratory, Los Alamos, New Mexico 87545, USA. --First order many body theory has been used for the calculation of differential cross sections, complete set of electron impact coherence parameters and fine-structure effect spin-polarization functions for $1^1S_0 \longrightarrow 3^3P_{0,1,2}$ excitation of neon. Results will be reported for the above quantities for E=20,50, and 100eV incident electron energies. The calculations incorporate the spin-orbit coupling effect in the target-state wave-functions.

*Work supported by the National Science Foundation, International Programs, USA, Conselho Nacional de Pesquisa, Brazil, and the U. S. Department of Energy.

H-23 Orientation and Alignment Parameters in $e^{\pm}$ Impact Excitation of Hydrogen-Like Positive Ions. ASHOK JAIN, N.C. DEB, N.C. SIL and C.D. LIN, Physics Department, Kansas State University. --The orientation ($\langle L_y \rangle$) and alignment angle (γ) of the excited 2p state of hydrogenlike positive ions by high-energy electron and positron impact are calculated under the Coulomb-Born approximation. The behavior of $\langle L_y \rangle$ and γ is found to be qualitatively similar as in the case of $e^{\pm}$ impact excitation of the helium atom. We also analyze the shape and the rotation of the excited state in terms of the dipole and velocity vectors resulting from the coherences between 2s and 2p levels. The dependence of $\langle L_y \rangle$ and γ parameters on the projectile velocity and on the strength of target nuclear charge Z is also investigated. These results reveal that the classical grazing model, which interprets positive (negative) $\langle L_y \rangle$ in terms of attractive (repulsive) force between the projectile and the target, is not valid in general. We also report the orientation and the alignment angle for the 3d state of He^+ excited by electron and positron impact.

*Work supported by USDOE.

H-24 Comparison of the Differential Magnetic Sublevel (m_ℓ=0) Cross Section for the 3^1P State of Helium for 60 and 80 ev Electrons.* N.W.P.H. PERERA and D.J. BURNS, Behlen Laboratory of Physics, University of Nebraska, Lincoln, Nebraska 68588--The 3^1P state was excited by 60 and 80 ev electrons. The 501.6 nm ($3^1P \rightarrow 2^1S$) photon was detected in coincidence with electrons which had excited the state. Both electrons and photons were detected in the scattering plane, so that a coincidence is only produced for atoms decaying from the m_ℓ=0 state. The relative differential magnetic sublevel (m_ℓ=0) cross section for 60 and 80 ev electrons at various scattering angles from 10°-60° will be presented and compared to a number of theoretical models of Madison[1] and others.

*Work supported by NSF.
[1]private communication with D.H. Madison.

H-25 Density and Rotational Temperature of $SiH_3(X^2A_1)$ Radical in Silane Plasma*, T. GOTO, N. ITABASHI, N. NISHIWAKI and K. KATO, Nagoya Univ., C. YAMADA and E. HIROTA, Inst. for Molecular Science -- The SiH_3 radical density has never been measured although SiH_3 radical is an important precursor of amorphous silicon thin film. In this work, first the densities of several rotational levels belonging to the $SiH_3(X^2A_1)$ radical have been measured in pulsed silane plasma with infrared diode laser absorption spectroscopy, and the rotational temperature and density of the $SiH_3(X^2A_1)$ radical have been determined. The experimental conditions have been as follows: a hollow cathode tube of 117 cm long and 10 cm inner diameter, a discharge current of 1 A, a SiH_4/H_2 pressure of 0.2/1.8 Torr and a gas flowing rate of 60 sccm. The measured density of one rotational level ($v=0^+$, $J''=4$, $K''=0$) of SiH_3 has been 4.3×10^9 cm^{-3}. The rotational temperature obtained with the densities of several rotational levels has been 320 K and the determined SiH_3 (X^2A_1) radical density has been 6.3×10^{11} cm^{-3}.
*Supported by Grant-in-Aid for Scientific Research on Priority Areas of the Ministry of Education, Science and Culture.

H-26 Time-Dependence of the Scattering Amplitudes for the 3^1D State of Helium,* E. J. MANSKY, Georgia Institute of Technology - The multichannel eikonal theory results for the complex scattering amplitudes $f_m(\theta_e;\rho,x=vt;E)$ for the electron-impact excitation of the 3^1D state of helium are examined. The behavior of the scattering amplitudes f_m, as a function of electron scattering angle θ_e, and impact parameter ρ, for the 3^1D_m states of helium gives a detailed, dynamical, picture of the time evolution of the final state probabilities, phase angles and the change cloud of the 3^1D state of helium. Comparing the dynamical behavior of the f_m for the 3^1D state with the dynamics of the scattering amplitudes for the 2^1P and 3^1P states provides direct information on the time evolution of the excitation process during the scattering event.

*Research supported by U. S. Air Force Office of Scientific Research under Grant No. AFOSR-84-0233.

H-27 Electron-Photon Coincidence Studies of Heavy Rare Gas Excitation by Electron Impact,* J.J. CORR, P. PLESSIS and J.W. McCONKEY†, University of Windsor, Canada--Excitation of the resonance levels of Kr and Xe is studied at various incident electron energies and scattered electron angles by measuring the appropriate polarization correlations both in and perpendicular to the scattering plane. Significant spin-dependent effects are observed which increase with target mass. Agreement with theory is quite good at small scattering angles (<20°) for some of the parameters but serious disagreements exist particularly with respect to predictions regarding the magnitude of spin-dependent effects.

* Supported by the Natural Sciences and Engineering Research Council of Canada.

† Canada Council Killam Fellow.

H-28 Polarization of VUV Radiation from the Rare Gases Excited by Electron Impact,* W. KARRAS, K. BIRD, P. HAMMOND and J.W. McCONKEY†, University of Windsor, Canada--Accurate polarization data has been obtained for VUV radiation emitted from He, Ne, Ar, Kr and Xe following electron impact excitation in the energy range from threshold to 500 eV. Some spectral filtering is achieved with the more massive targets by the use of a LiF window. Use of the polarization signature allows various effects to be identified and studied particularly in the near threshold region.

* Research supported by the Natural Sciences and Engineering Research Council of Canada.

† Canada Council Killam Fellow.

H-29 Molecular Dissociation Studies Using Laser Induced Fluorescence,* M. DARRACH and J.W McCONKEY†, University of Windsor, Canada--An experiment will be described in which crossed electron, laser and supersonic pulsed gas beams are used to probe the electron impact dissociation of simple molecules. Data will be presented as a function of incident electron energy and wavelength of the LIF detection stage.

* Research supported by the Natural Sciences and Engineering Research Council of Canada.

† Canada Council Killam Fellow.

H-30 Fragmentation of CF_4 Following Electron Impact,* S. WANG and J.W. McCONKEY†, University of Windsor, Canada--Fragmentation of CF_4 following electron impact has been studied over the energy range from threshold to 500 eV by monitoring the VUV radiation produced from the excited fragments. Radiation from both neutral and ionic species has been observed in the wavelength range 45-130 nm and cross-sections for production of individual features have been established using secondary standards in the rare gases and H_2. The fragmentation pattern is similar in many respects to that observed for SF_6.[1]

* Supported by the Natural Sciences and Engineering Research Council of Canada.

† Canada Council Killam Fellow.

[1] Forand et al., Can. J. Phys. 64, 269 (1986).

H-31 VUV Emissions Produced by Electron Collisions with Halogen-Containing Molecules*, F.M. OLCHOWSKI, Z.J. JABBOUR and K. BECKER*, Lehigh University -- As part of our ongoing program to study electron collisions with the reactive constituents of processing plasmas[1] we measured absolute photo-emission cross sections for the various fragment emissions in the vacuum ultraviolet (VUV) produced by dissociative electron impact on NF_3, CF_4, SF_6 and CCl_2F_2. We also determined appearance potentials for these emissions which in many cases allowed a unique identification of the break-up mechanism of the parent molecule.

[1]Z.J. Jabbour et al., J. Chem Phys. 88, 4252 (1988) and references therein

#Supported by NSF through grant CBT-8614513

*Present Address: City College, New York

H-32 Electron Degradation Spectra and Yields by Subexcitation Electrons in O_2 and CO_2 Gases*--M. KIMURA, K. KOWARI, M. A. ISHII†, A. PAGNAMENTA‡, and M. INOKUTI, Argonne National Laboratory--Electrons arriving in the energy domain below the first electronic excitation threshold are termed "subexcitation electrons." These subexcitation electrons are known to play an important role in radiation chemistry and biology. We have systematically studied the moderation of subexcitation electrons in O_2 and CO_2 molecular gases using time-dependent and time-independent versions of the Spencer-Fano equation, as well as the continuous slowing-down approximation. Our study reveals the important influence of negative ion formation as a competing process to vibrational excitation processes on the electron degradation process.

*Work supported in part by the U.S. Dept. of Energy, OHER, under Contract W-31-109-Eng-38.

†Summer Research Participant, University of Minnesota, Minneapolis, MN.

‡Permanent address: Dept. of Physics, University of Illinois, Chicago, IL.

H-33 Electron Distribution in a Dense Gas of Repulsive Scatterers. T. F. O'MALLEY, San Jose, CA -- Nearly all existing measurements of electron mobility, μ, in gases at high density, N, are closely reproduced by a previously derived physical model[1]. For *repulsive* scatterers, it gave the formula:

$$\mu(N)/\mu(0) = \exp[-(E_c - E_0)/kT],$$

which predicted the exponential falloff of μ for many gases through more than 2 orders of magnitude. The model argued that $E_0 = -\Gamma$ (the induced width or uncertainty), and that $E_c = 0$. The present work puts the derivation on a much firmer mathematical basis. E_0 is now rigorously found to be $-1/(4L^2)$ Ry, where $L = 1/(Nq_T)$ is the mean free path. Finding E_c is harder. It is done by using a result of Kubo's for stochastic processes to *derive* a Ioffe-Regel like criterion for "non-propagating" electron states, viz. $\lambda > L\pi$. This leads to the final result $E_c - E_0 = 4/L^2$, which duplicates the experimentally confirmed results at very high N, while predicting for the first time an observed quadratic N dependence for low N.

[1]T. F. O'Malley, J. Phys. B 13, 1491 (1980).

H-34 Measurement of the Mobility and Longitudinal Diffusion Coefficients of SF_5^+ in SF_6.* J. DE URQUIJO, I. ALVAREZ, H. MARTINEZ AND C. CISNEROS, Insituto de Física, UNAM, Cuernavaca, Mor., 62191, México. A drift tube with variable drift distance and mass analysis at its exit end has been used to measure the mobility and longitudinal diffusion coefficients of SF_5^+ in SF_6 over the range 31-510 Td, and gas pressures of 3.33 and 6.67 Pa. The mass-analyzed mobilities agree well with those of Fleming and Rees[1] up to 170 Td. The peak of the mobility curve lies well below that calculated by Brand and Jungblut[2]. We are unaware of any previously published longitudinal diffusion data for SF_5^+ over this range.

*Research partially supported by CONACyT, ICEXNA-050230.

1. I.A. Fleming and J.A. Rees, J.Phys.B 2, 776 (1969).
2. K.P. Brand and H. Jungblut, J.Chem.Phys. 78, 1999 (1983).

H-35 Excited States in Partially Ionized Hydrogen.* S.S.POPOVIĆ, Institute of Physics, Beograd, Yugoslavia--Polarizabilities of excited states can be a few order of magnitude higher then those of ground states. Consequently, cross-sections for momentum transfer from electrons to excited atoms should be substantially higher than corresponding ground-state quantities. Higher cross-sections, multiplied by lower population densities, and summed over quite a number of states that may exist in a low pressure discharge, are not necessarily negligible as it is usually assumed. To exemplify, total collision frequencies for electron momentum transfer in low pressure plasmas at temperatures between 5000 and 15000 K, including excited states, were calculated. Voltampere characteristics of high current hydrogen thyratrons happen to be quite sensitive to the influence of excited states.

* Submitted by B. Bederson

H-36 Measurements of Electrode Temperature Evolution by Laser Light Reflection, H. KEMPKENS*, W.W. BYSZEWSKI and W.P. LAPATOVICH, GTE Labs., Waltham, MA -- The electrode temperature rise during starting of an arc discharge was measured using the temperature dependent reflection coefficient of metal surfaces. Reflected He-Ne laser light is collected by an integrating sphere and detected by a photodiode and fast lock-in technique. The temporal resolution we achieved was 3ms (adequate to resolve 60Hz electrode heating phenomena) limited by the lock-in integration time and the chopper frequency. Calbration was obtained by pyrometric measurements of tungsten and molybdenum incandescent ribbon lamps operated at constant, regulated current levels. This related the observed signal during electrode heating in the electric discharge to electrode temperature. This technique affords a non-intrusive method for measuring transient electrode temperature in an obstructed environment with an accuracy of about 20%. Ordinary pyrometric electrode temperature measurements fail during an arc starting process when plasma radiation obstructs the incandescent radiation of the heated electrode not yet in a full thermionic stage.
*On leave from U. of Dusseldorf, W. Germany.

H-37 Experimental Investigation of Arc Root Ignition on Cold Cathodes,* K.P. NACHTIGALL and J. MENTEL Allgemeine Elektrotechnik und Elektrooptik, Ruhr-Universität Bochum, FRG - The hot plasma of a switching arc of several hundred amps. is blown magnetically against a cathodic commutation electrode which is inserted laterally into the discharge vessel. By a voltage increasing linearly with time between the cathode and the arc plasma in front of the cathode arc roots are ignited initiating arc commutation. The arc can be switched off after some 100 ns so that the traces of arc ignition at the cathode could be recorded by scanning electron microscopy (SEM). The arc root ignition was investigated at cathodes of copper, steel and graphite, materials with approximately the same work function, and at cathodes of magnesium and cerium which have much lower work functions. For the ignition delay time cumulative frequency distributions are found with a first steep rise at short times (≈250 μs) and a second steep rise at long times (≈400 μs).
* Research supported by DFG.

H-38 Effect of UV Radiation on Operating Voltage in the High-Voltage Hollow Cathode Discharge, T. ARAI, H. AKIBA, Kanagawa Inst. of Tech., T. IIJIMA, Tokyo Voca. Train. Col., and T. GOTO, Nagoya U. --The purpose of this work is investigation of the photoelectric effect on the high voltage operation of hollow cathode discharge. The clyindrical hollow cathode is 6cm in length and 15mm in inner diameter. The cylindrical insulator with openings was coaxially placed at proper intervals inside a hollow cathode pipe. When the opaque quartz tube with openings is mounted in the hollow cathode, a slope of the I-V characteristics becomes steeper. Then, when the opaque quartz tube is replaced by the transparent quartz tube with openings, the slope of I-V characteristics becomes small and oprating voltage decreases remarkably. The opaque quartz does not transmit uitraviolet light as compared with transparent quartz tube.
The result shows that the one reason for maintaining the voltage in the high voltage hollow cathode discharge by restricting partially the cathode inner surface is due to reduction of photoelectric effect.

SESSION I

3:45 PM - 6:00 PM, Wednesday, October 19

Radisson Plaza Hotel - Ballroom

POSTERS: GASEOUS ELECTRONICS III

Chairperson: L. Bigio, General Electric R&D Center

(All posters may be posted from 1:00 PM onwards, manned from 3:45 PM to 6:00 PM, and taken down at 6:00 PM.)

I-1 Electrical Conductivity Measurements of the NRL Laser-Initiated-Reduced-Density Channels,* K. R. STALDER, M. S. WILLIAMS and D. J. ECKSTROM, SRI International--We have used a 35-GHz microwave interferometer to measure the conductivity of reduced-density channels resulting from laser-guided discharges. The density channels are formed by discharging capacitor banks along paths created by laser ionization of aerosol-seeded air. The channels hydrodynamically expand in 100 μs to a pressure equilibrated diameter of 2 to 8 cm, depending on the capacitor bank energy and then become turbulent with a corresponding reduction in conductivity due to gas cooling. The interferometer probed chordwise conductivity profiles; Abel inversion yields radial profiles of the conductivity. Results show that the DC conductivity reaches 0.5-2 x 10^{10} sec^{-1} in 500 μs, then decreases as turbulent cooling takes effect. Corresponding electron densities reach 1 to 6 x 10^{12} cm^{-3}. The temperatures deduced from the conductivity levels indicate equilibrium temperatures up to 3800 K. Results of upcoming measurements using a 94-GHz interferometer also will be discussed.
*Work supported by DARPA through NSWC contract N60921-85-C-0210.

I-2 Temperature Dependence of VUV Fluorescence Yield of Xe_2^*, I. Messing*, M. S. Williams, and D. J. Eckstrom, SRI International--Past studies have shown that the fluorescence efficiency of 172-nm emission from Xe_2^* when room-temperature xenon at atmospheric pressures is pumped by electron beams of moderate current is at the theoretical limit of approximately 43%. We have now studied the variation of the fluorescence intensity as a function of temperature. We used a shock tube to heat xenon to temperatures as high as 2500K. A Febetron 706 electron beam (600 keV, ~2000 A, 3 ns) was fired through the endwall of the shocktube to excite the VUV fluorescence. The gas density was held constant to maintain constant excitation rates. The fluorescence was found to decrease exponentially with temperature approximately as exp[-(T-300)/950]. Static cell experiments with $T \leq 400K$ confirmed the decrease of fluorescence yield even at slightly elevated temperatures. We have not identified a good explanation for the observed results, although enhanced self-absorption of the VUV emission and impurity interference with the electron-ion recombination kinetics are under consideration.
*Permanent address: RAFAEL, Haifa, Israel.

I-3 Excitation Temperature Determination in Non-Equilibrium, Low-Pressure, Ar-Cs Plasmas. M.A. GIESKE, J. MYERS and S.D. MARCUM, Miami University, Oxford, OH, B.N. GANGULY, AFWAL, WPAFB, OH -- A method of determining excitation temperatures in cesium in low pressure (< 2.5 Torr) Ar-Cs plasmas is presented. The method assumes that the dominant creation and destruction processes are electron impact excitation and spontaneous emission, respectively. Using measured emission line intensities and published electron impact cross section and oscillator strength data, numerical integration of the cross sections over the electron energy distribution function yields excitation temperatures from each pair of suitable emission lines. Current focus is on extension of the method to high n states. By contrast, excitation temperature measurements for argon give substantially higher values, indicating the non-equilibrium nature of the Ar-Cs plasmas.

I-4 Electron Temperature Relaxation in Ar-Cs Plasmas as a Function of Cathode Temperature. J.L. MYERS, M.A. GIESKE and S.D. MARCUM, Miami University, Oxford, OH, B.N. GANGULY, AFWAL, WPAFB, OH -- Excitation (electron) temperatures for cesium have been measured in low pressure Ar-Cs discharges. The discharge cell is a six-way cross fitted with sapphire viewports and a set of flat, circular Ni electrodes (4.3 cm diameter, 1 cm gap), one of which can be maintained at temperatures between ambient and 1000 K. Spatially resolved emission spectra were measured as functions of discharge current density and cathode temperature. Cesium excitation temperatures are extracted using a method based on ratios of emission line intensities. Average excitation temperatures of roughly 3000 K are found at ambient cathode temperature, falling to nearly 1500 K at high cathode temperatures. At low cathode temperature and near the negative glow, several high n states of Cs show population inversions. This is possibly explained by collisional dexcitation of argon with a contribution by optical pumping by the 805.3 nm Ar resonance line.

I-5 Measured and Predicted Etch Characteristics of Sulfur Hexafluoride RF Discharges, H.M. Anderson, Univ. of New Mexico - Experimental measurements made in SF_6/O_2 RF discharges used to etch Si wafers reveal numerous peculiarities. Single crystal Si etch rates can be as high as 10-20 μm's/min, whereas poly-Si rates under comparable conditions are lower by a factor of four. Small additions of O_2 to SF_6 increase poly-Si etch rates, whereas single crystal Si rates monotonically decrease with O_2addition. DC bias, at least in large scale commercial planar diode reactors, appears to be not only a function of power, but also oxygen percent. Finally, recombination rates in SF_6 discharges appear to be very fast, radically influencing extent of dissociation depending on pressure [1]. In this study, Monte Carlo simulation of the electron kinetics is used along with a kinetics code for gas phase chemistry to better understand which events and reaction paths dominate discharge behavior and lead to the above experimental observables.

1) K.E. Greenberg and P.J. Hargis, paper FA-1, 40th GEC, Atlanta, GA (1988)

I-6 Pulsed-Laser Generation of Acoustic Resonances in High Pressure Mercury and Metal Halide Discharges JERRY KRAMER AND WALTER LAPATOVICH GTE Labs --We describe a technique for probing gas temperature in operating arc lamps using acoustic resonances. Acoustic resonances were generated in high pressure 60 Hz discharges by pulsed-dye laser irradiation. The laser was fixed at wavelengths which were non-resonant with the vaporized species in the discharges and directed perpendicular to the discharge axis. The acoustic resonances were detected as a change in voltage, in analogy with the optogalvanic effect. The transient voltage waveforms observed yield information about the radial and azimuthal acoustic resonances. The average sound velocity and the average temperature in the radial plane were calculated from the frequency of the radial acoustic resonances. Differences in average temperature were easily observed between the Hg and metal halide discharges using this technique. Measurements were made as a function of voltage phase angle and axial position to examine the temporal temperature dependence and effects of segregation. A mechanism for generating the acoustic resonances is described. The interaction of the acoustic wave and the current carrying channel is addressed.

I-7 Radial Temperature Distributions in High Pressure Xenon Discharges.* S.S.POPOVIĆ, J.KOCEIĆ, Institute of Physics, Beograd, Yugoslavia-- Radiation intensity profiles of high pressure pulsed discharges in xenon were measured in a single shot by using a combination of telecentric imaging and multichannel detection techniques. Observations were made on several wavelengths ranging from ultraviolet to near infrared. Radial temperature distributions were obtained by comparing the intensity profiles with a 12000K-xenon radiation source which was calibrated by tungsten lamp, and by using the standard diagnostic techniques for optically thick plasmas. The results indicate that the choice of observation wavelength is quite critical with respect to validity of assumptions incorporated in diagnostic methods.

* Submitted by B. Bederson

I-8 Emission of Radiation from a Xenon Discharge at Medium Pressures, J. K. Berkowitz and P. Moskowitz, GTE Products Corp--We have investigated resonant 1467Å emission from a medium pressure (10-100 Torr) Xe discharge. For this work we have used a fluorescent lamp jacket with standard fluorescent cathodes as our discharge chamber. At these pressures, with AC or Pulsed DC operating conditions, we see a correlation between the peak in 1467Å emission and the period in the discharge operating cycle wherein there is a cold, relatively dense, electron gas (voltage crossover for AC operation, voltage turnoff for pulsed DC operation). Spectroscopic and laser probe techniques have been employed in investigating this phenomena. Details of our experimental work will be presented.

I-9 Stark Spectroscopy of Rydberg States in Plasmas, J. R. Shoemaker, B. N. Ganguly and A. Garscadden, Wright-Patterson Air Force Base OH 45433. --- Optogalvanic detection of high principal quantum number excitations in discharges provides spectra that illustrate line-broadening and splitting, line shift and intensity transfer caused by the Stark effect. Experimental spectra show the total effects of applied fields, self-consistent fields and microfields. Theory and experiments have been performed to demonstrate separation of these effects for plasma diagnostics. Model calculations for hydrogen and helium show the initial overlap of high n manifolds (Inglis-Teller relation) to be a sensitive diagnostic for low electric fields if modifications are made for finite laser linewidth, polarization and quantum defects. Nomographs relating "last 100% modulated level", linewidth and electric field have been generated for discharge parameters of gaseous electronics interest.

I-10 Electric Field Profile Measurement in an Obstructed Hydrogen Discharge, B. N. Ganguly, J. R. Shoemaker and A. Garscadden, Aero Propulsion Laboratory, Wright-Patterson Air Force Base OH 45433. --- Spatially resolved axial and radial electric field values have been measured in a planar diode dc hydrogen discharge with PD $<$ 0.3 torr cm and current density $<$ 1ma/cm^2. The electric field values are obtained from spontaneous emission measurements of Stark splitting and broadening of polarization dependent H_β and H_γ lines. The electric field profile and the atomic emission intensities show that this discharge behaves like a collisional sheath suggesting formation of an obstructed discharge. The electric field gradient is approximately linear over most of the interelectrode distance. Very high field values (greater than 1 kv/cm) are measured throughout the interelectrode space. The discharge also displays a positive impedance characteristic. Small radial variation of electric values are observed over most of the electrode diameter indicating essentially one-dimensional characteristics of this discharge.

I-11 Space and time resolved electric field vector measurements in two dimensional DC and RF discharges using laser Stark spectroscopy of NaK : H. DEBONTRIDE, J. DEROUARD, N. SADEGHI, Univ. of Grenoble I, France -- We shall present results concerning the determination of the electric field in glow discharges established in potassium/rare gas mixtures by means of the laser e-f Stark mixing spectroscopy[1] in NaK[2]. Analysis of the polarization of the laser induced fluorescence signal of NaK is used to determine the electric field lines in two dimensional DC discharges : a large radial component is seen close to the edge of the electrodes, and also in the bulk of the plasma when the length of the shieth is not small in front of the electrode radius. We find also that the onset of the negative glow is an equipotential. We have also performed experiments to study the oscillation of the electric field in RF (0.3 - 1.3 MHz) discharges.

[1]R.A. Gottscho, Phys. Rev. A36, 2233 (1987)
[2]J. Derouard and N. Sadeghi, Opt. Comm. 57, 239 (1986).

I-12 Electric Field Measurements in the Cathode Fall Region of DC Glow Discharges Using the Relative Intensity of Stark Enhanced Forbidden Transitions, H. SHAN, M.A. CAPPELLI and S.A. SELF, Stanford University- Measurements of the electric field strength have been made in both normal (J=0.5 mA/cm^2) and abnormal (J=4 mA/cm^2) DC glow discharges in helium using the ratio of emitted intensities of forbidden and allowed transitions with the same upper level. Absolute measurements required estimates of the far infrared oscillator strengths or oscillator strength ratios. Agreement has been obtained between the measured electric fields and the fields predicted using a simple model of the cathode fall region, based on semi-empirical expressions for the ion mobility and net charged species generation rate. The results indicate a close to linear decrease in the electric field with distance from the cathode and are in close agreement with other recent measurements using laser optogalvanic spectroscopy. In general, this technique is applicable to any atomic species and can be used in conjunction with laser induced fluorescence in both DC and time-varying discharges. It is suitable for measurements of low field strengths (< 100 V/cm) when careful selection of the forbidden and allowed line pairs is made.

I-13 Ion Bombardment Angle and Energy Distributions in Argon and SF_6 rf Discharges, J. LIU, J.W. BUTTERBAUGH, G.L. HUPPERT, and H.H. SAWIN, M.I.T.-- The ion-impact angle distributions from a glow discharge have been measured using an orifice array in the electrode and spherical retarding grids. A large fraction of the ions do not strike perpendicularly on the surface; in an argon discharge, the peak ion impact angle ranges from about 5^o to 20^o off normal for pressures of 15 mtorr to 200 mtorr, respectively. These results are similar to that predicted by Thompson *et al*[1]. Data will be presented on the ion impact energy distribution for pressures ranging from 15 mtorr to several torrs and power ranging from 0.05 to 1 W/cm^2. In addition, the sheath thickness was observed by spatially resolved plasma induced emission. This was used to calculate the number of ion mean free paths in the sheath which is needed for comparison with the previous model.

[1]B.E. Thompson, H.H. Sawin, and D.A. Fisher, J. Appl. Phys. 63(7), 2241 (1988).

I-14 Numerical Calculation of Breakdown Channels in a Dielectric-Barrier Discharge, B. ELIASSON and W. EGLI, ASEA BROWN BOVERI, Corporate Research, 5405 Baden, Switzerland - Numerical calculations of the breakdown characteristics of dielectric-barrier discharges are presented. The discharge gap consists of plane and parallel electrodes which are separated by a gap of a few mm. One of the electrodes is covered by a dielectric of arbitrary thickness. Molecular oxygen at about atmospheric pressure was used to test the calculations. By applying a field across the gap which is larger than the corresponding Paschen- field the gap breaks down resulting in a statistical distribution of microdischarge channels. We calculate the temporal and spatial distribution of the electric field, ions and electrons within such a current filament. Some of the calculated parameters, like the current pulse and charge, are compared to measured data [1]. The time-dependent problem was solved in two dimensions (axial and radial) by solving the equation of continuity for the electrons and ions and the Poisson equation for the electric field. All ions were assumed to be stationary during the duration of the current pulse (< 100 nsec). The Poisson equation was solved with a fast Poisson solver and the equation of continuity with a method of characteristics.

[1]G. Mechtersheimer, B. Eliasson and U. Kogelschatz, Proceedings of the IX Int. Conf. Gas Discharges and Their Applications, Venice, September 19-23, 1988.

I-15 The role of ionization by fast atoms and ions in the electrical breakdown of Ar at high voltages and low pressures,* A.V. PHELPS† and B.M. JELENKOVIĆ,‡ JILA, University of Colorado and NBS. -- A recent[1] model of electron, ion, and fast atom motion in Ar at very high E/n is applied to electrical breakdown. The highly nonequilibrium electrons are treated using a single-beam, energy-balance model. The Ar^+ are in equilibrium with the field and produce fast Ar in charge transfer collisions. If experimental breakdown voltages > 1 kV are modeled using only electron-impact ionization, the derived secondary electron yields at the cathode are much larger than measured by beam techniques at the calculated ion energies (≈ 100 eV). Experimental breakdown voltages and realistic secondary electron yields are obtained by adding to the model ionization by ions, fast atoms, and electrons backscattered from the anode.

[1] A.V. Phelps and B.M. Jelenković, Phys. Rev.(in press).

* Supported in part by Lawrence Livermore Laboratories.

† Quantum Physics Division, NBS and Physics Dept., CU.

‡ Permanent address: Institute of Physics, Belgrade, Yugoslavia.

I-16 Streamer Propagation in Attaching Gases, S. K. DHALI and A. SARKAR, Southern Illinois University --The results of computer simulations of streamer development and propagation are reported for SF_6 and SF_6/N_2 mixtures. This is an extension of an earlier work on streamer propagation in pure N_2 and SF_6.[1,2] The transport, ionization and attachment coefficients in SF_6/N_2 mixtures are calculated using the Monte Carlo technique. The relevant continuity equations and Poisson's equation are solved self-consistently to simulate the propagation of streamers. The role of attachment, space-charge field, secondary electrons, and the shape and size of the initiating charge have been determined.

[1] S.K. Dhali and P.F. Williams, J. Appl. Phys. 62, 4696 (1987)

[2] S. K. Dhali and A. K. Pal, J. Appl. Phys. 63, 1355 (1988).

I-17 Copper Contamination in An Electric Arc, G.Y. Zhao, M. Dassanayaki, K. Etemadi, Department of Electrical and Computer Engineering State University of New York at Buffalo, The impact of the contamination of copper vapor, evaporated either from the cathode or from the anode, on the entire plasma region is studied by a numerical method. The arc is generated between a cone-shpaed cathode and a flat anode operating at atmospheric pressure with an electrode gap spacing of 1 cm and at a current of 200 A. In the case of cathode contamination, the copper vapor in the cathode region has a velocity of 210 m/s with a mass concentration above 90% within 0.5 mm from the arc axis. In the anode region the velocity of the vapor drops to 90 m/s with more than 90% copper vapor still concentrated within 0.9 mm from the arc axis. In the case of anode contamination, the effect of the vapor in the cathode region and core of the arc is negligible.

I-18 Experimental Studies of Anode Boundary Layers in High-Intensity Arcs, E. LEVERONI & E. PFENDER, U. of Minnesota -- The plasma near the anode of free-burning, high-intensity argon arcs, characterized by strong deviations from kinetic & chemical equilibrium, was investigated by means of electric probes.Electric probes provide data which can be interpreted without introducing assumptions about the thermodynamic state of the plasma.Results of parametric studies are presented for clarifying the effects of arc current, electrode gap (flow field), and operating pressure on the properties of the boundary layer.The electron temperatures are shown to remain in the order of 10^4K whereas the heavy species temperature drops to the temperature of the water cooled anode. Diffusional effects due to the steep gradients are related to the relative magnitude of the measured ion and electron currents, & to the existence of conditions which make a reversal of the electric field[1] in the boundary layer possible. The effects on the heat transfer to the anode are discussed.

[1]H.A.Dinulescu & E. Pfender, J. Appl. Phys. 51, 3149 (1980).

I-19 Nucleation and Growth of Plasma-Synthesized Powders*, C.-P. CHIU, R. MUNO and S. L. GIRSHICK, U. of Minnesota—Fine particle formation in a thermal plasma reactor typically results from homogeneous nucleation of a highly supersaturated vapor. Depending on the chemical system, in many cases the subsequent particle growth can be described as an irreversible Brownian coagulation, determined by free-molecule kinetics of monomer, clusters and particles. Final particle size is affected by reactant concentrations and flow times. For a constant gas cooling rate, we show that the resulting particle size distribution follows a modified self-preserving form which accounts for the fact that coagulation rates for a given particle size increase as the gas cools. We discuss applications and limitations of this model for actual plasma synthesis conditions. We have recently constructed an apparatus consisting of an inductively-coupled rf plasma tube, a porous-wall reaction tube with injected flow to suppress wall deposition, and an aerosol sampling probe for on-line particle size measurements. Experimental results will be presented if available at the time of the Conference.

*Work supported by National Science Foundation, Grant No. CBT-8805934, and by the Graduate School of the University of Minnesota.

I-20 Two-dimensional magnetic field effects in inductively-coupled atmospheric-pressure hydrogen plasmas*, W. YU and S. L. GIRSHICK, U. of Minnesota—Recent calculations for inductively-coupled argon plasmas were reported which included a two-dimensional magnetic field based on the electromagnetic vector potential formalism, and the results were compared to calculations which assumed a one-dimensional magnetic field[1]. We report similar calculations for hydrogen plasmas. The effects of the radial magnetic field were found to be generally greater for hydrogen than for argon. In particular, Lorentz forces in the hydrogen plasma were found to have a large peak axial component in the direction opposite to the flow—of the same order as the peak magnitude of the radial component—while this effect was weaker for argon. Hence flow recirculation and on-axis flow reversal in the coil region are caused by axial forces as well as by radial pinch.

*Work supported by the Graduate School of the University of Minnesota and by the Minnesota Supercomputer Institute.

[1]Mostaghimi, J. and Boulos, M., *Plasma Chem. Plasma Process.*, in press (1988).

I-21 Photodissociation of H_3* P. C. Cosby and H. Helm, SRI International - We report the first observation of H_3 photodissociation. A fast beam of H_3 molecules is prepared by charge-transfer of H_3^+ in Cs and is intersected by a tunable dye laser. Predissociation of the optically prepared $3s\,^2A_1'$ and $3d\,^2E''$ states by the $X\,^2E'$ ground state is detected by monitoring the production of correlated pairs of H_2 molecules and H atoms with a position and time sensitive detector.[1] Product rovibrational excitation is resolved by the detector and is found to be highly dependent on H_3 electronic and nuclear configuration. Evidence is also found for dissociation into three H atoms. The observed spectra provide estimates of the vibrational spacings in the 2p, 3s, and 3d states and, in combination with recent photoionization measurements,[2] provide the first accurate experimental value for the dissociation energy of H_3^+.

*Research supported by AFOSR.
[1]H. Helm and P. C. Cosby, J. Chem. Phys. 86, 6813 (1987).
[2]H. Helm, Phys. Rev. Letters 56, 42 (1986); Phys. Rev. A 38 (in press).

I-22 Laser-Induced Photodetachment of O^- in an Oxygen dc Glow Discharge* G. GOUSSET, J. JOLLY and M. TOUZEAU, L.P.G.P., Univ. Paris-Sud, Orsay, France -A quasi-neutral theory of the positive column in electronegative gases, based on fluid momentum equations, was used to describe charged particle concentrations and radial profiles. In order to verify the negative ion spatial distributions predicted by the theory, laser-induced photodetachment experiments were performed, using a second harmonic generation Nd-Yag laser (532 nm) with an energy up to 200mJ in 10ns pulse duration. According to the reaction $O^- + h\nu \rightarrow O + e + 0.87$ eV, the detached electrons induce in the positive column of the discharge ($p = 0.1$-5 torr, $I = 1$-100 mA) an intense optogalvanic signal (1-20 mA). Detailed study of spatially-resolved optogalvanic signals allows the determination of the radial profile of negative ions. The optogalvanic currents calculated from the negative ion and electron radial densities predicted by the model are in good agreement with the experimental data.

*Research supported by CNRS

I-23 Resonant Multiphoton Ionization Spectroscopy in an Hydrogen Flowing Afterglow Experiment,* G. SULTAN, G. BARAVIAN, G. JOLLY, and P. PERSUY, L.P.G.P., U. of PARIS-SUD 91405 ORSAY FRANCE -Resonance-enhanced multiphoton ionization is studied in a flowing afterglow discharge in hydrogen (P= 1-10 Torr, I=10-100 mA). The laser beam is focused 30 cm downstream the discharge where electrical charges resulting from multiphoton ionization are collected. When the laser wavelength is tuned in the range 305-308 nm, several resonances occur and a spectrum is recorded. Resonances are interpreted as molecular and atomic 3 photon excitation, the absorption of one more photon leading to ionization. The slope of the curve giving the electron signal versus the laser energy, in a log-log plot and at a wavelength of 307.26 nm is found to be 2.5 for laser energies less than 5mJ and 1.2 for greater energies.

* Work supported by DRET and CNRS.

I-24 Positron and Electron Differential Elastic Scattering from Inert Gases at Intermediate Energies*, STEVEN J. SMITH, G.M.A. HYDER, W.E. KAUPPILA, C.K. KWAN, and T.S. STEIN, Wayne State U. --A crossed-beam experiment[1] is being used to measure relative elastic differential cross sections (DCS's) for intermediate energy (up to 300 eV) positrons and electrons scattering from helium, neon, and argon at angles ranging from 30-135°.[2] An incentive for this work relates to the observed[2] merging (to within 2%) of the respective positron and electron total cross sections for helium at 200 eV, and near merging for neon and argon. Our results for argon[1] and preliminary results for neon and helium indicate that the positron DCS curves monotonically decrease with increasing scattering angle, while the electron curves may exhibit considerable structure. Comparisons of these measurements with each other and with theoretical calculations may help lead to a better understanding of the static and polarization interactions as they contribute to positron and electron scattering by atoms and molecules.

*Research supported by NSF Grant PHY-8706120.

[1] G.M.A. Hyder et al., Phys. Rev. Lett. 57, 2252 (1986).
[2] W.E. Kauppila et al., Phys. Rev. A 24, 725 (1981).

I-25 Total Cross Section Measurements for Positron- and Electron-Na and Rb Collisions,* T.S. STEIN, M.S. DABABNEH, W.E. KAUPPILA, C.K. KWAN, R.A. LUKASZEW, S.P. PARIKH, and Y.J. WAN, Wayne State U.--We are using a beam transmission technique[1] to measure total scattering cross sections (Q_T's) for positrons and electrons (4 to 100 eV) colliding with Na and Rb. These preliminary measurements along with our earlier results for potassium[1] indicate mergings (or at least near-mergings) of the corresponding positron- and electron-alkali atom Q_T values as the energy is increased just above 30 to 40 eV, while as the energy is lowered below 30 eV, the positron Q_T's tend to become increasingly higher than the corresponding electron Q_T's. This is in sharp contrast[1] to the cases for all of the room-temperature gases for which positron- and electron- Q_T comparison measurements have been made, where the positron Q_T's tend to be significantly lower than the corresponding electron Q_T's at low energies, and mergings tend to occur at considerably higher energies than where they have been observed for the alkali-metal atoms.

*Work supported by NSF grant PHY-8706120

[1]T.S. Stein et al., in: Atomic Physics with Positrons, edited by J.W. Humberston and E.A.G. Armour, (Plenum Press, New York, 1987), p. 251.

I-26 Absolute elastic differential cross sections of electrons scattered by $3^2P_{3/2}$ sodium,* M. ZUO, T.-Y. JIANG, L. VUŠKOVIĆ, AND B. BEDERSON, New York U,--We report on the first measurements of absolute differential cross sections (DCS) for electrons elastically scattered by $3^2P_{3/2}$, F=3 laser-excited sodium at 3 eV, over an angular range of 25^o to 40^o. The excitation is by σ^+ or π light resulting in atomic sublevel populations of polarized and aligned distributions respectively. Photon recoil[1] is used to both separate and assay the relative populations of ground and excited states. In the same angular range we also measure the corresponding ground-state elastic DCS's 3S→3S. The excited state CS's are about one order of magnitude larger than the ground state ones; the CS's with excitation by σ^+ are about 20% smaller than by π light. Measurements will be compared with available computations.

*Supported by NSF

1. B. Jaduszliwer et al, Phys. Rev. A, 33, 3792 (1986)

I-27 Electron Impact Ionization Cross Section Measurements of the Cu, Fe, P and Si Atoms. R. S. FREUND, R. C. WETZEL, and R. J. SHUL, AT&T Bell Laboratories ---- Absolute electron impact cross sections for single and double ionization of the copper, iron, phosphorous, and silicon atoms have been measured from threshold to 200 eV, with an accuracy of ±15%. Ions formed in a dc discharge are accelerated to 3 keV and are neutralized by charge transfer with triethylamine. Threshold measurements are used to determine the fraction of excited state atoms in the neutral beam. All 4 atoms have single ionization cross sections which peak at about 4 times the threshold energy. These are the first reported measurements of the Fe, P and Si cross sections. Of 3 previous Cu measurements, our results agree best with those of Pavlov et al. [Sov. Phys. JETP 25, 12 (1967)].

I-28 Electron-impact excitation of atomic oxygen*. S. S. TAYAL and RONALD J. HENRY, Louisiana State University -- Excitation of several excited states of atomic oxygen has been studied in detail for electron impact energies from 13.87 to 100 eV by use of a close-coupling approximation. The target states included in the expansion of the total wave function are represented by accurate configuration-interaction wave functions. We include the twelve low-lying states $2p^4\ ^3P$, $2p^3 3s^{5,3}S^o$, $2p^3 3p^{5,3}P$, $2p^3 4s^{5,3}S^o$, $2p^3 3d^{5,3}D^o$, $2p^3 4p^{5,3}P$, and $2p^3 3s^3D^o$. The present results are in good agreement with recent experiments for the dipole-allowed ^3P-$3s^3S^o$ and ^3P-$3d^3D^o$ transitions, but for the forbidden ^3P-$3p^3P$ transition a large unresolved discrepancy exists.

*Work supported in part by NASA grant NAGW-48.

I-29 Integral and Differential Cross Sections for $e^-+He(2^{1,3}S)$ Collisions,* E. J. MANSKY AND M. R. FLANNERY, Georgia Institute of Technology - The multichannel eikonal theory results for the integral and differential cross sections for $e^-+H(2s)$ and $e^-+He(2^{1,3}S)$ collisions for incident electron energies E from 20 eV to 1 keV are examined. Comparison with available experimental data indicates that careful examination of the convergence of the integral and differential cross sections, with respect to the complex excitation amplitudes, must be made in order for accurate results to be obtained. Cross sections for electron-impact excitation of $H(1s)$ and $He(1^1S)$ will also be presented and compared with available experimental data.

*Research supported by U. S. Air Force Office of Scientific Research under Grant No. AFOSR-84-0233.

I-30 Electron Impact Vibrational Excitation of Small Molecules* S. ALSTON,+ G. SNITCHLER, and D. NORCROSS,‡ JILA, Univ. of Colo. and NBS -- The electron impact excitation of H_2 and HF has been studied using a fully vibrational close-coupling (VCC) program. An exact treatment of exchange is used in the separable representation. Correlation and polarization are represented by parameter-free model potentials (BTAD[1] and VCOP). Results are compared with measurements, model exchange VCC calculations, and with the adiabatic nuclei approximation.[1]

*Research supported by National Science Foundation grant PHY86-04504 to the University of Colorado.
+Present Address: Dept. of Physics, Penn. State Univ., Lehmann, PA, 18627
‡Quantum Physics Division, National Bureau of Standards

[1]M. A. Morrison and B. Saha, Phys. Rev. A 34, 2786 (1986); and personal communications.

I-31 Studies of Low – Energy Electron Scattering by Molecules*, H. PRITCHARD, C. WINSTEAD, K. WATARI†, V.MCKOY,California Institute of Technology, M. A. P. LIMA, F. J. daPAIXAO, and L. M. BRESCSANSIN, Instituto de Fisica, Unicamp, S. P. Brasil. – Elastic and inelastic scattering of electrons by several molecules have been studied using the Schwinger Multichannel method. Elastic differential, integral, and momentum transfer cross sections have been studied for e-NH_3, e-C_2H_4, and e-C_2H_6 from 5 to 20eV. These results are compared with recent experimental data. Electron impact excitation cross sections for H_2 ($a^3\Sigma_g^+$, $b^3\Sigma_u^+$,$c^3\Pi_u$), CO ($a^3\Pi$,$a'^3\Sigma^+$,$d^3\Delta$,$e^3\Sigma^-$) , and N_2 ($A^3\Sigma_u^+$,$W^3\Delta_u$, $B'^3\Sigma_u^-$) have been obtained from multichannel calculations, results of which will be reported. Preliminary results of impact excitation of the lowest energy $^3B_1$ and $^3A_1$ states of H_2O will also be discussed. Extension of the method to open-shell systems and results of its application to e-O_2 collisions will also be discussed[2].

*Supported by NASA-Ames Cooperative Agreement NCC 2-319, NSF Grant PHY- 8604242, and the Innovative Science and Technology Program of SDIO Contract DAAL 03-86-K-0140.
†Supported by CNPq(Brasil).
[1]M. A. P. Lima, F. J. daPaixao, L. M. Brescansin, and V. McKoy, Phys. Rev. A (to be published).

I-32 Use of the PDE Method in Dissociative Recombination C.A. WEATHERFORD†, Florida A&M U., W.M. HUO, NASA Ames Research Center – We describe the use of the Partial Differential Equation (PDE) method[1,2] in dissociative recombination. The PDE method is a non-iterative solution of the Schrödinger equation by finite differences and avoids a partial-wave decomposition. New features of the PDE method developed for electron-positive ion collisions are: (1) the use of Coulomb functions on the asymptotic PDE boundary; and (2) the explicit calculation of the continuum orbital. The computed width for the $e^- + H_2^+ \rightarrow H + H$ reaction will be compared with experiment and other calculations.

†Supported by NASA Grant NCC 2-492
[1]A. Temkin in *Symposium on Electron – Molecule Collisions*, ed. by I. Shimamura and M. Matsuzawa (U. of Tokyo, Tokyo, 1979),p.55.
[2]E.C. Sullivan and A. Temkin, Comp.Phys.Comm. 25,97(1982).

I-33 Dissociative Ionization of Laser Excited N_2^* by Electron Impact,** D. P. WANG and L. C. LEE, San Diego State U. and S. K. SRIVASTAVA, JPL, Calif. Inst. of Tech.--N_2 molecules were excited by ArF (193 nm) laser photons and then dissociatively ionized by electron impact. The apparatus includes an electron beam, an excimer laser and a molecular beam. N^+ ion signals enhanced by laser irradiation were observed, and the dependence of the enhanced signals on laser power, N_2 pressure, and low electron beam current were investigated. The enhanced ion signal is attributed to electron impact ionization of the laser excited N_2^* which is mainly in the $A^3\Sigma_u^+$ state. The excitation function for the production of N^+ ions by electron impact on N_2^* was measured in the 17-32 eV region. The threshold for the laser enhanced signal is about 17 eV.

**Work sponsored by the SDIO/IST and managed by ONR under Grant No. N00014-86-K-0558.

I-34 Electron Impact Excitation of the $a^3\Pi$, $a'^3\Sigma^+$, $d^3\Delta$ and $A^1\Pi$ States of CO at Low Energies*, P. W. ZETNER, I. KANIK, J. C. NICKEL ans S. TRAJMAR, Jet Propulsion Lab., Caltech and U. of Calif. Riverside – Differential excitation cross sections were determined at 12.5 and 15.0 eV impact energies in the 10° to 140° angular range. Normalization of the data to the absolute scale was achieved by a recently established procedure described elsewhere by Nickel et al.(1) Integral cross sections were obtained by extrapolation and integration. The results and comparison with recent theoretical calculations will be presented.

* Work supported in part by the National Aeronautics and Space Administration and in part by the National Science Foundation.

(1) J. C. Nickel, P. W. Zetner, G. Shen and S. Trajmar (To be submitted to J. Phys. E).

I-35 Total Low-Energy Electron Scattering Cross Sections for SiF_4,* Phillip B. Lieschesk, Ce Ma, Kyung-Hee Chung and R.A. Bonham, Chemistry, Indiana U. -- Total electron scattering cross sections for SiF_4 are measured by a simple transmission experiment. A low-current electron beam from a low-energy adjustable (4-50 eV) electron gun is allowed to pass through static gas into a Faraday cup. With the Faraday cup and a Keithley 642 electrometer, the transmission of the electron beam is measured. The gas pressure within the chamber is monitored by three MKS capacitance gauges and an MKS spinning-rotor gauge. The scattering distance can be changed by adjusting the positions of the electron gun and/or the Faraday cup within the chamber. While maintaining constant pressure, temperature and incident electron energy the effective scattering length is varied in order to measure the total cross section.

* Work supported by the National Science Foundation through grant number CHE-8600746.

I-36 A Study Of The Angular Momentum Dependence Of Phase Shift For Finite Range and Coulomb Potentials, S.R. VALLURI, University of Western Ontario, London, Canada, and W.J. ROMO, Carleton University, Ottawa, Canada - The dependence of the phase shift delta (L,K) on the angular momentum L is studied. An analytic expression for the derivative of the phase shift with respect to angular momentum is derived for a class of potentials that include complex and real potentials. The potentials behave like the finite range potential for small R and like a coulomb potential for large R. Specific examples like the square well, the pure point charge coulomb and a combination of a square well and the coulomb potential are analytically treated. Possible applications in heavy ion collisions are expected.

I-37 Laser Induced Fluorescence Studies in Hg-Ar rf Discharges, J.L. Streete, J.M. Christman and L. Maleki, Jet Propulsion Laboratory, California Institute of Technology--We will report on a laser induced fluorescence (LIF) study in Hg-Ar rf discharges, performed to determine the relative populations of Ar and Hg under various discharge conditions. The rf discharge was produced in a cell containing a small amount of Hg and Ar at pressures ranging from 100 mTorr to 1 Torr. The $^3P_2$ level of Hg populated in the discharge was excited via the 546.1 nm transition by resonant laser light. The laser's influence on the discharge was first determined through measuring the optogalvanic and fluorescence signals for the $^3P_2$ $^3S_1$ transition at each Ar pressure, discharge power, and laser power. LIF signal for the level of interest was then measured and compared to these signals to infer the laser's influence on the population of the level under study. Results will be given for a number of transitions in Ar, Hg, and Hg ion.

I-38 New Variational Approaches to Electron-Molecule Scattering* T. N. RESCIGNO, LLNL and C. W. McCURDY, OHIO STATE UNIV.,--Recent progress in applying the complex S- or T-matrix versions of the Kohn variational method to low-energy electron-diatomic molecule scattering is described. Results are presented for electron-impact dissociation of H_2. We will also describe an extention of the method suitable for application to polyatomic targets. Special methods are needed to evaluate continuum matrix elements. These include adaptive three-dimensional quadrature techniques, specifically tailored to handle Coulomb singularities at the nuclear centers, as well as pseudospectral methods.

* Work performed under the auspices of the U. S. Department of Energy by the Lawrence Livermore Laboratory under contract W-7405-ENG-48.

SESSION JA

8:00 AM - 8:50 AM, Thursday, October 20

Radisson Plaza Hotel - East Ballroom

SILANE PLASMAS

Chairperson: G. Hays, Sandia National Laboratories

JA-1 Negative Ion Kinetics in Silane Plasmas, Alan Garscadden, Wright-Patterson Air Force Base 45433. --- Negative ions in plasmas are trapped by self-bias and ambipolar fields and their losses are determined by detachment and recombination rather than by diffusion. Calculations have been made of ion formation rates in silane using the new cross section data of Srivastava et al, for dissociative attachment (DA). In argon-silane, 95:5, rates at 80 Td are: ionization $k(I)=10^{-10}$, $k(DA)\ 10^{-11}$ and detachment by electron collisions, $k(ED) = 10^{-8} cm^{-3} s^{-1}$. The ED rates were obtained by analogy to experimental results for ionization of H^- by electron impact. The data confirm that silane is a weak attacher. The usual plasma boundary conditions and ED being dominant over neutral collisional induced detachment, will, however, permit the build-up of negative ion densities to $k(DA)Na/k(ED)$ where Na is the attacher density. Large concentrations will result in weakly ionized plasmas. $k(I)$ is a strong function of E/N and $k(DA)$, $k(ED)$ are relatively weak functions, however, $[d \ln k(DA)/d(E/N)]\ [d \ln k(I)/d(E/N)]$ may exceed unity indicating instability.

JA-2 Measurements of Electron Swarm Parameters in Silane, D. K. DAVIES, Westinghouse R&D Center -- Measurements of electron and ion mobility and net ionization coefficient have been carried out in pure silane using a pulsed drift tube. The electron mobility has been measured over the range $0.1 \leq E/N \leq 1000$ Td and, for $E/N > 65$ Td, the present values are the first to be reported. For $E/N \leq 65$ Td, the present values are in excellent agreement with those of Pollock.[1] For values of $E/N < 1$ Td, the mobility is found to be constant, having a mean value of $(3.10 \pm 0.03) \times 10^3$ cm^2/Vs; this value corresponds to thermal electrons. Measurements of positive-ion mobility and net ionization coefficient have been made over the range $200 \leq E/N \leq 1400$ Td. For values of $E/N < 500$ Td, the positive-ion mobility has a constant value of 1.28 ± 0.01 cm^2/Vs and is tentatively identified with the thermal mobility of the SiH_3^+ ion. The present values of the net ionization coefficient differ from the only other previous measurements[2] by up to 35% in the region of overlap.

[1]W. J. Pollock, Trans. Faraday Soc. 64, 2919 (1968).
[2]M. Shimozuma and H. Tagashira, J. Phys. D19, L179 (1986).

JA-3 The Plasma-Surface Interface in PECVD of Amorphous Silicon,* MICHAEL J. MCCAUGHEY and MARK J. KUSHNER, University of Illinois, Urbana, IL--The PECVD of amorphous hydrogenated silicon (a-Si:H) is usually performed in RF discharges sustained in silane. Electron impact dissociation of silane generates SiH_3 and SiH_2 radicals which are adsorbed on the substrate. The rate of incorporation of those radicals into the film depends on plasma conditions such as ion bombardment. Some fraction of the radicals will desorb from the substrate, enter the plasma, and may influence the electron kinetics. In this paper we report on a Monte Carlo computer simulation of the plasma-surface interface in PECVD of a-Si:H. The model examines the adsorption of SiH_3 from the plasma, incorporation into the lattice, and its subsequent desorption from the surface as Si_2H_6 due to its low sticking coefficient. The generation rate of Si_2H_6 from the surface reactions are compared to the generation rate due to plasma reactions. The effects of Si_2H_6 from this source on the plasma chemistry is examined.

* Work supported by Army Research Office.

JA-4 Low Temperature, Low Pressure, RF Plasma Synthesis of Ultrafine, Ultrapure Ceramic Powders, H. M. Anderson, University of New Mexico -- Gas-phase nucleation and particulate formation during plasma processing for thin film applications is generally regarded as a "pernicious problem." Regrettably, it is little known that powders formed in low pressure discharges may also possess quite desirable properties as precursors to structural and electronic ceramics. In this study, it is shown that a SiH_4/NH_3 discharge can be adjusted to encourage gas-phase nucleation and production of ultrapure, submicron sized powders. Dependent on discharge parameters, the silicon nitride powders can be tailored to be stoichiometric, Si-rich, or N-rich, and virtually free from oxygen contamination, a frequent problem to other non-oxide ceramic powder synthesis techniques. The as-produced powders are shown to be weakly agglomerated, amorphous aggregates of primary particles in the range of 20-40 nm. These results are examined in light of the present knowledge of the gas-phase kinetics of silane and ammonia discharges. Subsequent heating of the powders results in transition to α-crystalline Si_3N_4 which is critical for ceramic applications.

SESSION JB

8:00 AM - 9:20 AM, Thursday, October 20

Radisson Plaza Hotel - West Ballroom

BEAM-PLASMA INTERACTIONS

Chairperson: J. L. Shohet, University of Wisconsin

JB-1 A Hollow Cathode Arc Source for Beam-Plasma Experiments* J. B. ROSENZWEIG, Argonne National Laboratory - The experimental observation of Plasma Wake-field Acceleration (PWFA) requires use of a dense, quiescent plasma source which has a reliably reproducible, nearly uniform density profile along an axis of symmetry. We have developed a hollow cathode arc source which satisfies the unique requirements for studying this beam-plasma interaction at the Argonne Advanced Accelerator Test Facility. We present here the operational characteristics of the source, and results of the PWFA experiments. The diagnosis of this device is discussed, with emphasis on the new, novel determination of the plasma density from direct observation of the frequency of the PWFA waves (the plasma frequency) by a bunched electron probe beam.

*Work supported by U. S. Dept. of Energy, Division of High Energy Physics, Contract No. W-31-109-ENG-38.

JB-2 Monte Carlo Simulation of Ion Cooling in EBIT.* B. M. PENETRANTE and J. N. BARDSLEY, Lawrence Livermore National Laboratory -- The Electron Beam Ion Trap (EBIT) at LLNL produces and confines very highly charged ions (HCI). The charge limit and confinement time reached by these HCI's are effectively increased by continuously injecting a coolant composed of low-charged ions (LCI). The LCI's absorb energy from the HCI's through ion-ion collisions and escape the trap faster, thus cooling the HCI's. We perform a Monte Carlo simulation of this ion-collisional cooling mechanism in order to quantitatively assess and predict the charge states, energy loss and escape rates of the ions in EBIT. Results are presented for a Au-Ti ion mixture, for which EBIT has successfully trapped Au(69+) for several minutes.

Work performed under the auspices of the U. S. Department of Energy by the Lawrence Livermore National Laboratory under contract number W-7405-ENG-48

JB-3 Electron Energy Deposition in Partially Ionized Atomic Nitrogen Plasmas,* B. M. PENETRANTE and J. N. BARDSLEY, Lawrence Livermore National Laboratory -- We use a discrete-energy-bin code to study high-energy electron-beam deposition in partially ionized atomic nitrogen plasmas. The degradation of energy to plasma heating, electron-ion pair production and excitation processes are computed. Two types of applications are considered: one in which energetic electrons are completely stopped by the medium; the other in which a continuous beam passes through the plasma. We show that the functional dependence of the energy loss rates on the beam energy and ionization degree strongly depend on the type of application. Thus, for electron-beam propagation studies, for example, the radial energy loss modes will be different from the axial ones.

*Work performed under the auspices of the U.S. Department of Energy by the Lawrence Livermore National Laboratory under contract number W-7405-ENG-48.

JB-4 Model of Multiphoton Ionization Resonant UV Laser-Atmosphere Interactions",* J. E. STOCKLEY, G. J. FETZER, L. D. NELSON, and L. J. RADZIEMSKI,** OPHIR Corporation --A model has been developed to simulate the effects of resonant multiphoton ionization due to a uv laser pulse directed vertically through the atmosphere. The model simulates the propagation of a 315.2 nm laser pulse from sea level to the upper homosphere. This wavelength has a 3+1 multiphoton ionization resonance with the $3p^5 4s\ ^1P_1^o$ excited state in naturally occuring argon. The purpose of the model is to examine the spatial and temporal perturbation of the local ion and electron concentrations in the atmosphere due to interaction of the laser radiation with the atmosphere. Both linear and nonlinear effects on the laser pulse propagation are taken into account. Using a rate equation formalism and a detailed collection of atmospheric chemistry reactions the model determines the concentrations of electrons and ions of major atmospheric constituents as functions of altitude, time and laser energy.

*This work supported by the Department of Energy under contract number DE-AC03-86SF16039.

**Physics Department of New Mexico State University Box 3D, Las Cruces NM 88003-0004.

JB-5 High Energy Heavy Ion Beam Pumped Plasmas. D. E. MURNICK, AT&T Bell Laboratories, Murray Hill, NJ 07974, A. ULRICH, B. BUSCH, W. KROTZ and G. RIBITZKI, Technical University, Munchen, 8046 Garching, FRG.-In a program to study the feasibility of pumping shortwavelength lasers with heavy ion beams, the *vuv* emission from gaseous and solid targets was studied by time resolved optical spectroscopy. Ion beams ranging from ^4He to ^{238}U were used with maximum instantaneous power of 1 MW in a 1 ns pulse. Intense excimer light from Ne_2 (74 nm), Ar_2 (127 nm), Kr_2 (146 nm) and Xe_2 (176 nm) were the dominant spectroscopic features from the rare gases at pressures above about 100 mtorr. The time evolution of the excimer formation and decay in the ion beam induced glow could be modelled. Interesting time evolution of the 3rd continuum band at 200 nm as well as that of various atomic and ionic lines in argon were noted. Experiments are now being designed for the synchrotron storage ring facility SIS/ESR under construction at GSI where heavy ion beam powers up to 200 GW will be available.

JB-6 Electron Beam Initiated Discharge Studies in Hydrogen Azide (HN_3) Gas Mixtures. M. W. WRIGHT and L. A. SCHLIE, Advanced Laser Technology Division (AFWL/ARBI), Air Force Weapons Laboratory, Kirtland AFB, N. M. 87117-6008.-The behavior of short pulse electron beam initiated discharges in hydrogen azide (HN_3) gas mixtures is reported. This highly energetic azide gas is of interest because its molecular kinetics indicates it has much potential for future visible/ultraviolet laser systems. Previously, no investigation of its electron kinetic/plasma physics behavior has been reported. Via a 3 nsec, 600 KeV electron ionizing pulse, the spectral and plasma behavior of such gas mixtures for different applied E/N values was obtained. The electron decay shows the effect of both recombination and attachment processes. Conditions are shown for the optimum production of the excited N_2(A,B,C) states. These excited states are very useful as energy reservoir for potential nitrogen metastable transfer laser systems. Some results may be presented on hydrogen azide mixtures with hydrogen sulfide (H_2S) and xenon difluoride (XeF_2).

SESSION KA

8:50 AM - 9:45 AM, Thursday, October 20

Radisson Plaza Hotel - East Ballroom

NON-EQUILIBRIUM ELECTRON TRANSPORT

Chairperson: Y. Li, GTE Laboratories

KA-1 Local Moment Theory of Electron Transport in Gases,* E. E. KUNHARDT and I. T. LU, Weber Research Institute, Polytechnic University --A theoretical description of the behavior of electrons in a background gas under the influence of an electric field is presented. It is based on the concept of local moments of the distribution. In contrast to the usual global moments (i.e., weighted velocity integrals with contributions from all velocity space), the contribution to the velocity integrals defining the local moments comes mainly from a finite interval in velocity space. Thus, local moments provide a measure of the local properties (in velocity) of the distribution. The formulation in terms of local moments is accomplished with the use of a generalized Gabor expansion.[1] The equations of evolution for the local moments are obtained using bi-orthogonality properties that have been obtained for the basis functions. The principal features of the theory are illustrated with an example.

*Work supported by the Office of Naval Research.

[1]N. J. Bastiaans Optik. 57, 95 (1980).

KA-2 The Influence of Electron Generation and Depletion on the Electron Kinetics in Gases,* G. SCHAEFER and P. HUI, WRI, Polytechnic University of New York -- The Monte Carlo Flux method was used to calculate steady state and transient electron distribution functions. Electron generation and depletion processes were incorporated directly into the Monte Carlo Flux code. This allows the direct calculation of the electron density for both steady state and transient conditions. The influence of electron generation and depletion mechanisms on the energy distribution is demonstrated.

* Work supported by NSF.

1. G. Schaefer and P. Hui, GEC Abstract, MB-3, p.171, Oct., 1987 and POLY-WRI-1518-87.

2. G.Schaefer, G.F.Reinking and K.H.Schoenbach, J. Appl. Phys., vol.61, pp. 120-125, Jan. 1987.

KA-3 Convective Scheme Modeling of Swarm Experiments and the Cathode Fall* T. J. SOMMERER, W. N. G. HITCHON, and J. E. LAWLER. U. of Wisconsin.—A convective scheme[1] (CS) has been used to model both swarm experiments and the cathode fall region of various DC glow discharges. The CS is an efficient algorithm for solving kinetic equations which reduces to an explicit finite difference scheme in the limit of small time steps. However, it is not restricted by the Courant-Friedrichs-Levy (CFL) criterion, and larger time steps may be used. Particles are allowed to traverse several grid spacings in a single time step, which is chosen based upon the physics of the problem (specifically, $\Delta t_{CS} < \min \tau(v) = \min [N\sigma(v)v]^{-1}$) rather than the specifics of the grid and the maximum velocity of the particles in the grid ($\Delta t_{CFL} < \Delta x / v_{MAX}$). The CS results will be compared to previous experiments and Monte Carlo calculations of swarms and the cathode fall region. Since the statistics of the CS (where all particles are tracked) are better than a Monte Carlo simulation, self-consistent electric field calculations are possible and will also be discussed.

* Supported by the AFOSR.

[1] J. B. Adams and W. N. G. Hitchon, J. Comput. Phys. **76**, 159 (1988); W. N. G. Hitchon, D. J. Koch, and J. B. Adams, Sandia Report No. SAND88-8652 (1988), to be published.

KA-4 Flux-Corrected Transport for Solution of the Spatially Dependent Boltzmann's Equation,* JOHN V. DICARLO and MARK J. KUSHNER, University of Illinois, Urbana, IL--We present a solution of the spatially dependent Boltzmann's equation in the cathode fall region of a He discharge based on the use of flux-corrected transport. The solution averts the use of the local field approximation and thus can be used for highly non-equilibrium conditions such as abnormal glows. A major difficulty in the solution of first-order hyperbolic equations, such as Boltzmann's equation, is that of accurately simulating evolution of shock and contact discontinuities in the particle flow. In the cathode fall, this problem arises because of large gradients in ion and electron densities in both spatial coordinate space and in velocity space. Many finite differences techniques suffer from excessive numerical dissipation under these conditions. The flux-corrected transport method is used in this work to help alleviate this difficulty. We discuss the spatial dependence of the ion and electron energy distribution functions for a variety of discharge conditions.

* Work supported by Sandia National Laboratory.

SESSION LA

10:00 AM - 11:30 AM, Thursday, October 20

Radisson Plaza Hotel - East Ballroom

NEUTRAL PARTICLE DISTRIBUTIONS

Chairperson: M. Cappelli, Stanford University

LA-1 Measurement of the Density and Temperature of Ground-State Hydrogen Atoms and of Vibrationally Excited Hydrogen Molecules in a Plasma.* A. S. SCHLACHTER, G. C. STUTZIN, A. T. YOUNG, J. W. STEARNS, K. N. LEUNG, W. B. KUNKEL, Lawrence Berkeley Laboratory, G. T. WORTH, R. R. STEVENS, H. V. SMITH, and E. PITCHER Los Alamos. - A diagnostic system to determine the density and temperature of ground-state hydrogen atoms in a plasma by vacuum-ultraviolet laser-absorption spectroscopy has been applied to H^- ion-source discharges: a dc volume production ion source and a pulsed Penning ion source. Ground-state H^0 densities between 10^{12} and 10^{15} atoms/cm^3 have been measured, as have atom temperatures in the range 0.1-3 eV. The populations of vibrational levels of H_2 up to v=5 and rotational levels up to J=8 have also been measured. The translational velocity distribution and vibrational and rotational state populations provide information on the chemistry in the discharge. This information is crucial to incresing our understanding H^- production in ion sources. The same diagnostic methods have many additional applications.

* This work was supported by Los Alamos National Lab, Air Force Office of Scientific Research, and U. S. DOE under Contract No. DE-AC03-76SF00098.

LA-2 Spatially Resolved Temperature Measurements in an Abnormal Glow N_2-Ar Discharge Using Coherent Anti-Stokes Raman Spectroscopy (CARS). P. P. YANEY, J. E. OLEKSY,* W. A. FOWLER, U. of Dayton**; S. W. KIZIRNIS, USAF Aero Propulsion Lab. -- A stable discharge was setup between nickel-iron doorknob electrodes spaced 18 mm with ≈ 31 Torr N_2 and ≈ 9 Torr Ar at E/N = 56 Td and J ≈ 0.16 A/cm^2. Rotational (gas) and apparent vibrational temperatures of N_2 were measured axially using the "folded" BOXCARS beam geometry giving an axial resolution of ≈ 50 μm. These temperatures were obtained by computer fitting the observed CARS spectra. A ≈ 600 K jump in T_v to 2290 K occurred between 9 and 11 mm from the cathode coincident with the tip of the positive column. The T_r peaked at 11 mm to give 890 K and dropped to ≈ 740 K near the electrodes. The spectra showed some evidence of deviations from the Boltzmann distribution at low J values near the cathode.
* In partial fulfillment of the requirements for the M.S. degree in Electro-Optics.
** Supported by USAF Contract F33615-86-C-2722.

LA-3 Plasma Etching Diagnostics Using Gated-rf Discharges, P. J. HARGIS, JR., and K. E. GREENBERG, Sandia National Laboratories -- Optical emission which interferes with laser Raman measurements in plasma etching discharges was suppressed by using a gated-rf discharge. A timing pulse synchronized with the laser was used to gate off the rf signal applied to the powered electrode. Raman measurements were than carried out during the time the discharge was gated off (typically 5 μsec to 1 msec). Based on optical emission spectra from NF_3 discharges and the rates of reactions between atomic nitrogen and NF_x radicals it is generally believed that N_2 is a dominant dissociation product. Raman measurements in gated rf discharges through 750 mTorr NF_3 showed that less than 50 mTorr N_2 is formed under conditions of greater than 95% NF_3 dissociation, suggesting that the nitrogen is contained in other dissociation products. Measurements of atomic fluorine (using electronic Raman scattering from the spin-orbit-split ground state) were also made in gated-rf discharges through NF_3. The versatility of the gated-rf discharge is demonstrated by dissociation and recombination measurements in SF_6 discharges.

LA-4 Characterization of CF_4 Plasma Kinetics by Modulated Power Relaxation, L.D. BASTON and H.H. SAWIN, MIT -- Kinetic coefficients governing the gas-phase chemistry of a CF_4 plasma have been measured from the observed relaxation of individual species in the plasma. The perturbation of species concentrations caused by electron density modulation due to power modulation were monitored using Plasma Induced Emission, Laser Induced Fluorescence, and Mass Spectrometry. Plasma conditions are approximately 0.5 Torr, interelectrode spacing of 1.0 cm, 13.5 MHz excitation, and 3 Watts/cm^3. Primary species monitored are F, CF, CF_2, and C_2F_6. Transfer function analysis[1] is used to compare the experimental kinetic results with simulations of CF_4 chemistry developed using published rate coefficients and mechanisms of the CF_4 plasma.[2]

[1]R.H. Jones, et.al., J. Vac. Sci. Technol., 9(6), 1429 (1972).

[2]K.R. Ryan and I.C. Plumb, Plasma Chem. Plasma Process., 6(3), 231 (1986).

LA-5 Infrared Absorption Laser Diagnostics of Deposition Plasmas* J. WORMHOUDT, Aerodyne Research, Inc.--Laser diagnostics, including long path infrared diode laser absorption and dye laser induced fluorescence (LIF), are able to provide microscopic information on the gas phase of such important semiconductor fabrication processes as plasma etching and plasma enhanced chemical vapor deposition. It is possible to measure temperatures, concentration profiles, and absolute concentrations if independent laboratory measurements of quantitative spectroscopic parameters have been made. We will discuss observations in a newly constructed apparatus which allows multipass absorption and LIF diagnostics of a large volume of plasma. Among the molecular radicals studied by a combination of discharge observations and laboratory band strength measurements are CH_3 and CF_2.

*Supported by AFOSR Contract No. F49620-87-C-0052.

LA-6 Detection of Sulfur Dimers in Sulfur Hexafluoride Etching Discharges, K. E. GREENBERG and P. J. HARGIS, JR., Sandia National Laboratories -- The optical emission from rf plasma etching discharges in sulfur hexafluoride is dominated by broadband emission between 2800 and 5500 Å and by atomic fluorine emission between 6000 and 8500 Å. We have found that the broadband emission at shorter wavelengths is due to the B-X transitions of sulfur dimers. A nitrogen laser was used to pump from the v''=4 vibrational level in the X (ground) state to the v'=2 level in the B state and subsequent radiation back to the ground state was monitored. Using this laser induced fluorescence (LIF), the relative population density of the v''=4 level was observed as a function of various discharge parameters (rf power, etc.). An estimate of the absolute sulfur dimer density was obtained using the ratio of the intensity of a dimer LIF peak to the nitrogen Raman signal intensity measured when the discharge chamber was filled with a known nitrogen density. The radiative lifetime of the v'=2 level of the B state was measured to be 51.4 ± 0.2 ns.

SESSION LB

10:00 AM - 11:30 AM, Thursday, October 20

Radisson Plaza Hotel - West Ballroom

HEAVY PARTICLE INTERACTIONS

Chairperson: B. Bederson, New York University

LB-1 Interaction of Low-Energy $O^-(^2P)$ and $O(^3P)$ Beams with a MgF_2 Surface,* A. CHUTJIAN, O. J. ORIENT and E. MURAD, JPL/Caltech and AFGL -- Optical emissions have been observed in the interaction of 5eV, $O^-(^2P)$ ions with a MgF_2 surface. The background pressure was 1 x 10^{-6} torr. Measurements were made at ion fluxes of 5.0 x 10^{12} ions/cm^{2}s and 1.0 x 10^{14} ions/cm^{2}s. The observed emissions differed markedly under these two conditions. Work is presently underway to observe emission at lower and higher energies, and to observe the analogous emission spectrum under $O(^3P)$ exposure. The $O(^3P)$ is formed by photodetachment of $O^-(^2P)$[1]. A description of the magnetically-confined source, and interpretation of the emission phenomenon will be given.

* Work carried out at JPL/Caltech, and supported by the Air Force Geophysics Laboratory in agreement with NASA.

[1] O. J. Orient, A. Chutjian and E. Murad, XVth Int. Conf. Phys. Electron. Atom. Collisions (Brighton, July 1987). Abstracts p. 813.

LB-2 Rate Constants for the Reaction $^{22}Ne^+ + {}^{20}Ne$ as a Function of Collision Energy at Several Temperatures, R.A. MORRIS, A.A. VIGGIANO, T. SU, and J.F. PAULSON, Air Force Geophysics Laboratory-Rate constants for the symmetric charge transfer reaction $^{22}Ne^+ + {}^{20}Ne$ have been measured as a function of center of mass translational energy over the temperature range 85 - 450 K. The measurement were made in a variable temperature selected ion flow drift tube (SIFDT) apparatus. The rate constants were found to increase with increasing temperature and energy. At high energies ($>$0.5 eV) the rate constants exceeded the Langevin limiting value. This suggests that the repulsive part of the potential is important in determining the collision rate constant, even at the relatively low temperatures employed in the experiments. A theoretical treatment of the reaction rate constant by classical trajectory calculations is presented to test this hypothesis.

LB-3 Mutual Neutralization Studies Using Chemical Releases in Space Plasmas*. P.A. BERNHARDT and P. RODRIGUEZ, Naval Research Laboratory, Washington, DC 20375-5000-- We have developed a new technique to study ionic recombination. A gas which dissociatively attaches electrons to form negative ions is released into the ionosphere from a sounding rocket or from an orbiting satellite. The reactions between the newly created negative ions and the ambient O^+ ions are monitored with ground-based radars, in-situ density probes, and ground-based or space-borne optical instruments. During the AFGL sponsored IMS program, SF_6 was released at 350-km altitude to produce SF_5^- and SF_6^- ions. The reaction between SF_6^- and O^+ yielded enhanced 777.4 nm emissions from $O(^5P)$ states. Future experiments such as the NASA sponsored NICARE and CRRES missions will examine the energy dependence on the reaction rates and excited species production by generating ionospheric negative ions with energies between 0 and 40 eV.

*Research sponsored by NASA.

LB-4 Predissociation Product Distributions from H_3*, P. Devynck, W. G. Graham, and J. R. Peterson, SRI International- Using a translational spectroscopic technique used earlier for D_3^+ dissociative electron capture in Cs,[1] we now include H_3^+ and isotopic mixtures. Near-resonant capture in Cs populates the first Rydberg states of H_3, 2s A_1' and 2p A_2'',[2] even though the beam ions are rovibrationally hot (~2 eV).[1] As from D_3^+, we find both $H + H_2$ and $H + H + H$ products in the ratio ~ 2:1, and with very similar dissociation kinetic energy release spectra. However, the dissociation branching of HD_2 to $H + D_2$ and $D + HD$, each compared to $H + D + D$, is vastly different; $H + D_2$ dominates, and D appears mostly in the three-particle channel. Yet from H_2D, $H + HD$ is readily seen. An interesting dynamical problem exists. The H_2 products are rovibrationally very hot (3 eV),[1,3] which may aid production of H^- in Cs-seeded ion sources.

*Research supported by NSF and AFOSR.
[1]J. R. Peterson and Y. K. Bae, Phys. Rev. A 30, 2807 (1984).
[2]H. Helm Phys. Rev. Lett. 56, 42 (1986).
[3]J. R. Peterson, Proc. 4th Neg. Ion Conf. Brookhaven (1986); A.I.P. Conf. Proc. No. 158 (1987).

LB-5 Dissociative Charge Transfer in $H^+(H_3^+)$ + SiH_4 Reactions.* H. H. Michels and R. H. Hobbs, UTRC----An *ab initio* study of the potential energy reaction surfaces for the dissociative charge transfer reaction: $H^+ + SiH_4 \rightarrow SiH_n^+ + mH_2 + lH_2$, (n=0,3; n+l+2m=5) has been undertaken. The basis set employed was the standard 6-31G* representation, augmented with diffuse functions (Si:3d, H:2p) for an accurate description of the polarizability of SiH_4. Dissociative channels connecting to SiH_2^+ and SiH^+ exhibit, surprisingly, significant reaction barriers relative to the SiH_3^+ product channel. The dissociative channel leading to Si^+ from either SiH_2^+ or SiH^+, however, exhibits no reaction barrier. The dominant product ion is found to be SiH_3^+, formed from a hydride abstraction mechanism. A preliminary calculation of the rate for SiH_3^+ formation, using a modified R-matrix propagator technique, yields results close to the Langevin prediction, $k_L = 5.2 \times 10^{-9}$ cm^3/sec. The chemistry of the $H_3^+ + SiH_4$ reaction is qualitatively similar with $SiH_3^+ + 2H_2$ formed as primary products.

*Supported in part by AFWAL Contract F33615-87-C-2718.

LB-6 Center of Mass Distribution of H^- Produced by the Dissociation of H_3^+.* O. YENEN, L. WIESE, and D. H. JAECKS, University of Nebraska-Lincoln--We have determined the center of mass (c.m.) energy distribution of H^- produced by the collision induced dissociation of H_3^+ from He targets for incoming beam energies ranging from 2.417 to 7.0 keV. The most probable H^- c.m. energy is found to be .8 eV. We have also determined, from the FWHM of the laboratory H^- energy peaks that the maximum H^- energy in the c.m. is 2.31±.2 eV. Moreover, we obtained the most probable inelastic energy loss of 60±12 eV from the shift of the position of the H^- lab peaks. These results and the energies of the excited states of H_3^+ and H_3 suggest that H^- is produced by a double excitation of H_3^+ with subsequent dissociation into $H^+ + H^+ + H^-$. In this case the motion of the two H^+ are highly correlated, and we put a lower limit of 160^o, in the c.m., on the correlation angle between the protons.
* This work is supported by NSF.

SESSION M

1:30 PM - 3:20 PM, Thursday, October 20

Radisson Plaza Hotel - Ballroom

RF GLOW DISCHARGE MODELING

Chairperson: A. Mitchell, AT&T Bell Laboratories

M-1 Modeling of RF Glow Discharges. J.-P. BOEUF, CNRS, Université Paul Sabatier, Toulouse, France. - Self-consistent fluid models of RF glow discharges are presented. Depending on frequency, pressure, power and gap length, the mechanisms of energy deposition in the RF plasma may change drastically. A good representation of these mechanisms is of paramount importance for the developpment of realistic glow discharge models. Energy deposition by secondary electrons accelerated in the sheaths is dominant at low frequency; the RF plasma is, in that case similar to the negative glow of a DC discharge; wave riding electrons gaining their energy from the sheath expansion are more important at higher frequency; at lower pressure "electron-sheath collisions" may become more probable than electron-molecule collisions, and the mathematical description of the electron momentum and energy balance is more complicated.

The ability of fluid models to provide a good description of these mechanisms as well as the limits of the fluid approach are discussed.

M-2 Continuum Modeling of SF_6 and Ar RF Discharges, and Comparison with Experimental Measurements, E. GOGOLIDES, J.P. NICOLAI and H.H. SAWIN, MIT -- SF_6 and Ar discharges were modeled using continuity equations for positive, negative ions and electrons; time derivative of Poisson's equation (current continuity); a force balance for the inertial effects of ion transport; and an electron energy balance. Using kinetic rate coefficients derived from swarm experiments, the above equations were solved in one dimension. The Ar and SF_6 discharges exhibit different electrical impedances as was experimentally observed, and the results show that electron-impact ionization is peaked at the bulk-sheath interface. For a SF_6 discharge, the peak coincides with the anodic phase of the rf cycle. In contrast for an Ar discharge, the peak occurs during the cathodic part of the cycle. These results are in agreement with time and space resolved optical emission data from our laboratory.

M-3 Modeling of Molecular RF Glow Discharges for Semiconductor Processing*, T.J. GRIMARD, M.S. BARNES AND M.E. ELTA, University of Michigan-A pair of interactive numerical models describing a molecular rf glow discharge (which include reactor flow and gas phase chemistry) are used to simulate a reactive ion or plasma etch reactor. The large-signal rf glow discharge model[1] treats charged particle effects and predicts the electrical properties as well as the electron impact generation rates for input to the subsequent model. The chemical kinetics model includes gas phase chemistry and gas flow with the boundary conditions defined by the mass flow controllers and the pumping stack. Results from this simulation set for CF_4 in a parallel plate batch reactor are presented. DC bias measurements from a SEMI 1000 TP/CC RIE tool are compared with rf glow discharge model results. Radical species trends from actinometry experiments are compared with chemical kinetic results.

[1] M.S. Barnes et. al., JAP, **61**(1), 81 (1987)
*This work is supported by the Semiconductor Research Corporation.

M-4 Computational Limitations in RF Glow Discharge Modeling*, M.S. BARNES, T.J. GRIMARD AND M.E. ELTA, University of Michigan-Large-signal continuum rf glow discharge models are potentially very useful tools for enhancing the understanding of semiconductor plasma processing. Difficulties arise in accuracy, stability and efficiency as a result of the complexity of the underlying physical mechanisms. The accuracy of the rf glow discharge models will be discussed both in terms of discretization of the simulation as well as the underlying assumptions. For instance, the "drift-diffusion" models reported in refs. 1 and 2 do not model electron energy and momentum effects whereas the energy momentum model outlined in ref. 3 does not include ion momentum effects in the electrode sheath regions. Other accuracy problems to be discussed include sheath discretization effects and the accuracy of the swarm parameters utilized in the large-signal simulations. In brief, it appears to be necessary to utilize numerical schemes which allow more grid points to be concentrated in the sheath regions where the dependent variables change more over an rf cycle. Moreover, it will be shown that variations in the swarm parameters can significantly alter simulated results. Numerical stability and efficiency effects related to the aforementioned issues will also be discussed.

[1] M.S. Barnes et. al., JAP, **61**(1), 81 (1987)
[2] J.P. Bouef, Phys. Rev. A, **36**(6), 2782 (1987)
[3] M.S. Barnes et. al., J. Computat. Phys., to be published, Aug. 1988
*This work is supported by the Semiconductor Research Corporation.

M-5 Modeling of RF Glow Discharge Plasmas,* T. MAKABE *Keio University* --- A dynamic model for RF glow discharge in a parallel plate geometry has been developed from the continuum theory, considering phenomenological description of relaxation kinetics for the momentum and energy of the electron and ion. The idea of the *effective field*, E_{eff} plays an important role. The second-stage investigation, i.e, the behaviour of the excited species has been also simulated in order to judge the validity of the procedure by comparison with the results of the optical emission spectroscopy. The driving source has a voltage or current form $A(t)=A_o\cos(2\Pi ft)$. Numerical analysis is done using Newton-Raphson method after expressing the timederivative by 6th-order Gear's algorithm. Result is obtained for the condition, A_o=100 V, W=0.03 Wcm^{-3}, p=1 Torr at d=2 cm, f= 13.56 MHz in accordance with the observation. Maximum of N_e and N_+ are $3x10^9$ cm^{-3}. Current leads voltage by 72°. Time-averaged profile of $Ar[2p_1, \varepsilon=13.5eV:\tau=20ns]$ shows the reasonable coincidence with the experimental $Ar[3p_1, \varepsilon=14.7eV:\tau=71ns]$. $Ar[^3p_{0,2}, \varepsilon=11.5eV:\tau>1.3s]$ has the diffusion profile with maximum of $1.5x10^{11}$ cm^{-3}. The discharge for 100 k $\leq f \leq$ 13.56 MHz and 0.01 $\leq p \leq$ 1 Torr has been also studied.

*Supported by Grant-in-Aid for Sci.Res.on Priority Areas

SESSION N

3:40 PM - 5:35 PM, Thursday, October 20

Radisson Plaza Hotel - Ballroom

BREAKDOWN AND SWITCHING

Chairperson: M. Gundersen, University of Southern California

N-1 Stochastic Properties of Negative Corona (Trichel) Pulse Discharges in Electronegative Gases,* R.J. VAN BRUNT and S.V. KULKARNI, National Bureau of Standards--The stochastic behavior of ultra-violet sustained Trichel-type corona discharge pulses generated in a point-plane gap have been investigated for the electronegative gas mixtures N_2/O_2 and SF_6/O_2 using a new technique that allows direct measurement of various conditional pulse-height and time-separation distributions from which correlations among successive discharge pulses can be determined. It is shown that the amplitude of a given discharge pulse can be strongly correlated with the amplitude and time separation from the preceding pulse, and the degree of correlation is explained by the influence of the negative-ion space-charge cloud from the preceding pulse on the magnitude of the electric field near the cathode at the time that the next pulse is initiated. The discharge process is shown to be Markovian, i.e., the correlation exists only between nearest neighbor pulses.

*Supported in part by U.S. Department of Energy.

N-2 Ionization and current growth in N_2 at very high E/n,* V.T. GYLYS,** B.M. JELENKOVIĆ,‡ and A.V. PHELPS† JILA, University of Colorado and NBS. -- Measurements are reported of current growth in low-current, prebreakdown discharges in N_2 at 1 kTd < E/n < 52 kTd and $6 \times 10^{18} < nd < 3 \times 10^{20}$ m^{-2}. Ratios of charge collected during the electron transit time to that collected subsequently due to the initial ions and to delayed ionization by ions or fast neutrals are used to test ionization models. Data were corrected for secondary avalanches using ratios of N_2^+ 391.4 nm emission integrated over all avalanches to that for the photoelectron pulse. These results confirm the single-beam, energy-balance electron model[1] at high E/n and show that ionization by fast ions and neutrals is small.

[1] A.V. Phelps, B.M. Jelenković, and L.C. Pitchford, Phys. Rev. 36, 5327 (1987).

* Supported in part by Lawrence Livermore Laboratories.

** Present address, Rockwell International/Rocketdyne Division, Canoga Park, CA.

‡ Permanent address: Institute of Physics, Belgrade, Yugoslavia.

† Quantum Physics Division, NBS and Physics Dept., CU.

N-3 Overshoot in Ionization Rates at High E/N,* J. T. VERDEYEN, U. of Illinois, L. C. PITCHFORD and Y. M. LI, GTE Laboratories, J. B. GERARDO and G. N. HAYS, Sandia National Laboratories -- When an electron gas is subjected to an intense transient field, the velocity distribution evolves in time as it approaches a hydrodynamic equilibrium at the given E/N. For any gas, the ionization frequency has a maximum and thus it is not a monotonic increasing function of the electron energy. This can lead to an overshoot in the ionization frequency for high values of E/N. We have observed this effect experimentally by measuring the transient ionization growth rate caused by a pulsed microwave field at cyclotron resonance. The maximum in the ionization frequency is most clearly demonstrated in a dynamic fashion by the existence of a negative "induction time"[1] which is the extrapolated delay time for the electrons to reach hydrodynamic equilibrium. Reasonable agreement between the multibeam model, Monte Carlo simulations, and the experimental observations of the induction times has been achieved.

*This work performed at Sandia National Laboratories, supported by the U.S. Department of Energy under contract number DE-AC04-76DP00789.

[1]G. N. Hays, L. C. Pitchford, J. B. Gerardo, J. T. Verdeyen, and Y. M. Li, Phys. Rev. A 36, 2031 (1987).

N-4 An Investigation of Streamer Properties and Multi-Streamer Interactions,* M. C. WANG and E. E. KUNHARDT, Weber Research Institute, Polytechnic University--Quantitative dependence of streamer properties (streamer velocities, charged-particle densities, and streamer shapes) on the initial parameters (applied E field, initial electron density distribution) in N_2/SF_6 mixtures has been determined using the 2-D numerical simulation scheme of Wu and Kunhardt.[1] The transition from transient to steady-state streamer behavior has been elucidated. Streamer initiating and sustaining fields for different gas mixtures/initial electron density distributions have been examined and compared with previous results. These results are used in the characterization of streamer dynamics. We have also investigated the interactions between multiple streamers and the influence of the space-charge distribution and applied field on this interaction.

*Work supported by the Office of Naval Research and National Science Foundation.

[1]C. Wu and E. E. Kunhardt, Phy. Rev. A37, 4396 (1988).

N-5 Distributed Element Model Giving Spontaneous Thresholds for Electric Discharges*, W. B. MAIER II, A. KADISH, Los Alamos National Laboratory, and R. T. ROBISCOE, Montana State University—We model freely propagating discharges such as lightning and punch-through arcs, by Maxwell's equations and the condition[1] $\partial \vec{J}/\partial t = \omega^2(\vec{E} - E^* \hat{J})$. $\hat{J} = \vec{J}/J$; $\vec{J}$ is the current density in the discharge; $\vec{E}$ is the electric field; t is time; ω^2 is related to geometry and medium; and E^* is a positive constant[1] characteristic of the medium. If $\vec{J}$ is restricted to a single direction between parallel, planar cathode and anode, then $\vec{J}$ and the electric field colinear with $\vec{J}$ are driven by electromagnetic waves propagating between cathode and anode. This model predicts threshold behavior and discharges which initiate and may quench before any charge has been transported the entire cathode-to-anode distance. Analytic and computer solutions will be presented.

* Work conducted under the auspices of the U.S. DOE.

[1] Cf. R. T. Robiscoe, A. Kadish, and W. B. Maier II, J. Appl. Phys. (accepted).

N-6 **Effects of Unsteady Flow and Radiation on Recovery of a Spark Gap Switch,*** **A.K. COUSINS, V.C.H. LO and W.J. THAYER, Spectra Technology Inc. -- Analytical and computational modeling of a convectively-purged spark gap switch have been performed. The switch has been characterized experimentally for purge flow rates of 10-150 m/s and voltages of 65-100 kV. The flow channel was "tuned" to utilize the energy of unsteady gasdynamic processes to augment the convective purging. A separated-flow model was used to predict the time and purge flow rate required for complete recovery of the breakdown voltage. Analysis indicates that a significant fraction of the energy deposited into the gas is radiated away to the device walls. With a correction for the radiative losses, the computational results using the separated-flow model are shown to predict the experimental data well. The experimental results have demonstrated that steady and unsteady gasdynamic processes control the recovery of the spark gap switch for pulse rates up to 2.5 kHz and switched energies of approximately 100 J.**

***Work supported by the Department of Energy.**

N-7 Simulation of an Optically Triggered Pseudo Spark Thyratron,* HOYOUNG PAK and MARK J. KUSHNER, University of Illinois, Urbana, IL--Pseudo spark discharges are being developed as replacements for conventional thyratrons. The Back-Lit-Thyratron (BLT) is one such pseudo-spark device using optical triggering. In this paper, we present a computer simulation of the BLT. The model uses a 2-dimensional time dependent continuum formulation, and the local field approximation is used to calculate the transport properties. Gas pressure, gas composition, and geometry are user defined. Secondary electron emission by electrons, ions, and photons are included in the model. Comparisons are made to experiments for anode delay time and rate of current rise. We find switching behavior largely dependent on formation of a virtual anode. Long anode delay times (100-200 ns) result from the necessity to generate sufficient positive space charge to create the virtual anode.

* Work supported by Los Alamos National Laboratory.

N-8 Excitation of Mercury in a Dielectric-barrier Discharge, B. ELIASSON, B. GELLERT and U. KOGELSCHATZ, ASEA BROWN BOVERI, Corporate Research, 5405 Baden, Switzerland - It is demonstrated that the electron energy distribution in dielectric-barrier discharges can be optimized for the excitation of the mercury resonance levels in Hg/Ar mixtures. The discharge is initiated between electrodes which are a few mm apart. At least one of the electrodes is covered with a dielectric layer. The total gas pressure varies from mbars to a few bars. The discharge consists of ns-current filaments which are statistically distributed in time and space. The electron energy in the filaments can be adjusted by varying the pressure and the gap width. Special effort has been put into optimizing the output of the UV-resonance lines at 185 nm and 254 nm. For example one can obtain ratios of intensity (185)/intensity (254) in excess of 1 in this discharge. Some of the recorded spectral features are most likely due to excimers. At higher pressures this discharge favours the formation of excimers. One can obtain electron energies which are considerably above those of the classical low-pressure mercury lamp. This allows for a greater flexibility in optimizing the UV-radiation. In this way intense UV radiation can be generated. Model calculations based on the solution of the Boltzmann equation for the gas mixtures used and taking the breakdown field of the filaments into consideration have been made. Experimental trends are confirmed.

SESSION O

8:30 AM - 9:05 AM, Friday, October 21

Radisson Plaza Hotel - Ballroom

PHYSICS IN A POSITRON TRAP

Chairperson: R. Gottscho, AT&T Bell Laboratories

0-1 Physics in a Positron Trap,* C.M.SURKO** AT&T Bell Laboratories --We have built a device which is designed to efficiently accumulate and store positrons in an electrostatic trap.[1] Among other things, this has allowed us to study various aspects of positron-molecule interactions. Studies of the positron confinement in the trap provide evidence that positrons can bind to neutral molecules, when the molecules are sufficiently large; and a model of this binding process will be discussed. The ultimate limits on positron confinement will also be discussed, as well as several of the potential uses of large numbers of positrons in the laboratory, including the creation of an antimatter plasma.

*In collaboration with A. Passner, M. Leventhal and F. J. Wysocki.

**Present address, Physics Department, University of California, San Diego.

1. F. J. Wysocki, M. Leventhal, A. Passner and C. M. Surko, Proceedings of ANTIMATTER '87, to be published in Hyperfine Interactions (1988).

SESSION PA

9:20 AM - 11:15 AM, Friday, October 21

Radisson Plaza Hotel - East Ballroom

LOW-PRESSURE DISCHARGES: EXPERIMENTAL

Chairperson: R. Gerber, Sandia National Laboratories

PA-1 Negative Ion Flux Enhancement From RF Processing Discharges,* Lawrence J. Overzet† and Joseph T. Verdeyen, University of Illinois Center for Compound Semiconductor Microelectronics, Champaign, IL 61820--The negative ion flux impinging on a surface in contact with a glow is usually quite small because of the sheaths formed to contain the very mobile electrons. We have found that the flux of the negative ions can be enhanced by factors of 50 to 1000 by SQuare Wave Modulating (SQWM) the RF discharge. During the off-time, the sheaths disappear on the time scale of electron attachment, and the negative ions drift under the influence of the self-bias field. Data will be presented for CF_4 and F_2 in helium discharges, along with the correlation with a simple model.

* Work supported by JSEP and the NSF-ERC.
† Present address: The University of Texas at Dallas,
P.O. Box 830688
Richardson, TX 75083-0688

PA-2 Electrical Characteristics of rf Parallel Plate Discharges with Added Attachers and Their Interpretation, P. Bletzinger, Wright-Patterson Air Force Base OH 45433.---Electrical characteristics of an rf discharge in argon with the addition of .25 to 50% of SF6, CF4 and C2F6, pressure range from .08 to 2 Torr at 7.1,10.1,14.1 and 20MHz were measured. Adding attaching gases increases the discharge impedance shifts the impedance minimum to lower pressures, reaching .1 Torr at 50% SF6, for example. This minimum corresponds to the pressure at which the wave-riding energy deposition process and the volume collisional process are equally important. In the range of .1 to 1 Torr, the wave riding process is lessimportant as the amount of attacher increases. The equivalent circuit model predicts a decrease of effective sheath thickness at 14.1MHz, 1 Torr from 5mm with 1%SF6 to .5mm with 50%SF6. The impedance with added CF4 is approximately 70%, with C2F6 about equal, compared to the impedance with the same amounts of added SF6. Considering the large difference in threshhold energies of the attachment cross sections of these gases, these results require the mean electron energy to be >4 eV.

PA-3 Spatial Distributions of a-Si:H Film Producing Species in Silane Glow Discharges,* D. A. DOUGHTY and A. GALLAGHER,** JILA, Univ. of Colorado and NBS -- Dielectric fibers (5 and 30 μm diameter) are used to probe the distribution of SiH_4 decomposition products that produce a-Si:H films throughout DC and RF silane discharges. The film thickness on the fiber as a function of distance from the electrodes yields information about the source of depositing species within the discharge. In the case of low power RF discharges the film precursors appear to be produced in the negative glow region and then diffuse to the substrate without reacting. The preliminary results for the DC case, however, indicate a more complicated source function. These spatial distributions of film thickness and the derived source functions are compared with the spatial variation of the optical emission from the discharge. The perturbative nature of these probes on the discharge environment is also addressed.

*Work supported in part by the Solar Energy Research Institute.

**Staff member, Quantum Physics Division, National Bureau of Standards.

PA-4 rf Potential Measurements in the Model 5000 Magnetron Etcher. S.E. Savas* and K.G. Donohoe, Applied Materials Corp., Santa Clara, CA 95054 —Measurements of rf potential both in the plasma and on the surface of the powered electrode have been made for a range of realistic process conditions. The spatial variation in the plasma is measured about 1 1/2 cm above the wafer on diameters both parallel to the time-independent magnetic field and perpendicular to it. The electrode surface potential is measured at a point near the center of the wafer being processed. All measurements are made with custom designed rf probes whose output is fed to an rf spectrum analyzer. Calibration ($< \pm 5\%$) is against a Tektronix 1000X HV probe. Sheath voltages above the wafer inferred from the measured potentials will be presented for a range of pressures, rf power levels and magnetic field strengths. Discharge mechanisms accounting for the observed potentials will be discussed.

*Consultant and Visiting Scientist
SRI International.

PA-5 Electrical Characteristics of Cylindrical Magnetron RF Discharges for Etching and Deposition,* GUEN Y. YOEM and MARK J. KUSHNER, University of Illinois, Urbana, IL--Direct current magnetron discharges typically operate at lower (<10 mTorr) pressures and higher plasma densities than conventional glows due to the advantageous confinement of low energy electrons by E x B drift. Radio frequency (rf) cylindrical magnetron discharges also have these properties, and additionally operate with lower dc bias than diode discharges. The high plasma density and low dc bias (enabling low energy ion bombardment) make these discharges ideal for semiconductor etching. In this paper, measurements of electrical properties (ion density, dc bias, plasma emmission, potential distribution) of a cylindrical magnetron rf discharge are presented and related to the etching of Si in CF_4 plasmas. We find that the dc bias may be eliminated by a magnetic field of $\lesssim$100 G while maintaining high etching rates (>1000's A/s) and good anisotropy. The reactor tends to operate in the magnetron mode only on alternate half cycles.

* Work supported by Joint Services Electronics Program.

PA-6 A Microwave Discharge for Plasma Processing Using a Slotted Metal Coupler,* S. KUO, E. E. KUNHARDT and G. SCHAEFER, Weber Research Institute, Polytechnic University--A slotted metal, microwave coupler has been used for the production of microwave plasmas. Slots in opposite directions are connected in series with the length of each slot matched to 1/2 of the input microwave wavelength. Devices using this concept can be built in a variety of geometries such as planar, cylindrical, etc. They can utilize single or multiple, phase matched coupler configurations. Such devices are efficient in exciting homogeneous field distributions similar to low order cavity modes, but independent of dimensions. They allow using open-ended structures which are well-suited for producing a flowing homogeneous plasma column that is separated from the wall. This column can be directed towards the specimen table located outside the coupler. The table can be biased relative to the plasma potential. Experimental results for plasmas in various gas mixtures of interest to plasma processing are presented.

*Work supported by the Office of Naval Research and National Science Foundation.

PA-7 Electrode Design for Diffuse Gas Discharges, A.E. RODRIGUEZ and W.M. MOENY, Tetra Corporation, Albuquerque, NM -- The primary problem of electrode design for diffuse glow discharge devices (such as TEA lasers and glow discharge switches) is avoiding electric field enhancements, which can lead to arcs and breakdown. Analytical solutions (e.g. Rogowski or Chang) apply only for idealized conditions (vacuum or uniform conductivity). Conventional finite-element electric field codes typically degrade in accuracy on conductor surfaces for all but trivial contour shapes. This paper will describe the development and use of an electric field code for electrode design based on finite differences in a computer-generated boundary-fitted grid system. We will include several examples of in-house electrode designs for glow discharge and vacuum breakdown applications including strongly nonhomogeneous and nonlinear conductivities due to plasma interactions with the E-field. The emphasis will be on design approach, applications and experimental results, rather than the numerical techniques. Advantages, limitations, and future plans will be summarized.

PA-8 A Reflex Electron Beam Discharge as a Plasma Source for Electron Beam Generation,* C. MURRAY, J. J. ROCCA and B. SZAPIRO, Electrical Engineering Department, Colorado State University -- The plasma from a reflex electron beam glow discharge in helium has been studied as source of electrons for broad area electron beam generation. An electron current of 120 A (12 A/cm^2) was extracted from the plasma and accelerated in the gap between two grids to energies greater than 1 keV in 10 usec pulses. The mechanism of electron beam generation has been studied, and is shown to be in agreement with the theory of Zharinov et. al for grid-controlled plasma cathodes [1].

*Work supported by Wright Patterson A.F.B.

[1] A. V. Zharinov, Yu.A. Kovalenko, I.S. Roganov and P.M. Tyuryukanov, Sov. Phys. Tech. Phys., 32, 413, (1986).

PA-9 Design Criteria for an Optical Ionizing Radiation Particle Track Detector*, S. R. HUNTER, W. A. GIBSON, and G. S. HURST, Oak Ridge National Laboratory and Pellissippi International - A new type of ionizing radiation particle track detector has been developed,[1] based on the electron detection technique used in the Cavalleri diffusion experiment.[2] The position and density of the particle track in a gas is imaged by the optical radiation produced in electronic excitation collisions of the surrounding gas with the electrons in the particle track when subjected to a pulsed high frequency AC electric field. The performance of the detector in terms of its ultimate resolution and sensitivity has been calculated as a function of the total gas pressure and the RF pulse voltage, frequency, and duration using a simple equilibrium model. A prototype detector has been constructed and the resolution found to compare favorably with these calculations.

*Research sponsored by OHER and ONS, USDOE under contract DE-AC05-84OR21400 with Martin Marietta Energy Systems, and by the National Cancer Institute under contract with Pellissippi International, Inc.

[1]S. R. Hunter, Nucl. Instru. Methods, A206, 469 (1987).
[2]G. Cavalleri, Phys. Rev. 179, 186 (1969).

SESSION PB

9:20 AM - 11:15 AM, Friday, October 21

Radisson Plaza Hotel - West Ballroom

ELECTRON-MOLECULE COLLISIONS

Chairperson: R. Bonham, University of Indiana

PB-1 Multichannel Studies of Low – Energy Electron Impact Excitation of Molecules*, C. WINSTEAD, H. PRITCHARD, K. WATARI†, V. MCKOY, California Institute of Technology and M. A. P. LIMA‡, F. J. daPAIXAO, L. M. BRESCANSIN Instituto de Fisica, Unicamp, S. P. Brasil. – The Schwinger method[1] has been used to carry out multichannel calculations of electron impact excitation of triplet states of several molecular targets. Differential and integral cross sections are reported for impact excitation of H_2, N_2, CO, and H_2O. These cross sections are compared with experimental measurements and results of two-channel calculations. Extension of the method to open-shell molecules and results for e-O_2 collisions will also be discussed[2].

*Supported by NASA-Ames Cooperative Agreement NCC 2-319, NSF Grant PHY- 8604242, and the Innovative Science and Technology Program of SDIO Contract DAAL 03-86-K-0140.
†Supported by CNPq(Brasil).
‡Instituto de Estudos Avançados,CTA,São José dos Campos, Brasil

[1]K. Takatsuka and V. McKoy, Phys. Rev A**24**, 2473(1981); **30(4)**, 1734(1984).
[2]M. A. P. Lima, F. J. daPaixao, L. M. Brescansin, and V. McKoy, Phys. Rev. A (to be published).

PB-2 Electron-Impact Dissociation of Simple Molecules*, P. C. Cosby and H. Helm, SRI International - Absolute cross sections and fragment kinetic energy releases are measured for the dissociation of O_2, CO, N_2, CO_2, and NO_2 into neutral fragment pairs by low energy (0-200 eV) electron impact. A fast (3 keV) beam of molecules is created by charge transfer and is intersected at right angles by the electron beam. The correlated fragments produced by the dissociation of individual molecules are detected by a time and position sensitive detector. The detector identifies not only the kinetic energy release and fragment angular distribution accompanying the dissociation, but also the mass ratio of the fragments. Identification of both the dissociative molecular states produced by the electron interaction and the internal energy states of the products can generally be made for the diatomic molecules.

*Research supported by USAF Aero Propulsion Lab., WPAFB, OH.

PB-3 New Developments in Dissociative Recombination, J.B.A. MITCHELL and F.B. YOUSIF, U. of WESTERN ONTARIO, Canada.* - Recent merged beam experiments[1] using ions with low vibrational populations have (a) confirmed that H_3^+ (v = 0) recombination is slow (b) shown that the HeH^+ recombination rate coefficient is not negligible (c) raised questions about accepted values for N_2^+ recombination rates (d) demonstrated that a decay channel leading to long lived (>10^{-7}s) excited H_3 rydberg states plays a significant role in H_3^+ recombination. A discussion of these findings and related theoretical calculations will be presented.

* Work supported by AFOSR and NSERC.

1 Mitchell, J.B.A. and Yousif, F.B. in Dissociative Recombination Theory Experiment and Applications, eds. (J.B.A. Mitchell and S.L. Gubeman) World Scientific, N.Y. 1988.

PB-4 Attachment and Ionization Cross Sections in CF_4

P.J. CHANTRY and C.B. FREIDHOFF, Westinghouse R&D Center.--Only two negative ions are produced to any significant extent, F^- and CF_3^-. Their cross sections were measured individually, and summed to give the total attachment cross section. The result agrees well with the value we find by total ion collection. Our peak cross section of 1.50 x 10^{-18} cm^2 also agrees well in magnitude with previous "swarm unfolded" data[1], but lies 0.5 eV lower in electron energy, at 6.85 eV. Our positive ion measurements concentrated on CF_3^+ near threshold, to supplement the extensive data of Stephan et. al.[2] (SDM). We measured the CF_3^+ appearance curve on energy scales calibrated against the Xe^+ and Ne^+ thresholds, and the resulting scales agree to within 0.1 eV. To reconcile our data with that of SDM, we find it necessary to shift their data to higher energies by 0.55 eV. The agreement is then satisfactory, given the better energy resolution (0.1 eV) of the present measurements.

1. Hunter, S.R. and Christophorou, L.G.; J. Chem. Phys. 80, 6150 (1984).
2. Stephan, K., Deutsch, H. and Mark, T.D.; J. Chem. Phys. 83, 5712 (1985).

PB-5 Monte Carlo Calculations of Electron Transport in CF_4 with Anisotropic Scattering, L. E. KLINE and T. V. CONGEDO, Westinghouse R&D Center -- We have predicted electron transport parameter values vs. E/n for CF_4 using Monte Carlo simulations (MCS). The MCS input data include cross sections for production of F^- and CF_3^-, and CF_3^+ near threshold, measured at Westinghouse R&D, total scattering and ionization from published measurements and vibrational excitation and neutral dissociation estimated in this work. The neutral dissociation cross section was obtained by subtracting a measured (dissociative) ionization cross section from a measured total dissociation cross section. The vibrational cross section was estimated by analogy with CH_4. Anisotropic scattering was assumed for all types of collisions in the MCS. A differential cross section was estimated from available experimental data and by comparing the predicted and measured drift velocities. The predicted attachment (η) and ionization (α) coefficient values in the range $50<E/n<100$ Td depend on the assumed shape of the neutral dissociation cross section near threshold. The predicted α values agree well with experiment at higher E/n values.

PB-6 Low Energy Structures in Emission Cross Sections from CCl_2F_2 and BCl_3#, Z.J. JABBOUR and K. BECKER*, Lehigh University -- We carried out detailed measurements in the low energy region (threshold to 50 eV) of the emission cross sections of various fragments produced by dissociative electron impact on CCl_2F_2 and BCl_3, e.g. $CCl(A \rightarrow X)$ and CCl^+ $(A \rightarrow X)$ from CCl_2F_2 as well as $Cl(A \rightarrow X)$ [1] and $B(^2S \rightarrow {}^2P^o)$ from BCl_3. In all cases complex structures with multiple onsets were found in the near-threshold region. An attempt is made to relate these onsets to different break-up mechanisms of the parent molecule that lead to the particular emitting species.

[1] Z.J. Jabbour et al., Z. Phys. D, in press

Supported by NSF through grant CBT-8614513

* Present Address: City College, New York

SESSION Q

11:15 AM - 12:00 Noon, Friday, October 21

Radisson Plaza Hotel - East Ballroom

FOLLOW-UP TO THE WORKSHOP ON THE DESIGN, CALIBRATION, AND MODELING OF RESEARCH RF PLASMA PROCESSING SYSTEMS

Chairperson: J. Gerardo, Sandia National Laboratories

INDEX OF AUTHORS

UNIVERSITY OF MINNESOTA
PROFESSIONAL DEVELOPMENT & CONFERENCE SERVICES
CONTINUING EDUCATION AND EXTENSION
NOLTE CENTER FOR CONTINUING EDUCATION
315 PILLSBURY DRIVE SOUTHEAST
MINNEAPOLIS, MINNESOTA 55455

registrants thru 10/19/88 COURSE # 40-04

41ST ANNUAL GASEOUS ELECTRONICS CONFERENCE

OCTOBER 18-21, 1988
RADISSON PLAZA HOTEL

JOSEPH ABDALLAH
LOS ALAMOS NATIONAL LAB.
P.O. BOX 1663
LOS ALAMOS NM 87545

WILLIAM F. BAILEY
AF INSTITUTE OF TECHNOLOGY
7012 HUBBARD DR.
HUBER HEIGHTS OH 45424

B. BEDERSON
NEW YORK UNIVERSITY
6 WASHINGTON SQUARE NORTH
NEW YORK NY 10002

BARBARA ABRAHAM-SHRAUNER
WASHINGTON UNIVERSITY
DEPT. OF ELECT. ENG.
BOX 1127 - BROOKINGS DR.
ST. LOUIS MO 63130

MARK E. BANNISTER
PRINCETON PLASMA PHYSICS LAB.
RF BALCONY, BOX 2, PPPL
P.O. BOX 451
PRINCETON NJ 08543

RICHARD G. BEELER
LAWRENCE LIVERMORE NAT'L LAB.
P.O. BOX 808, L-436
LIVERMORE CA 94550

HAROLD M. ANDERSON
UNIVERSITY OF NEW MEXICO
DEPT. OF CHEMICAL ENGINEERING
ALBUQUERQUE NM 87131

J.NORMAN BARDSLEY
LAWRENCE LIVERMORE NAT'L LAB.
UNIVERSITY OF CALIFORNIA
LIVERMORE
CA CA 94550

HANS BEIJERS
YILA
U OF COLORADO
CAMPUS BOX 440
BOULDER CO 80309

L.W. ANDERSON
UNIVERSITY OF WISC. - MADISON
DEPARTMENT OF PHYSICS
MADISON WI 53706

MICHAEL S. BARNES
UNIVERSITY OF MICHIGAN
1121 WESTERN DRIVE
ANN ARBOR MI 48103

DAVID E. BELL
AIR FORCE INST. OF TECHNOLOGY

BENJAMIN ARAD
SOREQ NUCLEAR RES. CTR.
YAVNE, ISRAEL

L.D. BASTON
MIT
~~66-219~~
77 MASSACHUSETTS AVE.
CAMBRIDGE MA 02139

ERIC BENCK
UNIV. OF WI - MADISON
PHYSICS DEPT.
1150 UNIVERSITY AVE.
MADISON WI 53706

MARTHA BACAL
ECOLE POLYTECHNIQUE
PALAISEAU, FRANCE

JAMES BEBERMAN
UNIV. OF ILL./GASEOUS ELECT.
607 E. HEALEY
CHAMPAIGN IL 61820

JEFFREY K. BERKOWITZ
GTE PRODUCTS CORPORATION
100 ENDICOTT STREET
DANVERS MA 01923

DOUGLAS BAER
BLDG. 520
MECHANICAL ENGINEERING DEPT.
STANFORD CA 94305

KURT H. BECKER
DEPT. OF PHYSICS
CITY COLLEGE OF CUNY
CONVENT AVE. AT 138TH ST.
NEW YORK NY 10031

JEAN PIERRE BEUF
UNIV. SABATIER
TOULOUSE, FRANCE

ASHOK BHATTACHARYA
GE LIGHTING
NELA PARK
CLEVELAND OH 44112

TIMOTHY BIANCHI
U OF MN
800 - N.E. 5TH ST.
MINNEAPOLIS MN 55413

LARRY BIGIO
GENERAL ELECTRIC R & D CENTER
P.O. BOX 8
BLDG. K1-4C34
SCHENECTADY NY 12301

RANDALL BLAIR
GENERAL DYNAMICS LASER SYS LAB
5452 OBERLIN DRIVE
SAN DIEGO CA 92121

PETER BLETZINGER
USAF/WPAFB
WRIGHT-PATTERSON AFB
OH 45433

RUSSELL BONHAM
INDIANA UNIVERSITY
DEPT. OF CHEMISTRY
BLOOMINGTON IN 47405

J. L. BOROWITZ
SOREQ NUCLEAR RESEARCH CENTRE
YAVNE, ISRAEL

JACEK BORYSOW
JOINT INSTITUTE FOR
LABORATORY ASTROPHYSICS
UNIVERSITY OF COLORADO
BOULDER CO 80309

R.W. BOSWELL
AUSTRALIAN NATIONAL UNIV.
PRL RS PHYS S, ANV, GPO BOX 4
CANBERRA, ACT
AUSTRALIA 2601

MARK S. BOWERS
SPECTRA TECHNOLOGY, INC.
2755 NORTHRUP WAY
BELLVUE WA 98004

MARY L. BRAKE
UNIVERSITY OF MICHIGAN
DEPT. OF NUCLEAR ENG.
ANN ARBOR MI 48105

DAVID G. BRAUN
LAWRENCE LIVERMORE NAT'L LAB.
P.O. BOX 808, L-436
LIVERMORE CA 94550

PHILIP G. BURKE
QUEENS UNIVERSITY BELFAST
BELFAST, N. IRELAND

PAUL D. BURROW
UNIV. OF NEBRASKA
DEPT. OF PHYSICS
LINCOLN NE 68588

JEFFERY W. BUTTERBAUGH
MIT
77 MASSACHUSETTS AVE.
RM. 66-219
CAMBRIDGE MA 02139

WOJCIECH BYSZEWSKI
GTE LABORATORIES INCORPORATED
40 SYLVAN ROAD
WALTHAM MA 02254

WENDELL J. CALEY
DELPHAX SYSTEMS
35 PACELLA PARK DRIVE
RANDOLPH MA 02368

JOHN M. CANFIELD
LITTON G & C SYSTEMS
5500 CANOGA AVE.
WOODLAND HILLS CA 91365

MARIO CAPITILLI
UNIVERSITY OF BARI
VIA AMENDOLA 173
BARI, ITALY

MARK A. CAPPELLI
STANFORD UNIVERSITY
MECHANICAL ENGINEERING
STANFORD CA 94305

R. CARMAN
MACQUARIE UNIVERSITY
NORTH RYDE
SYDNEY, AUSTRALIA

DAVID C. CARTWRIGHT
LOS ALAMOS NATIONAL LAB.
P.O. BOX 1663, MS-E527
LOS ALAMOS NM 87545

ROBERTO CELIBERTO
VIA AMENDOLA, 173
BARI, ITALY

PETER J. CHANTRY
WESTINGHOUSE R & D CENTER
1310 BEULAH RD.
PITTSBURGH PA 15235

BRIAN CHAPMAN
LUCAS LABS LTD.
1590 OAKLAND ROAD SUITE B113
SAN JOSE CA 95131

ROBERT E.H. CLARK
LOS ALAMOS NATIONAL LABORATORY
GROUP X-6 MSB226
LOS ALAMOS NM 87545

JAMES T. DAKIN
GE LIGHTING
NELA PARK
CLEVELAND OH

DAVID CHATFIELD
UNIVERSITY OF MINNESOTA
1869 JEFFERSON AVE.
ST. PAUL MN 55105

JOHN W. COBURN
IBM
K33/801
650 HARRY RD.
SAN JOSE CA 95120

MURRAY DARRACH
UNIVERSITY OF WINDSOR
PHYSICS DEPT., UNIV OF WINDSOR
WINDSOR, ONTARIO
CANADA N9B 3P4

DONGHAI CHEN
UNIVERSITY OF PITTSBURGH
314 MEYREN ST. 2ND FLOOR
PITTSBURGH PA 15213

MICHAEL COLGAN
RUTGERS UNIVERSITY
3 KING ROAD
LANDING NJ 07850

MAHENDRA DASSANAYAKE
STATE UNIVERSITY OF NEW YORK
DEPT. OF ECE
BUFFALO NY 14215

BLAKE CHERRINGTON
UT DALLAS
P.O. BOX 830688
RICHARDSON TX 75083

WILLIAM T. CONNER
UNIVERSITY OF WISC-MADISON
522 W. WILSON
#301
MADISON WI 53703

SANTOLO DE BENEDICTIS
ITALIAN C.N.R.
VIA G. AMENDOLA, 173
BARI, ITALY

CHIU CHIA-PIN
1231 RAYMOND AVE.
ST. PAUL MN 55108

JAMES COOK
BUSSMANN DIVISION
P.O. BOX 14460
ST. LOUIS MO 63178

JAIME DE URQUIJO
INSTITUTE DE FISICA UN AM
P.O. BOX 139-B
CUERNAVACA, MEXICO

MOO-HYUN CHO
UNIVERSITY OF WISC-MADISON
1500 JOHNSON DRIVE
MADISON WI 53706

JAY CORR
UNIVERSITY OF WINDSOR
PHYSICS DEPT., UNIV OF WINDSOR
WINDSOR, ONTARIO
CANADA N9B 3P4

CRAIG DENMAN
AIR FORCE WEAPONS LAB
ALBUQUERQUE NM 87117

SHI-CHUNG CHU
UNIVERSITY OF NEBRASKA-LINCOLN
260 BEHLEN
LINCOLN NE 68588

PHILIP C. COSBY
SRI INTERNATIONAL
333 RAVENSWOOD AVENUE
MENLO PARK CA 94025

R. DEVONSHIRE
SHEFFIELD UNIVERSITY
CHEMISTRY DEPT.
SHEFFIELD, YORK
U. K.

ARA CHUTJIAN
JET PROPULSION LAB./CALTECH
4800 OAK GROVE DR.
PASADENA CA 91109

GEORGE CSANAK
LOS ALAMOS NATIONAL LAB.
P.O. BOX 1663
LOS ALAMOS NM 87545

PASCAL DEVYNCK
SRI INTERNATIONAL
333 RAVENSWOOD AVENUE
MENLO PARK CA 94025

SHIRSHAK K. DHALI
SOUTHERN ILLINOIS UNIVERSITY
DEPARTMENT OF ELECTRICAL ENGINEERING
CARBONDALE IL 62901

BALDUR ELIASSON
ASEA BROWN BOVERI
BADEN, SWITZERLAND

RAYMOND FLANNERY
GEORGIA TECH
SCHOOL OF PHYSICS
ATLANTA GA 30327

JOHN DICARLO
UNIVERSITY OF ILLINOIS
607 EAST HEALEY STREET
CHAMPAIGN IL 61820

GILBERT EMMERT
UNIVERSITY OF WISCONSIN
1500 JOHNSON DR.
MADISON WI 53806

ROBERT S. FREUND
AT & T BELL LABS
ROOM 1D-256
600 MOUNTAIN AVE.
MURRAY HILL NJ 07974

J. P. DOERING
JOHN HOPKINS
DEPT. OF CHEMISTRY
BALTIMORE MD 21218

DOUGLAS W. ERNIE
UNIVERSITY OF MINNESOTA
123 CHURCH ST. S.E.
MINNEAPOLIS MN 55455

ALAN GALLAGHER
JILA
JILA, UNIV. OF COLORADO
BOULDER CO 80309

DOUGLAS A. DOUGHTY
JILA
UNIVERSITY OF COLORADO CB-440
BOULDER CO 80309

LEO D. ESKIN
STANFORD UNIVERSITY
BLDG 520, 521 J
STANFORD CA 94305

JEAN W. GALLAGHER
NIST
A323 PHYSICS BUILDING
GAITHERSBURG MD 20899

LAWRENCE DOWNES
MIAMI UNIVERSITY
DEPT. OF PHYSICS
133 CULLER
OXFORD OH 45056

JOHN F. EVANS
U OF MN
1519 E. RIVER TERR.
MINNEAPOLIS MN 55414

G. A. GALLUP
UNIVERSITY OF NEBRASKA
LINCOLN NE 68588

PAUL J. DRALLOS
WAYNE STATE UNIVERSITY
666 W. HANCOCK
DETROIT MI 48202

IAN S. FALCONER
UNIVERSITY OF SYDNEY
SCHOOL OF PHYSICS, A28
SYDNEY
AUSTRALIA 2006

BISH GANGULY
WRIGHT-PATT AFB
AFWAL/POOC-3
DAYTON OH 45433

MARK E. DUFFY
GE LIGHTING
NELA PARK
CLEVELAND OH 44112

TONY FARMER
CSIRO - APPLIED PHYSICS
P.O. BOX 218
SYDNEY
AUSTRALIA

NARENDRA K. GARG
CRAY RESEARCH, INC.
900 LOWATER RD.
CHIPPEWA FALLS WI 54729

DONALD J. ECKSTROM
SRI INTERNATIONAL
333 RAVENSWOOD AVENUE
MENLO PARK CA 94025

GREGORY J. FETZER
OPHIR CORPORATION
7333 W. JEFFERSON AVE.
#210
LAKEWOOD CO 80235

ANDREW M. GARVIE
WRI--POLYTECHNIC UNIVERSITY
ROUTE 110
FARMINGDALE NY 11735

JOHN E. GASTINEAU
LAWRENCE UNIVERSITY
115 S. DREW ST.
APPLETON WI 54911

VALERY GODYAK
GTE PRODUCTS CORPORATION
100 ENDICOTT STREET
DANVERS MA 01923

DAVID GRAVES
UNIV. OF CALIFORNIA, BERKELEY
CHEMICAL ENGINEERING
BERKELEY CA 94720

JAMES B. GERARDO
SANDIA NAT'L LAB.
DEPARTMENT 1120
P.O. BOX 5800
ALBUQUERQUE NM 87185

EVANGELES GOGOLIDES
MIT
77 MASS. AVE.
OFFICE: 66-217
CAMBRIDGE MA 02139

B. DAVID GREEN
PHYSICAL SCIENCES, INC.
RESEARCH PARK
P.O. BOX 3100
ANDOVER MA 01810

ROBERT A. GERBER
SANDIA NATIONAL LABS.
DIVISION 1275
P.O. BOX 5800
ALBUQUERQUE NM 87185

MARIO JOSE GONGALVES PINHEIRO
CENTRO DE ELECTRODINAMICA
DA U.T.L.
LISBON, PORTUGAL

KEN GREENBERG
SANDIA NAT'L LAB.
DEPARTMENT 1128
P.O. BOX 5800
ALBUQUERQUE NM 87185

ALIX GICQUEL
STANFORD UNIVERSITY
MECHANICAL ENG. DEPARTMENT
HIGH TEMP. GASDYNAMICS LAB.
STANFORD CA 94305

THOMAS GORCZYCA
JOINT INST. FOR LAB. ASTROPHY.
BOX 440
UNIVERSITY OF COLORADO
BOULDER CO 80309

DONALD C. GREGORY
OAK RIDGE NATIONAL LAB
BLDG 6003, MS 6372
P.O. BOX 2008
OAK RIDGE TN 37831

MARK A. GIESKE
MIAMI UNIVERSITY
DEPT. OF PHYSICS
OXFORD OH 45056

JOHN GOREE
UNIVERSITY OF IOWA
DEPT. OF PHYSICS
IOWA CITY IA 52242

TINA GRIMARD
UNIVERSITY OF MICHIGAN
1121 EECS BLDG.
ANN ARBOR MI 48109

DILECCE GIORGIO
C. N. R. - ITALIAN
VIA AMENDOLA, 173
BARI, ITALY

CLAUDINE GORSE
VIA AMENDOLA 173
BARI, ITALY

REX D. GROVES
GENERAL ELECTRIC
NELA PARK
CLEVELAND OH 44124

STEVEN L. GIRSHICK
U OF MN
MECH. ENG. DEPT.
111 CHURCH ST. S.E.
MINNEAPOLIS MN 55455

TOSHIO GOTO
DEPARTMENT OF ELECTRONICS
FURO-CHO, CHIKUSA-KU
NAGOYA, AICHI
JAPAN 464-01

MARTIN GUNDERSEN
UNIVERSITY OF SOUTHERN CALIF.
EE-ELECTROPHYSICS / SSC-420
LOS ANGELES CA 90089

THOMAS E. GIST
USAF AFWAL/POOC-3
WRIGHT-PATTERSON AFB
DAYTON OH 45424

R. A. GOTTSCHO
AT & T BELL LABS
RM. 1A-259
MURRAY HILL NJ 07974

V. T. GYLYS
ROCKETDYNE DIV.-ROCKWELL INT.
6633 CANOGA AVE.
CANOGA PARK CA 91303

PHILIP J. HARGIS
SANDIA NAT'L LAB.
DEPARTMENT 1120
P.O. BOX 5800
ALBUQUERQUE NM 87185

JOHN HEIDENREICH
IBM
T.J. WATSON RES. CTR.
YORKTOWN HEIGHTS NY 10598

SCOTT R. HUNTER
OAK RIDGE NATIONAL LABORATORY
P.O. BOX 2008
OAK RIDGE TN 37831

ROBERT L. HARTLEY
AIR FORCE INST. OF TECHNOLOGY
5599 BAYSIDE DR.
DAYTON OH 45431

ROLF HERNBERG
TAMPERE UNIV. OF TECHNOLOGY
P.O. BOX 527
TAMPERE
FINLAND SF-33101

WINIFRED M. HUO
NASA AMES RESEARCH CENTER
MOFFETT FIELD
MOFFETT FIELD CA 94035

DANIEL DEN HARTOG
U OF WI
1150 UNIVERSITY AVE.
MADISON WI 53706

ALAN E. HILL
PLASMATRONICS, INC.
BOX 5444-A, ROUTE 5
ALBUQUERQUE NM 87223

GILBERT HUPPERT
MIT
RM. 66-217
CAMBRIDGE MA 02139

ELIZABETH DEN HARTOG
U OF WI
1150 UNIVERSITY AVE.
MADISON WI 53706

W.N.G. HITCHON
UNIVERSITY OF WISC - MADISON
1415 JOHNSON DR.
MADISON WI 53706

SHELDON B. HUTCHISON
XMR INC.
5403 BETSY ROSS DR.
SANTA CLARA CA 95054

J.P. HAUCK
GENERAL DYNAMICS LASER SYS LAB
5452 OBERLIN DRIVE
SAN DIEGO CA 92121

GREG HOFMANN
UNIVERSITY OF WISC-MADISON
1500 JOHNSON DRIVE
MADISON WI 53706

JOHN INGOLD
GE LIGHTING
NELA PARK
CLEVELAND OH 44112

GERALD N. HAYS
SANDIA NAT'L LAB.
DEPARTMENT 1120
P.O. BOX 5800
ALBUQUERQUE NM 87185

SHAN HONGQING
STANFORD UNIVERSITY
DEPT. OF MECH. ENG., BLDG. 520
STANFORD CA 94305

TOM INTRATOR
UNIVERSITY OF WISC-MADISON
1500 JOHNSON DRIVE
MADISON WI 53706

GREG HEBNER
SANDIA NATIONAL LABORATORIES
DEPARTMENT 1144
P.O. BOX 5800
ALBUQUERQUE NM 87185

DAVID F. HUDSON
N S W C
10901 NH AVE.
CODE F43
SILVER SPRING MD 20903

GREGORY M. JELLUM
UNIVERSITY OF CALIFORNIA
201 GILMAN HALL
BERKELEY CA 94720

GLENN HEESTAND
LAWRENCE LIVERMORE NAT. LAB.
P.O. BOX 808, L-460
LIVERMORE CA 94550

DAVID L. HUESTIS
SRI INTERNATIONAL
333 RAVENSWOOD AVENUE
MENLO PARK CA 94025

RAINER JOHNSEN
UNIVERSITY OF PITTSBURGH
DEPT. OF PHYSICS AND ASTRONOMY
PITTSBURGH PA 15260

JERZY JUREWICZ
UNIVERSITY OF SHERBROOKE
2500 UNIVERSITY BLVD.
SHERBROOKE PQ J1K2R

KEN-ICHI KOWARI
ARGONNE NATIONAL LABORATORY
9700 SOUTH CASS AVE.
ARGONNE IL 60439

RUSS LAHER
R & D ASSOCIATES
4640 ADMIRALTY WAY
LOS ANGELES CA 92965

ABE KADISH
LOS ALAMOS NATIONAL LABORATORY
P.O. BOX 1663
LOS ALAMOS NM 87545

JERRY KRAMER
GTE LABORATORIES INCORPORATED
40 SYLVAN ROAD
WALTHAM MA 02254

Y.C. LAU
UNIVERSITY OF MINNESOTA
111 CHURCH ST. S.E.
MINNEAPOLIS MN 55455

WILLIAM KARRAS
UNIVERSITY OF WINDSOR
PHYSICS DEPT., UNIV OF WINDSOR
WINDSOR, ONTARIO
CANADA N9B 3P4

OLE O. KROGH
TEGHL CORP.
2201 S. MCDOWELL BLVD.
PETALUMA CA 94953

J. E. LAWLER
DEPT. OF PHYSICS
U OF WI
1150 UNIVERSITY AVE.
MADISON WI 53706

WALTER E. KAUPPILA
WAYNE STATE UNIVERSITY
PHYSICS DEPT.
DETROIT MI 48202

CHARLES H. KRUGER
STANFORD UNIVERSITY
TERMAN 214
STANFORD CA 94305

LONG C. LEE
SAN DIEGO STATE UNIVERSITY
DEPT. OF ELECTRICAL & COMPUTER
ENGINEERING
SAN DIEGO CA 92182

JOHN H. KELLER
IBM - E. FISH KILL
DEPT. 18Q, BLDG. 300-48A
HOPEWELL JCT. NY 12533

IGOR KUBELIK
DELPHAX
5030 TIMBERLEA BLVD.
MISSISSAUGA, ONTARIO
CANADA L4W 2S5

EMANUELE LEVERONI
UNIVERSITY OF MINNESOTA
125 MECH. ENG. DEPT.
MINNEAPOLIS MN 55455

M.A. KHAKOO
UNIVERSITY OF MISSOURI
PHYSICS DEPT.
ROLLA MO 65401

KENNETH C. KULANDER
LAWRENCE LIVERMORE NAT'L LAB.
P.O. BOX 808, MAIL CODE L-438
LIVERMORE CA 94550

YAN MING LI
GTE LABORATORIES INCORPORATED
40 SYLVAN ROAD
WALTHAM MA 02254

LARRY KLINE
WESTINGHOUSE R & D
PITTSBURGH PA 15235

ASHOK KUMAR JAIN
FLORIDA A & M UNIVERSITY
PHYSICS DEPT., BOX 981
TALLAHASSEE FL 32307

MICHAEL A. LIEBERMAN
UNIV. OF CALIFORNIA-BERKELEY
DEPT. OF EECS
BERKELEY CA 94720

DANIEL J. KOCH
UNIVERSITY OF WI-MADISON
1614 GREEN VALLEY DR.
JANESVILLE WI 53546

M. J. KUSHNER
UNIVERSITY OF ILLINOIS
607 EAST HEALEY STREET
CHAMPAIGN IL 61820

PHILLIP LIESCHESKI
INDIANA UNIVERSITY
DEPT. OF CHEMISTRY
BLOOMINGTON IN 47405

C. D. LIN
KANSAS STATE UNIVERSITY
DEPT. OF PHYSICS
MANHATTAN KS 66506

CHUN C. LIN
UNIVERSITY OF WISC-MADISON
1150 UNIVERSITY AVE.
MADISON WI 53706

TE-HUA LIN
INTEL CORP.
P.O. BOX 58125, MS:SC9-34
SANTA CLARA CA 95052

BRUCE J. LIND
HONEYWELL, SRC
3660 TECH. DR., MN 65-2600
MINNEAPOLIS MN 55418

G.K. LINDEBERG
3M COMPANY
208-1-01 3M CENTER
ST. PAUL MN 55144

JOANNE LIU
MIT
66-219
77 MASSACHUSETTS AVE.
CAMBRIDGE MA 02139

DONALD C. LORENTS
SRI INTERNATIONAL
333 RAVENSWOOD AVENUE
MENLO PARK CA 94025

ZHIPENG LU
UNIVERSITY OF MINNESOTA
125 MECH. ENGR. BLDG.
111 CHURCH ST. S.E.
MINNEAPOLIS MN 55455

GILLIAN C. LYNCH
CHEM. DEPT. U OF MN.
207 PLEASANT ST. S.E.
MINNEAPOLIS MN 55455

CE MA
INDIANA UNIVERSITY
DEPT. OF CHEMISTRY
BLOOMINGTON IN 47405

DON MADISON
UNIVERSITY OF MISSOURI - ROLLA
PHYSICS DEPT.
ROLLA MO 65401

WILLIAM B. MAIER
LOS ALAMOS NATIONAL LABORATORY
UNIVERSITY OF CALIFORNIA
P.O. BOX 1663, MS P234
LOS ALAMOS NM 87545

TOSHIAKI MAKABE
KEIO UNIVERSITY
FACULTY-SCIENCE & TECHNOLOGY
3-14-1 HIYOSHI
YOKOHAMA, JAPAN 223

LUTE MALEKI
JPL/CAL TECH
4800 OAK GROVE DR.
PASADENA CA 91109

ED MANSKY
GEORGIA INSTITUTE OF TECH.
SCHOOL OF PHYSICS
ATLANTA GA 30332

S. DOUGLAS MARCUM
MIAMI UNIVERSITY
DEPARTMENT OF PHYSICS
OXFORD OH 45056

JAKOB MAYA
GTE PRODUCTS CORPORATION
100 ENDICOTT STREET
DANVERS MA 01923

ARMIN METZE
HONEYWELL, INC. (SRC)
3660 TECHNOLOGY DRIVE
MINNEAPOLIS MN 55418

H. HARVEY MICHELS
UTRC
PHYSICS DEPT.
EAST HARTFORD CT 06108

RICHARD E. MIERS
INDIANA U/PURDUE U AT FT WAYNE
2101 COLISEUM BLVD E.
FORT WAYNE IN 46805

HELEN MISHURDA
UNIVERSITY OF WISC-MADISON
1500 JOHNSON DRIVE
MADISON WI 53706

ANNETTE MITCHELL
AT & T BELL LABORATORIES
600 MOUNTAIN AVE.
MURRAY HILL NJ 07974

J. BRIAN A. MITCHELL
UNIVERSITY OF WESTERN ONTARIO
DEPT. OF PHYSICS
LONDON, ONTARIO
CANADA N6A 3K7

WILLIAM M. MOENY
TETRA CORPORATION
4905 HAWKINS ST., NE
ALBUQUERQUE NM 87109

TOM MORATZ
MISSION RESEARCH CORPORATION
1 TARA BOULEVARD
NASHUA NH 03062

IAN J. MOREY
UC BERKELEY
EECS, CORY HALL
BERKELEY CA 94720

ROBERT A. MORRIS
AIR FORCE GEOPHYSICS
HANSCOM AFB
BEDFORD MA 01731

PHIL MOSKOWITZ
GTE PRODUCTS CORP.
100 ENDICOTT ST.
DANVERS MA 01923

HELMUT MULLER
UNIVERSITY OF KARLSRUHE
DURRENWETTERSHACHERSTR. 22
KARLSRUHE, WEST GERMANY

RAY MUNO
U OF MN - MECH. ENG.
111 CHURCH ST. S.E.
MINNEAPOLIS MN 55455

DANIEL E. MURNICK
RUTGERS THE STATE UNIVERSITY
101 WARREN ST.
PHYSICS DEPT., SMITH
NEWARK NJ 07102

JENNIFER MYERS
MIAMI UNIVERSITY
133 CULLER HALL
OXFORD OH 45056

MICHAEL J. McCAUGHEY
UNIVERSITY OF ILLINOIS
607 EAST HEALEY STREET
CHAMPAIGN IL 61820

JABEZ McCLELLAND
NAT'L INST. OF STDS & TECH.
MET B206
GAITHERSBURG MD 20899

DONALD J. McCLURE
3M
3M CENTER BLDG. 208-1-01
ST. PAUL MN 55144

J. WILLIAM McCONKEY
UNIVERSITY OF WINDSOR
PHYSICS DEPT., UNIV OF WINDSOR
WINDSOR, ONTARIO
CANADA N9B 3P4

MR. NACHTIJALL
MARKGRATEN STR. 14.
SCHWELUR, GERMANY

JEAN-PHILIPPE NICOLAI
MIT
RM. 66-219
DEPT. OF CHEM ENG.
CAMBRIDGE MA 02139

D. NORCROSS
JILA/NIST
NIST, QUINCIE ORCHARD DR.
AND CLOPPER RD.
GALTHERSBURG MD 20899

THOMAS O'BRIAN
UNIVERSITY OF WI - MADISON
1150 UNIVERSITY AVE.
MADISON WI 53706

THOMAS F. O'MALLEY
2276 LUCRETIA AVE. #4
SAN JOSE CA 95122

STEPHAN OFFERMANNS
PHILIPS RES. LABS.
WEISSHAUSSTR.
AACHEN, WEST GERMANY

MIEKO OHWA
UNIVERSITY OF ILLINOIS
607 EAST HEALEY STREET
CHAMPAIGN IL 61820

JAMES OLTHOFF
NAT. INST. OF STANDARDS & TECH
BLDG. 220 / ROOM B344
GAITHERSBURG MD 20899

YOSHI ONO
TEKTRONIX INC.
P.O. BOX 500, MS 59-234
BEAVERTON OR 97077

TSUEN OR
UNIVERSITY OF MINNESOTA
125 MECH. ENGR. BLDG.
111 CHURCH ST. S.E.
MINNEAPOLIS MN 55455

H. J. OSKAM
UNIVERSITY OF MINNESOTA
ELEC. ENGR.
123 CHURCH ST. S.E.
MINNEAPOLIS MN 55455

A.V. PHELPS
JILA UNIVERSITY OF COLORADO
BOULDER CO 80309

DAVID L. A. RALL
UNIVERSITY OF WI / PHYSICS
1150 UNIVERSITY AVE.
MADISON WI 53706

LAWRENCE J. OVERZET
UNIVERSITIES OF IL & TX
P.O. BOX 830688
RICHARDSON TX 75083

LAL A. PINNADUWAGE
UNIV. OF TENNESSEE - KNOXVILLE
DEPT. OF PHYSICS
401 NEILSEN BLDG.
KNOXVILLE TN 37996

THOMAS N. RESCIGNO
LAWRENCE LIVERMORE NAT'L LAB.
P.O. BOX 808
LIVERMORE CA 94550

HOYOUNG PAK
UNIVERSITY OF ILLINOIS
607 EAST HEALEY STREET
CHAMPAIGN IL 61820

SAEED PIROOZ
WASHINGTON UNIVERSITY
P.O. BOX 1198
ONE BROOKINGS DR.
ST. LOUIS MO 63130

KARL-ULRICH RIEMANN
RUHR UNIVERSITY
UNIV. STR. 150
BOCHUM
WEST GERMANY

AJIL PARANJBE
STANFORD UNIVERSITY
MECHANICAL ENG. DEPT.
STANFORD CA 94305

LEANNE PITCHFORD
UNIVERSITE PAUL SABATIER
TOULONSE, FRANCE

JAMES R. ROBERTS
NAT'L INST. OF STDS & TECH.
A1C7/221
GAITHERSBERG MD 20899

MICHAEL L. PASSOW
UNIV. OF MICHIGAN - NUC. ENGR.
121 COOLEY BLDG.
2355 BONISTEEL
ANN ARBOR MI 48109

BILL PLATT
HONEYWELL, SRC
3660 TECH. DR., MN 65-2600
MINNEAPOLIS MN 55418

VICTOR ROBERTS
GE R & D CENTER
P.O. BOX 8
SCHENECTADY NY 12301

BERNIE M. PENETRANTE
LAWRENCE LIVERMORE NAT'L LAB.
L-417
P.O. BOX 808
LIVERMORE CA 94550

R.K. PORTEOUS
AUSTRALIAN NATIONAL UNIV.
PRL RS PHYS S, ANV, GPO BOX 4
CANBERRA, ACT
AUSTRALIA 2601

DANIEL C. ROBIE
SRI INTERNATIONAL
333 RAVENSWOOD AVENUE
MENLO PARK CA 94025

N. W. PERERA
DEPT. OF PHYSICS
UNIVERSITY OF NEBRASKA
LINCOLN NE 68588

HOWARD P. PRITCHARD
CALIFORNIA INSTITUTE OF TECHN.
PASADENA CA 91125

JORGE ROCCA
COLORADO STATE UNIVERSITY
ELECTRICAL ENGINEERING DEPT.
FORT COLLINS CO 80523

JAMES R. PETERSON
SRI INTERNATIONAL
333 RAVENSWOOD AVENUE
MENLO PARK CA 94025

JOESPH M. PROUD
GTE LABORATORIES
40 SYLVAN RD.
WALTHAM MA 02254

GERALD L. ROGOFF
GTE LABORATORIES INCORPORATED
40 SYLVAN ROAD
WALTHAM MA 02254

JAMES ROSENZWEIG
ARGONNE NAT'L LABORATORY
9700 S. CASS AVE.
ARGONNE IL 60439

JAY T. SCHEUER
U OF WI
1500 JOHNSON DR.
MADISON WI 53706

XUEYING SHI
UNIVERSITY OF NEBRASKA-LINCOLN
2265 YST. #23
LINCOLN NE 68503

MICHAEL E. RUHLAND
UNIVERSITY OF MINNESOTA
111 CHURCH ST. S.E.
MECH. ENGR.
MINNEAPOLIS MN 55455

ALFRED S. SCHLACHTER
LAWRENCE BERKELEY LABORATORY
MS 4-230
BERKELEY CA 94720

BERNIE SHIZGAL
UNIV. OF BRITISH COLIMBIA
DEPT OF CHEM. - 2036 MAIN MALL
VANCOUVER, BC
CANADA V6T 1Y6

ANA BELA SA
CENTRO DE ELECTRODINAMICA
INSTITUTO SUPERIOR TECHNICO
LISBON, PORTUGAL

VERN SCHLIE
AIR FORCE WEAPONS LAB
KIRTLAND AFB, NM
ALBUQUERQUE NM 87117

JAMES R. SHOEMAKER
USAF
WRIGHT-PATTERSON AFB
DAYTON OH 45433

NADER SADEGHI
UNIVERSITY OF GRENOBLE
B.P. 87
38402-ST. MARTIN DHERES
FRANCE

M. BRUCE SCHULMAN
PHILIPS LIGHTING COMPANY
330 LYNNWAY
LYNN MA 01901

JUDA LEON SHOHET
UNIVERSITY OF WISC-MADISON
DEPT. OF ELECTRICAL AND
COMPUTER ENGINEERING
MADISON WI 53706

STEPHEN SAVAS
APPLIED MATERIALS
3050 BOWERS AVE.
SANTA CLARA CA 95054

SUE SCHULTHESZ
UNIVERSITY OF MINNESOTA
CHEMISTRY DEPT.
SMITH HALL, BOX E-11
MINNEAPOLIS MN 55455

PAUL SHUFFLEBOTHAM
UNIVERSITY OF MANITOBA
DEPT. ELECTRICAL ENGINEERING
WINNIPEG, MANITOBA
CANADA R3T 2N2

HERB SAWIN
MIT
RM. 66-409
CAMBRIDGE MA 02139

SIDNEY A. SELF
STANFORD UNIVERSITY
MECHANICAL ENG. DEPT.
STANFORD CA 94305

TONG W. SHYN
THE UNIVERSITY OF MICHIGAN
2455 HAYWARD STREET
ANN ARBOR MI 48109

RICHARD SAYKALLY
UNIVERSITY OF CALIFORNIA
BERKELEY CA 94720

BARRIE ANN SHAFFER
UNIVERSITY OF WISC-MADISON
1101 UNIVERSITY AVE.
MADISON WI 53706

DAVID SKATRUD
ARMY RESEARCH OFFICE
P.O. BOX 12211
RESEARCH TRIANGLE PK NC 27709

KARL SCHEIBUER
LAWRENCE LIVERMORE NAT'L LAB.
P.O. BOX 5508
LIVERMORE CA 94550

FRANCIS A. SHARPTON
NORTHWEST NAZARENE COLLEGE
623 HOLLY STREET
NAMPA ID 83686

STEVEN JOEL SMITH
WAYNE STATE UNIVERSITY
PHYSICS DEPT.
666 WEST HANCOCK
DETROIT MI 48202

GREGORY SNITCHLER
JOINT INST. FOR LAB. ASTROPHY.
BOX 440
UNIVERSITY OF COLORADO
BOULDER CO 80309

DAVID H. STONE
U.S. AIR FORCE
AFIT/ENP
WPAFB OH 45433

SWARAJ TAYAL
LOUISIANA STATE UNIVERSITY
DEPT. OF PHYSICS
BATON ROUGE LA 70803

STUART SNYDER
UNIVERSITY OF IDAHO
PHYSICS DEPT.
MOSCOW ID 83843

PETER STORMBERG
PHILIPS RES. LABS
WEISSHAUS STR.
AACHEN, WEST GERMANY

WILLIAM S. TAYLOR
EXTREL CORPORATION
240 ALPHA DR.
P.O. BOX 11512
PITTSBURGH PA 15238

TIMOTHY J. SOMMERER
UNIVERSITY OF WISCONSIN
1150 UNIVERSITY AVE.
MADISON WI 53706

KEN STRICKLETT
PACIFIC N.W. LABORATORIES
P.O. BOX 999
MAIL STOP K3-57
RICHLAND WA 99352

TIMM H. TEICH
SWISS FEDERAL INST. OF TECH.
PHYSIKSTR, 3
ZVERICH, SWITZERLAND

RONALD SPORES
UNIVERSITY OF MINNESOTA
125 MECH. ENGR. BLDG.
111 CHURCH ST. S.E.
MINNEAPOLIS MN 55455

ISAAC D. SUDIT
U.W. -MADISON
PHYSICS DEPT.
909 SPAIGHT ST. #3
MADISON WI 53703

MICHAEL F. TOUPS
U OF MN - DEPT. OF ELECT. ENG.
123 CHURCH ST. S.E.
MINNEAPOLIS MN 55455

KENNETH R. STALDER
SRI INTERNATIONAL
333 RAVENSWOOD AVENUE
MENLO PARK CA 94025

GILBERT D. SULTAN
LAB. PHYS. GAZ ET PLASMAS
ORSAY, FRANCE

SANDOR TRAJMAR
J. P. L.
4800 OAK GROVE DR.
PASADENA CA 91107

TALBERT S. STEIN
WAYNE STATE UNIVERSITY
DEPT. OF PHYSICS
DETROIT MI 48202

MAHESWARAN SURENDRA
U C BERKELEY
GILMAN HALL, DEPT. CHEM ENG.
BERKELEY CA 94720

DONALD G. TRUHLAR
U OF MN
DEPT. OF CHEMISTRY
MINNEAPOLIS MN 55455

MR. STEVEFELT
UNIVERSITY OF ORLEANS
B. P. 6759
ORLEANS
FRANCE 45067

C. M. SURKO
AT & T BELL LABORATORIES
1D432
MURRAY HILL NJ 07976

MAOEE TSEN
207 PLEASANT ST. S.E.
MINNEAPOLIS MN 55455

JAY STOCKLEY
OPHIR CORPORATION
7333 W. JEFFERSON AVE.
#210
LAKEWOOD CO 80235

YEHUDA TAMIR
BEN-GURION UNIV. OF THE NEGEV
P.O. BOX 653
BEER SHEVA, ISRAEL

SREERAM VALLURI
UNIVERSITY OF WESTERN ONTARIO
DEPT. OF APPLIED MATHEMATICS
LONDON ON N6A 5

RICHARD J. VAN BRUNT
NAT'L INST. OF STAND. & TECH.
BLDG. 220, ROOM B344
GAITHERSBURG MD 20899

JOHN J. WAGNER
CRAY RESEARCH, INC.
900 LOWATER RD.
CHIPPEWA FALLS WI 54729

AMY WENDT
UNIVERSITY OF WISC-MADISON
ROOM 331, NEES DEPT.
1500 JOHNSON ST.
MADISON WI 53706

PETER J. M. VAN DER BURGT
NORTH CAROLINA STATE UNIV.
DEPARTMENT OF PHYSICS
RALEIGH NC 27695

KEITH G. WALKER
POINT LOMA COLLEGE
PHYSICS DEPT.
3900 LOMALAND DR.
SAN DIEGO CA 92106

YILIN WENG
UNIVERSITY OF ILLINOIS
607 EAST HEALEY STREET
CHAMPAIGN IL 61820

JUHA VATTULAINEN
TAMPERE UNIV. OF TECHNOLOGY
P.O. BOX 527
TAMPERE
FINLAND SF-33101

DAVID L. WALL
LASER ANALYTICS
25 WIGGINS AVE.
BEDFORD MA 01730

THOMAS E. WICKER
PHILIPS RESEARCH LABS.
811 E. ARQUES AVE. MS 65
SUNNYVALE CA 94088

JOSEPH T. VERDEVEN
UNIVERSITY OF ILLINOIS
607 E. HEALEY
CHAMPAIGN IL 61820

DONG-PO WANG
E-204 DEPARTMENT OF ECE
SAN DIEGO CA 92182

FRAZER WILLIAMS
UNIVERSITY OF NEBRASKA
DEPT. ELECTRICAL ENGINEERINIG
LINCOLN NE 68588

PABLO A. VICHARELLI
GTE LABORATORIES, INC.
40 SYLVAN RD.
WALTHAM MA 02254

SHOUYE WANG
UNIVERSITY OF WINDSOR
PHYSICS DEPT., UNIV OF WINDSOR
WINDSOR, ONTARIO
CANADA N9B 3P4

J. F. WILLIAMS
UNIVERSITY OF WEST. AUSTRALIA
NEDLANDS
PERTH, AUSTRALIA

ROBERT J. VIDMAR
SRI INTERNATIONAL, BLDG. 301
333 RAVENSWOOD AVE.
MENLO PARK CA 94025

JOHN F. WAYMOUTH
16 BENNETT RD.
MARBLEHEAD MA 01945

CARL WINSTEAD
CALTECH
127-72 NOYES, CALTECH
PASADENA CA 91125

MAYO VILLAGRAN
COLORADO STATE UNIVERSITY
ERC CSU
FT. COLLINS CO 82523

CHARLES A. WEATHERFORD
FLORIDA A & M
PHYSICS DEPARTMENT
BOX 981
TALLAHASSEE FL 32307

HAROLD L. WITTING
GENERAL ELECTRIC CO./CRD
P.O. BOX 8 K-1 4C17
SCHENECTADY NY 12301

LEPOSAVA VUSKOVIC
NEW YORK UNIVERSITY
PHYSICS
4 WASHINGTON PLACE
NEW YORK NY 10003

YU WEIXING
ME DEPT. - U OF MN
1174 FIFIELD AVE. S-2
ST. PAUL MN 55108

CLAUDE R. WOODS
DEPT. OF CHEMISTRY
UNIVERSITY OF WISCONSIN
MADISON WI 53706

JODY WORMHOUDT
AERODYNE RESEARCH, INC.
45 MANNING ROAD
BILLERICA MA 01821

M. ZHAO
U OF MN.
DEPT. OF CHEMISTRY
SMITH HALL
MINNEAPOLIS MN 55455

MALCOLM WRIGHT
AIR FORCE WEAPONS LAB
KIRTLAND AFB, NM
ALBUQUERQUE NM 87117

HUILING ZHU
UNIVERSITY OF MINNESOTA
111 CHURCH ST. S.E.
MINNEAPOLIS MN 55455

CHUN YI WU
1223 FIFIELD AVE.
ST. PAUL MN 55108

J. DAVID ZOOK
HONEYWELL
10701 LYNDALE AVE. SOUTH
BLOOMINGTON MN 55420

PERRY P. YANEY
UNIVERSITY OF DAYTON
DEPT. OF PHYSICS
DAYTON OH 45469

Jonathan Storer
3M Corporation
219-1S-01 3M Center
St. Paul, MN 55144

ORHAN YENEN
UNIVERSITY OF NEBRASKA-LINCOLN
DEPT. OF PHYSICS
LINCOLN NE 68588

Michael Dillon
Argonne National Laboratory
9700 S. Cass Avenue
Argonne, IL 60439

ROBERT A. YOUNG
ROCKWELL INT'L ROCKETDYNE DIV.
6633 CANOGA AVENUE
CANOGA PARK CA 91304

Gerhard Schaefer
Polytechnic U. of Brooklyn
Route 110
Farmingdale, NY 11735

GAVIN ZAN
MIT
RM. 66-217
CAMBRIDGE MA 02139

Erich E. Kunherdt
Weber Research Institute
Polytechnic U. of Brooklyn
Farmingdale, NY 11735

PETER ZETNER
JET PROPULSION LABORATORY
4800 OAK GROVE DR.
#183-601
PASADENA CA 91109

Szu-Cherng Kuo
Polytechnic U. of Brooklyn
Route 110
Farmingdale, NY 11735

FORTY FIRST ANNUAL GASEOUS ELECTRONICS CONFERENCE

October 17-21, 1988 • University of Minnesota • Minneapolis, Minnesota

All sessions held on the third level of the Radisson Plaza Hotel, Minneapolis, Minnesota.

Monday, October 17			
6:30 PM - 9:30 PM		*Registration and Reception*	Prefunction Area & Minnesota Room
Tuesday, October 18			
8:00 AM - 8:10 AM		Welcome (Vice Provost V. R. Murthy)	Ballroom
8:10 AM - 10:00 AM	A	Electron-Atom Collisions (S. Trajmar)	Ballroom
10:20 AM - 12:00 Noon	B	Charged particle Distributions and Electric Fields (J. Wormhoudt)	Ballroom
1:30 PM - 3:30 PM	CA	Thermal and High Pressure Plasma Processes (S. Girshick)	East Ballroom
1:30 PM - 3:30 PM	CB	Electron and Photon Interactions (M. Dillon)	West Ballroom
3:45 PM - 5:45 PM	D	Workshop on the Design, Calibration, and Modeling of Research RF Plasma Processing Systems (J. Gerardo)	West Ballroom
7:30 PM - 10:00 PM	E	Posters: Gaseous Electronics I (P. Moskowitz) posted from 5:00 PM	East Ballroom & Minnesota Room
Wednesday, October 19			
8:00 AM - 9:50 AM	FA	Models and Diagnostics of Lighting Discharges (H. Witting)	East Ballroom
8:00 AM - 9:55 AM	FB	Electron Collisions, Including Excited States (C. C. Lin)	West Ballroom
10:10 AM - 12:05 PM	GA	Lasers (J. G. Eden)	East Ballroom
10:10 AM - 11:55 AM	GB	Plasma-Surface Phenomena (D. Graves)	West Ballroom
1:30 PM - 3:45 PM	H	Posters: Gaseous Electronics II (J. Evans) posted from 1:00 PM	Ballroom & Minnesota Room
3:45 PM - 6:00 PM	I	Posters: Gaseous Electronics III (L. Bigio) posted from 1:00 PM	Ballroom
Thursday, October 20			
8:00 AM - 8:50 AM	JA	Silane Plasmas (G. Hays)	East Ballroom
8:00 AM - 9:20 AM	JB	Beam-Plasma Interactions (J. L. Shohet)	West Ballroom
8:50 AM - 9:45 AM	KA	Non-Equilibrium Electron Transport (Y. Li)	East Ballroom
10:00 AM - 11:30 AM	LA	Neutral Particle Distributions (M. Cappelli)	East Ballroom
10:00 AM - 11:30 AM	LB	Heavy Particle Interactions (B. Bederson)	West Ballroom
11:30 AM - 12:00 Noon		*Business Meeting* (J. Proud)	East Ballroom
1:30 PM - 3:20 PM	M	RF Glow Discharge Modeling (A. Mitchell)	Ballroom
3:40 PM - 5:35 PM	N	Breakdown and Switching (M. Gundersen)	Ballroom
6:30 PM - 7:30 PM		*Social Hour*	Prefunction Area & Minnesota Room
7:30 PM -		*Banquet*	Ballroom
		After Dinner Speaker: Dr. G. E. Schuh, Dean, H. H. Humphrey Institute, University of Minnesota	
Friday, October 21			
8:30 AM - 9:05 AM	O	Physics in a Positron Trap (R. Gottscho)	Ballroom
9:20 AM - 11:15 AM	PA	Low-Pressure Discharges: Experimental (R. Gerber)	East Ballroom
9:20 AM - 11:15 AM	PB	Electron-Molecule Collisions (R. Bonham)	West Ballroom
11:15 AM - 12:00 Noon	Q	Follow-up to the Workshop on the Design, Calibration, and Modeling of Research RF Plasma Processing Systems (J. Gerardo)	East Ballroom